

VYSOKÉ UČENÍ TECHNICKÉ V BRNĚ  
BRNO UNIVERSITY OF TECHNOLOGY



FAKULTA STAVEBNÍ  
ÚSTAV VODNÍCH STAVEB

FACULTY OF CIVIL ENGINEERING  
INSTITUTE OF WATER STRUCTURES

PRAVDĚPODOBNOSTNÍ ŘEŠENÍ PORUŠENÍ  
OCHRANNÉ HRÁZE V DŮSLEDKU PŘELITÍ  
THE PROBABILISTIC SOLUTION OF DIKE BREACHING DUE TO OVERTOPPING

DISERTAČNÍ PRÁCE  
DOCTORAL THESIS

AUTOR PRÁCE  
AUTHOR

ING. ZAKARAYA ALHASAN

VEDOUCÍ PRÁCE  
SUPERVISOR

PROF. ING. JAROMÍR ŘÍHA, CSC.

BRNO 2016



## **ABSTRAKT**

Disertační práce se zabývá analýzou spolehlivosti ochranných hrází na základě odhadu pravděpodobnosti poruchy hráze. Práce na základě teoretických poznatků, experimentálních a statistických výzkumů, matematických modelů a terénního šetření rozšiřuje soudobé znalosti analýzy spolehlivosti hráze ohrožené porušením v důsledku přelití. Tato práce obsahuje výsledky pravděpodobnostního řešení možné poruchy levobřežní ochranné hráze řeky Dyje v místě vesnice Ladná v České Republice v důsledku jejího přelití. V rámci práce byl navržen matematický model popisující proces přelití a proces eroze hráze. Proces přelití hráze byl popsán jednoduchými hydraulickými rovnicemi. Po začátku přelití hráze dojde k jejímu porušení za předpokladu překročení odolnosti povrchu hráze proti erozi vlivem proudící vody na vzdušném líci. Proces eroze hráze byl popsán jednoduchými rovnicemi pro transport sedimentů. Tyto rovnice obsahují parametry, které byly stanoveny s využitím údajů z minulých reálných poruch hrází. V rámci rozboru modelu byly stanoveny nejistoty ve vstupních datech a následně byla provedena citlivostní analýza s použitím „screening“ metody. Za účelem dosažení pravděpodobnostního řešení byly vybrané vstupní parametry uvažovány jako náhodné veličiny s různým rozdělením pravděpodobnosti. Pro generování sady náhodných hodnot pro vybrané vstupní veličiny byla použita metoda Latin Hypercube Sampling (LHS). V procesu porušení hráze v důsledku jejího přelití byly identifikovány čtyři typické fáze. Konečné výsledky této studie mají formu pravděpodobností vzniku jednotlivých typických fází porušení hráze.

## **KLÍČOVÁ SLOVA**

Analýza spolehlivosti; citlivostní analýza; Latin hypercube sampling; nejistota; odolnost vymílání; porušení hráze; přelití hráze.

## **ABSTRACT**

Doctoral thesis deals with reliability analysis of flood protection dikes by estimating the probability of dike failure. This study based on theoretical knowledge, experimental and statistical researches, mathematical models and field survey extends present knowledge concerning with reliability analysis of dikes vulnerable to the problem of breaching due to overtopping. This study contains the results of probabilistic solution of breaching of a left bank dike of the River Dyje at a location adjacent to the village of Ladná near the town of Břeclav in the Czech Republic. Within this work, a mathematical model describing the overtopping and erosion processes was proposed. The dike overtopping is simulated using simple surface hydraulics equations. For modelling the dike erosion which commences with the exceedance of erosion resistance of the dike surface, simple transport equations were used with erosion parameters calibrated depending on data from past real embankment failures. In the context of analysis of the model, uncertainty in input parameters was determined and subsequently the sensitivity analysis was carried out using the screening method. In order to achieve the probabilistic solution, selected input parameters were considered random variables with different probability distributions. For generating the sets of random values for the selected input variables, the Latin Hypercube Sampling (LHS) method was used. Concerning with the process of dike breaching due to overtopping, four typical phases were distinguished. The final results of this study take the form of probabilities for those typical dike breach phases.

## **KEYWORDS**

Dike breaching; dike overtopping; Latin hypercube sampling; reliability analysis; scour resistance; sensitivity analysis; uncertainty.

## **BIBLIOGRAFICKÁ CITACE**

ALHASAN, Zakaraya. *The probabilistic solution of dike breaching due to overtopping*. Brno, 2016. 82 s., 11 s. příloh. Disertační práce. Vysoké učení technické v Brně, Fakulta stavební, Ústav vodních staveb. Vedoucí práce prof. Ing. Jaromír Říha, CSc.

## **PROHLÁŠENÍ**

Prohlašuji, že jsem celou disertační práci vypracoval samostatně s použitím odborné literatury a pod vedením školitele prof. Ing. Jaromíra Říhy, CSc.

Dále prohlašuji, že veškeré podklady, ze kterých jsem čerpal, jsou uvedeny v seznamu použité literatury.

V Brně dne 31. 8. 2016

.....

podpis

## PODĚKOVÁNÍ

Prvně bych chtěl poděkovat svému školiteli prof. Ing. Jaromíru Říhovi, CSc. za odborné vedení a podnětné připomínky při zpracování doktorské disertační práce.

Dále bych chtěl vyjádřit velké díky Ing. Davidu Duchanovi, Ph.D., který mě zasvětil do programovacího jazyka. On a kolegové mi byli vždy nápomocni s jakýmkoliv problémem nebo dotazem.

Na závěr zvláštní dík patří mé ženě a mé rodině za podporu a toleranci při dokončování této práce.

# CONTENT

1	INTRODUCTION .....	3
1.1	General remarks.....	3
1.2	Dike failure due to overtopping.....	4
1.3	Terminology .....	5
2	AIM AND SUBJECT OF THE WORK.....	8
2.1	Aim of the work.....	8
2.2	Subject of the work.....	8
3	PRESENT STATE REVIEW .....	11
3.1	Flood protection dikes .....	11
3.2	General publications .....	11
3.3	Modelling and simulation for dike and dam failure .....	12
3.4	Experimental researches .....	13
3.5	Statistical researches and reference studies .....	14
3.6	Reliability analysis of dam and dike.....	15
4	BASIC DEFINITIONS AND PARAMETERS OF DIKE BREACHING ..	16
4.1	General comments .....	16
4.2	Essential parameters in the temporal evolution of dike breaching.....	16
4.3	Dimensional parameters .....	18
4.4	Statistics for dike failures .....	19
5	MECHANISM OF DIKE BREACHING DUE TO OVERTOPPING .....	22
5.1	Dike breaching progression .....	22
5.2	Homogeneous dike breaching due to overtopping .....	24
6	Scour resistance of the dike surface.....	25
6.1	Introduction .....	25
6.2	Assessment of the dike surface resistance.....	26
6.2.1	<i>Unlined surfaces</i> .....	26
6.2.2	<i>Lined surfaces</i> .....	27
6.3	Conceptual approach .....	29
7	RELIABILITY ANALYSIS .....	33
7.1	General remarks.....	33
7.2	Qualitative analysis.....	34
7.2.1	<i>Checklists of the problem</i> .....	35
7.2.2	<i>Event tree analysis (ETA)</i> .....	35
7.3	Quantitative analysis.....	38
7.4	Formulation of the problem.....	39

8	Model of dike breaching .....	41
8.1	Conceptual model .....	41
8.2	Mathematical model .....	43
8.3	Numerical model .....	45
8.4	Schematization of the flood wave .....	46
9	PROBABILITY OF DIKE BREACHING DUE TO OVERTOPPING .....	48
9.1	Uncertainty in input parameters .....	48
9.2	Sensitivity analysis .....	48
9.3	Estimation of the probability of dike breaching .....	49
9.4	Latin hypercube sampling (LHS) method .....	49
9.5	Description of the outline algorithm.....	51
10	Case study .....	52
10.1	Description of the studied dike .....	52
10.2	Definition of the flood wave.....	53
10.3	Sensitivity analysis .....	53
10.4	Detailed computational algorithm .....	56
11	FINAL RESULTS.....	62
12	CONCLUSIONS.....	65
12.1	General remarks.....	65
12.2	Discussion.....	66
	REFERENCES .....	68
	NOTATION .....	75
	LIST OF ABBREVIATIONS .....	77
	LIST OF TABLES .....	78
	LIST OF FIGURES.....	79
	PUBLICATIONS OF THE AUTHOR .....	81
	LIST OF APPENDICES .....	82



# 1 INTRODUCTION

## 1.1 General remarks

Constructing dikes or levees began at riversides to protect the urban areas against floods namely to protect people and property against the destructive effects of floods. Therefore, dikes are considered a vital part regarding to the modern flood risk management. Most countries have many dikes in their river and coastal systems and it was estimated that there are several hundreds of thousands of kilometres of dikes in Europe and USA alone (Handbook 2013).

Potentially endangered areas cannot be absolutely protected against floods due to the fact that no dike design has 100 % reliability against the failure. For instance, during a flood event the design flood may be exceeded so the dike will be overtopped and it may consequently fail due to the overtopping incident.

The flood wave induced from the event of dike failure propagates into the floodplain and the area behind the dike. That event may be disastrous and may cause extensive economic damages, environmental disasters and loss of human lives. Therefore, the dike reliability as a research issue is still important topic.

Based on the data concerning historical failures of dikes and dams, causes of the failure may be generally classified as follows (Floods and reservoir safety 1996):

- The loss of stability. This failure can be described as a shearing failure along a sliding surface of the downstream and upstream slope or as a cracking in the dike body due to settlement or landslide. This case is not frequent and the dike failure rarely occurs due to this reason.
- **Dike overtopping** due to exceeding the design flood or dam overtopping due to insufficient spillway capacity. In this case, the failure is resulted from the surface erosion caused by overflowing water. This case is considered the most frequent case.
- Internal erosion. In this case, the failure is due to an extreme and uncontrolled leakage through the dike body or through the sub-base. This leads to increase the permeability of the dike material and to create cavities and erosion canals (piping) in the dike body.
- Failure due to erosion by water flow or due to the effect of wave in the stream.
- Other reasons like sabotage or damage due to war, tree uprooting, activities of burrowing animals or human activities.

## 1.2 Dike failure due to overtopping

As mentioned above, the problem of dike overtopping is one of causes of the dike failure. Depending on statistics for dike and embankment failures, the dike failure due to overtopping represents of about 40% of all embankment dam and dike failures (Jandora and Říha 2008).

Indeed, the fact that no dike design can ensure the absolute protection should be taken into account; since the dikes near the rivers are usually designed depending on a certain degree of protection of the area behind the dikes. When this degree is exceeded the dike overtopping occurs, the likelihood of dike failure rises and the area behind the dike is not protected anymore. For instance, the Morava River dikes (depending on the protection characteristic of the area behind the dikes) ensure protection against flood waves with return period from twenty years to one hundred years (Jandora and Říha 2008).

A statistical research about the dike failure causes in the Morava river basin in the Czech Republic during the period from 1965 to 2004 was carried out by Kadeřábková et al. (2005). Results of that research showed that 64% of dike failures occurred due to overtopping, the relative frequency of the failure due to several causes (Fig. 4.3) per 1 km of the dikes and over a period of 40 years can be expected to fall within an interval between 0.12 and 0.2; and the relative annual frequency of the failure falls into an interval between 0.003 and 0.005. The authors presented the frequency of occurrence of individual failure modes as a percentage of all modes (Fig. 4.4). A similar statistical research was carried out by Glac and Říha (2012) for dike failure causes in the Odra river basin in the Czech Republic during the period from 1960 to 2009. The results showed that 40% of dike failures occurred due to overtopping, the relative frequency of the failure per 1 km of the river dikes and over a period of 49 years equals to 0.26; and the relative annual frequency of the failure equals to 0.0053. The authors presented the frequency of occurrence of individual failure modes as a percentage of all modes (Fig 2.5).

In order to increase the dike safety regarding potential overtopping events, suitable technical measures can be carried out. For example, determining of the place for controlled overtopping and suggesting the suitable structural design of the dike at that place (Jandora and Říha 2008). In the case of an uncontrolled overtopping, it is very important to know and understand mechanism and course of the dike failure in order to draw up emergency plans and warning systems. The mechanism of dam failure due to overtopping (same mechanism in case of dikes) was analysed by several authors, e.g. (Fread 1988), (Singh 1996), (Wahl 1998) and others.

The outcomes of prediction of the dike failure process are used to build the flood control plans. Those flood control plans involve predicting the parameters and the extent of a potential flood and predicting the consequences of a dike failure event such as the resulting values of the water level and its course over time in the area behind the dike (Jandora and Říha 2008).

In the case of dike failure due to overtopping, the size of breach opening channel and the maximum value of breach discharge are the most important output parameters of the dike failure analysis. Those parameters mainly depend on characteristics of the flood wave characteristics, properties of the dike material and geometric characteristics of the dike body.

### 1.3 Terminology

Analysis of the problem of dike breaching usually uses specific procedures and methods varying based on the mechanism proposed to describe the dike failure. Likewise, terminology in the field of dike breaching is not unified. In this chapter, terminology in the dike breaching especially due to overtopping is used.

Terminology mentioned below was derived from valid terminological standards and was discussed by a wider team of experts working in the field of dams and dikes. Some related terms can be found in the relevant literature sources of dam engineering. Other terms are more general and used in other fields.

***Breach*** is a term used to denote the opening channel or erosion channel which formed due to scouring particles of the dike or dam body.

***Breach bottom*** is the highest elevation of the bed of the breach opening channel.

***Breach cross-sectional area*** is the area of water flowing through the breach opening channel.

This area is perpendicular at each point to the flow velocity vector and located at the cross section with the highest breach bottom elevation.

***Breach depth*** is the vertical distance of the breach opening channel measured from the dike crest to the breach bottom.

***Breach discharge*** is the volume of water flowing through the breach opening channel per unit time.

***Breach width at the breach bottom*** is the width of the breach opening channel measured at the breach bottom.

**Breach width at the breach top** is the width of the breach opening channel measured at the dike crest.

**Dike** is a natural or artificial structure used to regulate water levels in the rivers or to protect urban areas against hazards of flood events, called levee in American English.

**Failure** is the ability termination of a structure to perform the desired function. It occurs due to exceeding the threshold values for one or several parameters. Failure may be partial or complete. It is a phenomenon negatively influencing the function of a structure ranging from reduction until termination of its operability. The term of critical failure (fatal, catastrophic) is usually understood as a failure in which the structure is completely discarded or destroyed.

**Overtopping** is the case of water flowing over the dike crest, this phenomenon occurs when the water level in the stream exceeds the dike crest elevation during the flood event.

**Probability** is a way for expressing the knowledge or belief that an event will occur or has occurred. In mathematics this concept has been given an exact meaning in probability theory, it can be defined as a numerical dimensionless quantity characterizing the prediction degree of reliability as it indicates information regarding the occurrence of uncertain future event.

**Reliability** is the feature of a structure consisting of the ability to perform the required functions while retaining the specified values for operating parameters within limits and for a defined time according to the technical conditions. The quantification of reliability is implemented by using a set of reliability indicators which their values quantify the individual reliability parameters. Quantifier of the reliability indicators is the probability of non-failure which is estimated using the probability theory and mathematical statistics.

**Reliability analysis** is a process in which the load and the resistance of a structure are modelled as random variables in order to assess the uncertainty in the outputs, its result is mostly the probability of failure or the reliability index.

**Uncertainty** is a term used to describe the lack of certainty about things, properties or event. The degree of uncertainty can vary from a little lack of certainty to absolute distrust. Uncertainty can be understood in the context of the natural phenomena (the outcome is unknown or unproven) and in the context of the statement credibility (the conclusion is not completely demonstrable or is expressed by uncertain information). In many cases,

the uncertainty can be expressed using the probability. Uncertainty can be divided into two categories:

- *The inherent uncertainty* which we are unable to influence it. It is fully connected with the randomness of the outside world, and it can be spatial or temporal;
- *The uncertainty of knowledge* which comes from the lack of information, the lack of understanding of phenomena or the lack of data and documents from which conclusions are drawn.

***Water depth in the breach*** is the vertical distance of water flowing through the breach and measured from the breach bottom elevation to the water level in the stream.

## 2 AIM AND SUBJECT OF THE WORK

### 2.1 Aim of the work

The main goal of the thesis is to analyse the reliability of flood protection dike by estimating the probability of dike breaching due to overtopping. For this purpose, the method of qualitative and quantitative analysis is used. In terms of the qualitative analysis, the method of event tree analysis (ETA) is used, namely the possible incident scenarios during the progress of dike breaching due to overtopping (Fig. 2.1) are discussed. Then, the subsequent quantitative analysis of that event tree is used in order to achieve the probabilistic estimation of the dike breaching process involving its event scenarios. For the purpose of quantitative analysis, the Latin hypercube sampling (LHS) method is used as a statistical modelling method.

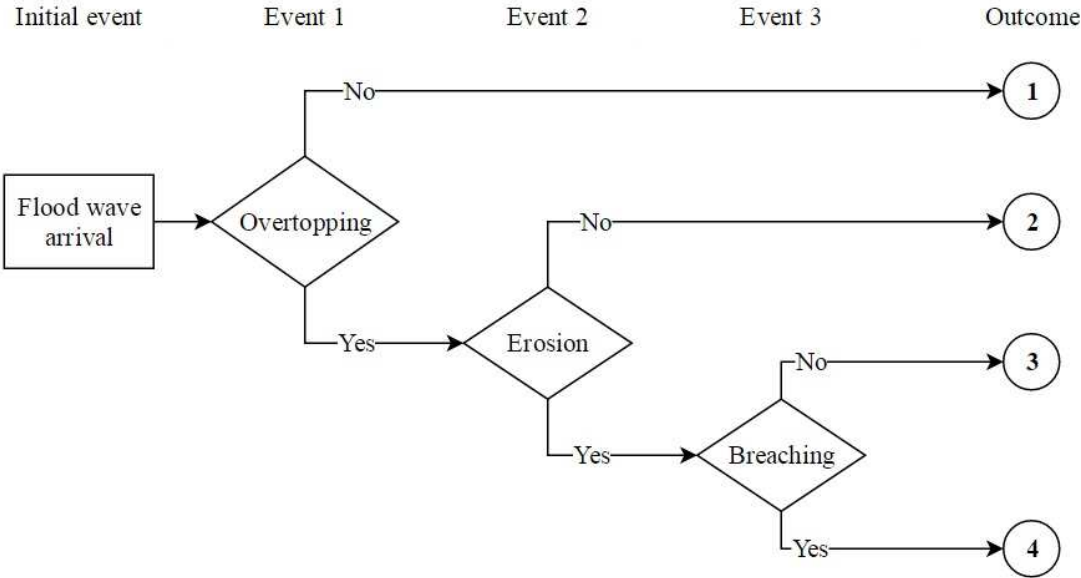


Fig. 2.1 Event tree for dike breaching due to overtopping

### 2.2 Subject of the work

The subjects of this thesis can be summarized as follows:

1. Proposal of a simple mathematical model of dike overtopping.
2. Definition of the resistance of dike material and its surface lining layer on the dike crest and its downstream slope in order to specify the erosion criteria for dike material.
3. Proposal of a simple mathematical model of dike material erosion.
4. Reliability analysis which involves qualitative and quantitative analysis:

4.1. Qualitative analysis includes the following steps:

- Completion of a checklist of the problems of dike breaching due to overtopping and a checklist of possible incident scenarios.
- Discussion of the possible incident scenarios using event tree analysis (ETA).

4.2. Quantitative analysis includes the following steps:

- Sensitivity analysis which means defining all parameters affecting the dike breaching process and then determining the influential and non-influential ones.
- Defining the probability distribution functions of the influential parameters.
- Developing a deterministic model.
- Estimating the probability of dike breaching using Latin Hypercube Sampling (LHS) method.

5. Evaluation of the final results.

According to the mentioned subjects of the thesis, this work contains the following chapters:

- Present state review: this chapter contains a summary of the current state of knowledge in the Czech Republic and abroad about the problem of dam and dike failure due to overtopping. Many references and researches with recognized efficiency and expertise in this field were studied and the list of references used for completion of this thesis was presented.
- Basic definitions and parameters of the problem of dike breaching: this chapter includes a description of time related and dimensional parameters and a citation of some statistical researches of dike breaching performed in the Czech Republic.
- Mechanism of the dike breaching due to overtopping: this chapter involves a description of cause and development of the failure and resistance of dike surface.
- Scour resistance of the dike surface: this chapter presents some procedures used for assessing the dike resistance with lined and unlined surface, and includes the conceptual approach adopted to analyse the process of dike breaching due to overtopping.
- Description of the reliability analysis procedure; involving describing the qualitative and quantitative analysis and formulating the problem.

- Description of the model of dike breaching due to overtopping: this chapter includes the determination of conceptual model, mathematical model and numerical model, and schematization of the flood waves that will be applied to the dike.
- Probability of dike breaching due to overtopping: this chapter contains the definition of uncertainty in input parameters and sensitivity analysis. The chapter also describes the method of estimation of the dike breaching, the use of Latin hypercube sampling (LHS) method and the outline algorithm.
- Case study: this chapter describes the interest locality, the studied dike and the input parameters of flood waves at that locality. The chapter also contains the final results of sensitivity analysis and the detailed computational algorithm.
- Final results of the probability of dike breaching
- Conclusions: this chapter contains general remarks of the work and discussion the final results.



### **3 PRESENT STATE REVIEW**

#### **3.1 Flood protection dikes**

Flood protection dikes belong among the most common structural arrangements that mostly constructed along rivers and waterways to protect urban areas against floods. Reliability of those constructions depends on their structural design and its parameters, compliance of project documentation during the constructing, maintenance works and regular technical and safety surveillance. The main parameters of the dike design are the control and design flow (respectively, the control and design water level in the stream) and elevation of the dike crest above an appropriate water level. Those design parameters are under the influence of the local conditions, the client's requirements and the provided relevant laws.

In accordance with the law and changes of other laws in the Czech Republic [254/2001] which concern the water works, there are constructions for protecting the water works against floods. The protection of those construction is defined in the §58 paragraph of that law. The 471/2001 Sb. announcement defines water works subjected to the Technical-Safety Supervision; in Czech: Technicko bezpečnostní dohled (TBD). Dikes are usually classified into the lowest categories of water works. For designing the dike, the technical standards historically published as branch standards (BS) or Czech national standards (CNS) can be used.

#### **3.2 General publications**

The issue of dike and dam failure due to overtopping in terms of analytical, mathematical and experimental modelling was dealt with numerous authors. A mathematical model for breach growth in sand-dikes and analytical steps of the breach erosion process observed in several laboratory and field experiments were presented by Visser (1988 and 1994). Singh (1996). In his book, the author presented some types of dam failure and causes of the failure; and provided an illustration of the hydraulics of dam breaching, the empirical models with dimensional and dimensionless solution, the mathematical models of dam breaching and comparative evaluation of dam breach models. Jandora and Říha (2008) summarised in their book knowledge about the mechanism of embankment dam failure due to overtopping. Authors analysed particular methods of modelling the breaching process, presented theoretical procedures of breaching and verified those procedures by experimental research and real accidents involving dams and dikes.

Another authors experimentally analysed the problem of dam failure due to overtopping. Chinnarasri et al. (2004) carried out their experimental research in order to propose the correlations between the variables of the embankment breach under falling reservoir level. Results obtained from the failure of real dams or field experiments were also published. Løvoll (2006) assessed the governing breach mechanisms and presented the results of 3 field tests carried out on 6 m high embankment dams in Norway during the period of 2001-2003 and discussed the breach initiation and formation of three different dam types. Alcrudo and Mulet (2007) described the event that led to the breach of the Tous Dam in Spain which broke due to overtopping on October 20th 1982 and displayed the effects of the flood. Goran and Goran (2009) presented the results of hydraulic analysis of the failure of two dams in Croatia with special focus on the first stage of breach formation when water flows through the initial breach and accelerates eroding soil. Gregoretti et al. (2010) conducted their laboratory experiments on the failure of homogeneous dams and they observed three failure types: overtopping, head-cutting and sliding of the downstream dam face. Similar series of embankment breach test due to overtopping were conducted by Pickert et al. (2011) where the authors divided the failure of homogeneous embankments into two breaching phases.

One of the most recent reference source is The International Levee Handbook, CIRIA (2013). This handbook involves a good practise in the management and design of dikes drawing on the skills found across Europe and in the USA. In this reference, the authors provided information about dikes in flood risk management and presented functions, forms and failure of dikes. The authors also addressed the concepts of operation, maintenance, inspection, assessment and risk attribution of dikes and they dealt with other topics as well.

### **3.3 Modelling and simulation for dike and dam failure**

In scope of modelling and simulation for dam failure, several studies and researches focused on development of mathematical and numerical models. Wahl (1997) examined empirical procedures and a numerical model used to predict dam breach parameters and to outline a program for development of an improved numerical model for the simulation for earth embankment dam breach events. Jun and Oh (1998) presented a simulation for dam-break process due to overtopping of the earth embankment and flood routing analysis of downstream reaches using the NWS DAMBRK model which is in good match with eyewitness evidence in terms of the dam crest overtopping and progress of breach formation. Holomek and Říha (2000) presented a comparison of breach modelling methods by applying them to the Slusovice earth

dam. A mathematical and physical model of dike failures due to overtopping was presented by Kratochvil et al. (2000). Other simulations for dam break were presented by Tingsanchali and Chinnarasri (2001) where a one-dimensional numerical model of dam failure due to flow overtopping is developed. In this model, the one-dimensional equations of continuity and momentum for unsteady varied flow over steep bed slopes are solved and the sediment transport equations are considered. The model has been successfully calibrated and verified using laboratory experimental data.

One, two or three dimensional dam breach model are provided by authors. Wang and Bowles (2006) developed the erosion and force equilibrium based three-dimensional dam breach model for the non-cohesive earth dam breach problem; and proposed a finite-difference scheme to simulate the dam breach outflow by solving the two-dimensional shallow water equations. Wang et al. (2006) physically developed a based numerical model to simulate the growth of a breach in an earth or rock-fill embankment due to overtopping. A one and two dimensional numerical dam-break flow model is provided by Galoie and Zenz (2011) where the shallow water equations are solved by means of the Finite Differences Method (FDM).

### **3.4 Experimental researches**

Use of the experimental data to verify and calibrate numerical models was addressed in a lot of articles. Aureli et al. (2000) were carried out their laboratory experiments to verify the numerical model under severe test conditions. Říha and Daněček (2000) compared the results obtained from analytical solution for different shapes of the breach channel with results of experiments carried out in the laboratory. Coleman et al. (2002) presented the experiments results of homogeneous small-amplitude embankments of non-cohesive materials breached by flow overtopping under constant reservoir level conditions. Chinnarasri et al. (2003) investigated the flow patterns and progressive damage of dike overtopping after analysing the data obtained from nine experimental runs and observed four stages in plane dike erosion. Rozov (2013) observed the breach process and flow through the pilot channel located at the embankment centre. Other experimental research performed by Franca and Almeida (2004); where the results obtained from their experimental tests were considered to fulfil the phenomenological aspects and the erosion process from the dam breach was modelled as a function of two erosion parameters and of the breach final geometry dimensions obtained from the experiments. Toledo et al. (2006) presented the results obtained from laboratory tests of rock-fill dam failure by overtopping. A similar experimental study of the embankment dam

breaching has been performed by Dupont et al. (2007) and the laboratory tests enabled to validate and to complete a numerical approach. An overview of the field test and laboratory experiments is given by Morris et al. (2007) under the IMPACT project which addressed the assessment and reduction of risks from extreme flooding caused by natural events or the failure of dams and flood defence structures. An overview on past hydraulic dike breach modelling due to overtopping was presented by and Schmocker and Hager (2009). Authors focussed on scale effects in laboratory dike-breach tests and presented model limitations for dike-breach experiments. A similar survey on laboratory breach tests was provided by Morris (2009). Roger et al. (2009) in their paper were compared the experimental model data (discharges, water level, and depth profiles of horizontal velocities) with numerical computations of dike-break induced flows. Schmocker and Hager (2012) investigated the plane dike-breach process of uniform granular dikes due to overtopping. other experimental research performed by Soares-Frazaio et al. (2012); in this research paper the experiments of two-dimensional dam-break flows over a sand bed were conducted at Université catholique de Louvain, Belgium. Their results were commented upon, in view of evaluating the modelling capabilities and identifying the challenges that may open pathways for further research.

### **3.5 Statistical researches and reference studies**

Review of previous researches, data collection and providing results of statistical researches about dikes and dams failed due to overtopping were presented in some articles. Lemperiere et al. (2006) presented a database of real world case studies of embankment dam failures and summarized the lessons learnt from the dam failures by overtopping to propose a new breach peak outflow empirical formula. In the statistical research carried out by Kadeřábková et al. (2005), an extensive database of historical floods and subsequent failures of dikes in the Morava river basin in the Czech Republic during the period from 1965 to 2004 was completed. Authors presented several causes of the dike failure incident and the frequency of occurrence of individual one was evaluated in percentage terms. A similar statistical research for dike failure causes in the Odra river basin in the Czech Republic during the period from 1960 to 2009 was carried out by Glac and Říha (2012). Wu et al. (2011) provided a review of common cases of earthen embankment breaching and reviewed previous laboratory experiments and field case studies. The authors summarised parametric, simplified physically-based and detailed multidimensional physically-based embankment breach models.

### **3.6 Reliability analysis of dam and dike**

Reliability assessment of dams and dikes (water works) was performed by several authors in the Czech Republic, e.g. (Votruba and Heřman a kol. 1993), (Jandora and Říha 2002), (Jandora and Říha 2008), (Říha a kol. 2008) or (Říha 2010).

In USA, the issue of reliability assessment was addressed by the organisation: United States Army Corps of Engineers (United States Army Corps of Engineers 1999). Wolff (2008) dealt with this topic at Michigan State University. From Asia, papers from Taiwan (Huang et al. 2015) can be cited.

In Europe, reliability of flood protection dikes was mostly addressed in the Netherlands because of the geomorphology of this country. Authors from the Delft University of Technology like Jonkman, van Gelder and Vrijling they dealt with this problem (Jonkman et al. 2002 and 2003). The Dutch Technical Advisory Committee on Flood Defences issued in 1999 the publication titled Technical Report on Sand Boils (Piping) (Calle et al. 1999). French dam Committee recently issued several guidelines (Royet and Peyras 2010), (Royet Peyras 2013) and recommendations (Peyras et al. 2008) dealing with the problems of reliability of dams and limit states. A similar topic was addressed by Farinha et al. (2015) in Portugal.

## **4 BASIC DEFINITIONS AND PARAMETERS OF DIKE BREACHING**

### **4.1 General comments**

The failure due to gradual erosion of the dike body resulting from water overflowing on the dike crest and its downstream slope is referred as the dike breaching due to overtopping. The most significant dike breaching parameters that influence the breaching progress are time related parameters; namely outflow through the breach opening (later referred as breach discharge), velocity and depth of the overflowing water on the dike crest and its downstream slope, shape and size of the breach opening. Those parameters depend on shape and geometry of the dike and on properties of the dike material.

The main parameters controlling the progress of dike breaching due to overtopping have been determined based on the gained experience from studying and analysing real previous events of dams or dikes failure due to overtopping. Those parameters can be classified into the following groups (Jandora and Říha 2008):

- Time related parameters;
- Characteristics of water flowing over the dike and through the breach opening including the maximum value of the breach discharge;
- Characteristics of the breach opening;

Those parameters basically depend on characteristics of the flood wave which causes the dike overtopping in addition the dike geometry and erodibility of the dike material. Values of the dike breaching parameters can be predicted using numerical calculations and some of those parameters may be estimated based on historical observations of dike and dam failures.

### **4.2 Essential parameters in the temporal evolution of dike breaching**

For the purposes of this work, the evolution over time of the dike breaching due to overtopping from the beginning of the flood wave until the complete collapse of the dike was clarified using the following parameters (Fig. 4.1) (Wahl 1998, Jandora and Říha 2008):

- Time of beginning of flood wave  $t = 0$ .
- Duration of flood wave arrival phase is the period during which water level gradually increases in the river and does not exceed the dike crest elevation (no overtopping).

- Time of beginning of overtopping  $t_o$  is the instant when water begins to overflow the dike crest.
- Duration of the resistance phase lasts from the instant of beginning of dike overtopping until the instant of beginning of dike erosion (overtopping – no erosion). Therefore, it represents the period during which the overflowing water on the dike crest and its downstream slope does not cause any erosion of the dike body. This period is attributed to the dike resistance caused by existence of the protective lining layer covering the dike crest and its downstream slope.
- Time of beginning of the dike erosion  $t_e$  is the instant when the load resulting from overflowing water on the dike crest and its downstream slope exceeds the dike resistance.
- Duration of breach initiation phase begins with the first erosion of the dike body on its crest or its downstream slope and ends with the instant of beginning of the dike breaching (erosion – no collapse). During this phase, a gradual backward erosion of the dike body initiates while the dike crest elevation remains constant.
- Time of beginning of the dike breaching  $t_b$  is the instant when the dike crest elevation decreases downward due to the backward erosion of the dike body. From this instant, there is a danger of the immediate dike failure. This danger usually initiates warning signals and the announcement of evacuation in the area downstream of the dike.
- Duration of breach formation phase is the period from the instant of beginning of the dike breaching until the end of the flood wave (collapse). During this phase, the maximum breach size and the maximum breach discharge are reached.
- Time of reaching the maximum breach discharge  $t_{max}$  is the instant when the maximum breach discharge  $Q_{bmax}$  flows through the breach opening. This time ( $t_{max}$ ) usually corresponds to the instant when the maximum breach size is attained.

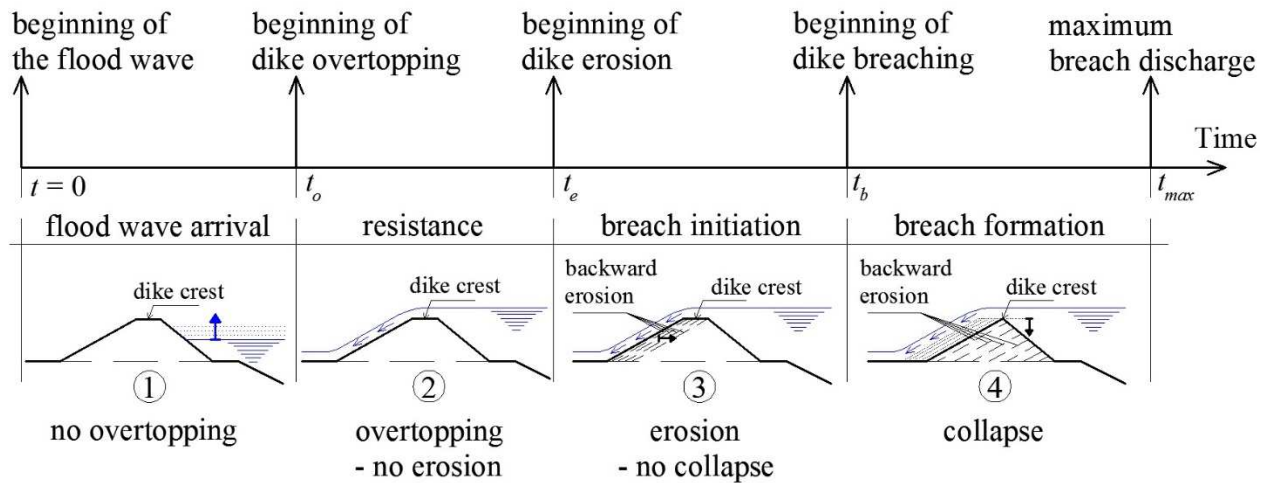


**Fig. 4.1** Time related parameters of the dike breaching due to overtopping

### 4.3 Dimensional parameters

During the dike breaching process, the dimensional parameters of the idealised shape of the breach which are time related parameters and also represent further significant parameters. Those dimensional parameters are the following (Fig. 4.2):

- Breach depth  $h_b$  is the vertical distance measured from the dike crest to the breach bottom.
- Water depth in the breach  $h$  is the vertical distance measured from the breach bottom to the water level in the stream.
- Breach width at the breach top  $b_1$  is the width of breaching channel measured at dike crest.
- Breach width at the breach bottom  $b_2$  is the width of the breaching channel measured at the channel bottom.
- Average breach width  $b$  is the average value of  $b_1$  and  $b_2$ .
- Average breach side slope factor  $s$  expresses the breach side slope angle and specifies the shape of the breach opening (Wahl 1998).
- Breach cross-sectional area  $A_b$  is the area of water flowing through the breaching channel. This area is perpendicular at each point to the velocity vector and located at the cross section A-A' with the highest breach bottom elevation.
- Breach discharge  $Q_b$  is the volume of water flowing through the breach cross-sectional area per unit time.
- Maximum breach discharge  $Q_{bmax}$  is the maximum value of the breach discharge  $Q_b$ .



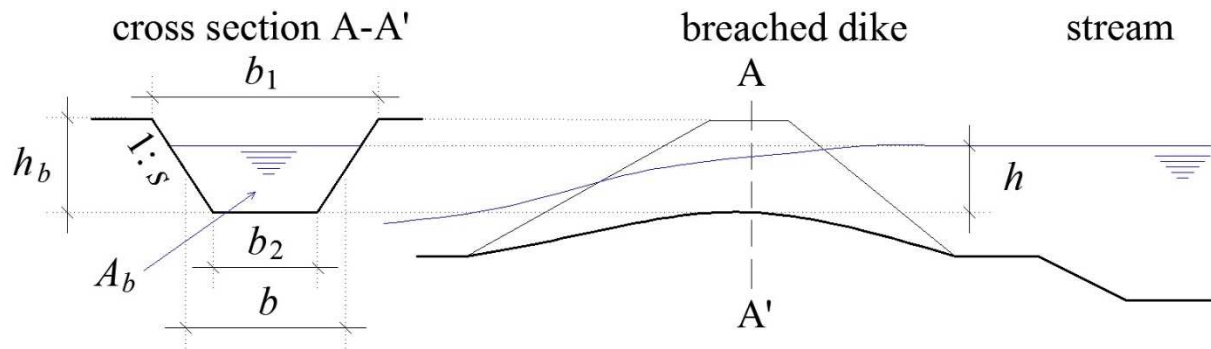


**Fig. 4.2** Dike cross section and idealized trapezoidal shape of the breach opening according to Jandora and Říha (2008)

#### 4.4 Statistics for dike failures

Considering the data of historical failures of dams and dikes, an important realization and recognition that no dike or dam is absolutely safe construction should be taken into account. This fact means that the existence and operation of any dike or dam are linked with a certain risk and that risk must be kept at an acceptable level (Jandora and Říha 2008).

Importance of analysis of the historical dam failures may also be related to analysis of dikes along the rivers. That importance can be clarified by the following utilities obtained from analysis of the historical failures (Jandora and Říha 2008):

- Discovering the errors and mistakes of dike designers or builders;
- Establishing a database and source of knowledge of the failure origin;
- Using those database and knowledge in order to suggest some convenient methods for increasing the safety of both existing dikes and newly constructed ones;
- Specifying the risk extent of the failure of a dike with similar type and similar parameters, using the mathematical statistics and estimating the potential damage;
- Ability for calibrating and verifying the analytical models describing the mechanism of dike failure and the mathematical models assessing the failure parameters;
- Proposing a potential scenario of the dike failure course and predicting the parameters used for drawing up the warning and evacuation plans in the floodplains and areas downstream of the dikes.

Since the failure of flood protection dikes commonly causes wide inundations, great damages and numerous losses, many researches and studies addressed the statistical aspect and data collection of recorded past events of dike failures were performed by several authors and researchers in the Czech Republic. For instance, an extensive database of historical floods and dike failures was completed in the statistical research carried out by Kadeřábková et al. (2005) and in the similar study provided by Glac and Říha (2012). Kadeřábková et al. (2005) carried out the statistics in the Morava river basin during the period from 1965 to 2004. Approximately 1300 km of dikes were assessed. Causes of the failures were classified and the frequency of individual failure modes was evaluated (Fig. 4.3). Four classes of the damage range were classified and the frequency of each class was also specified in percentage terms (Fig. 4.4). Glac and Říha (2012) carried out their statistics in the Odra river basin during the period from 1960 to 2009. Approximately 155 km of dikes were assessed. Causes of the failures were classified and the frequency of individual failure modes was evaluated (Fig. 4.5).

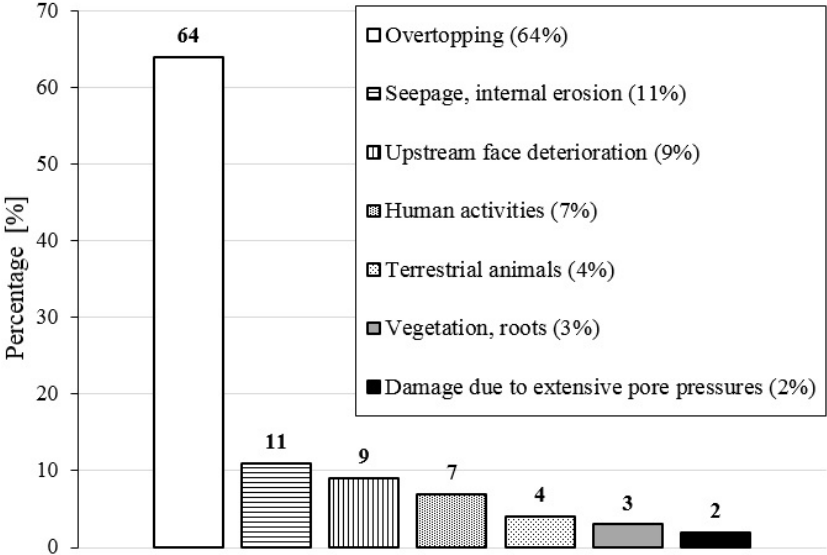


**Fig. 4.3** Occurrence of individual failure modes as a percentage of all modes, for dikes in the Morava river basin during the period from 1965 to 2004 (Kadeřábková et al. 2005)

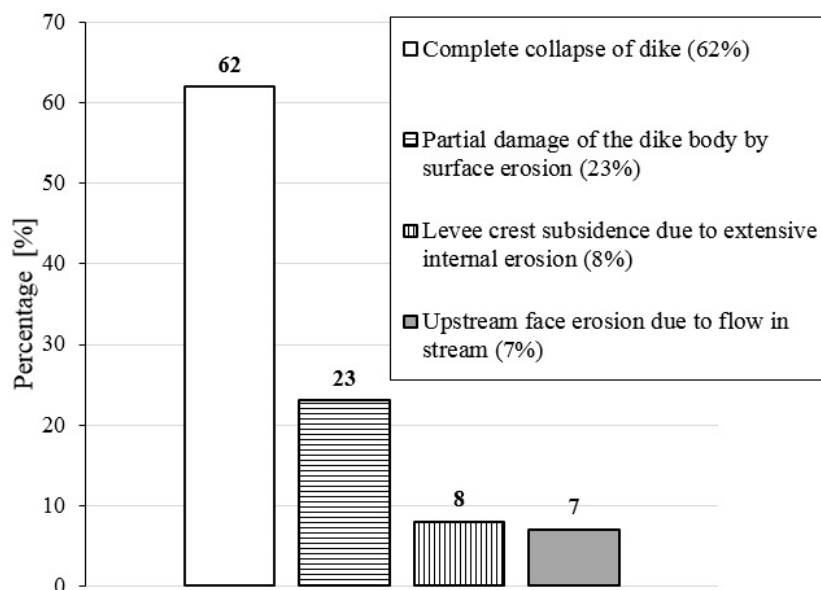


**Fig. 4.4** Percentages by damage type of the extent of dike damage in the Morava river basin during the period from 1965 to 2004 (Kadeřábková et al. 2005)

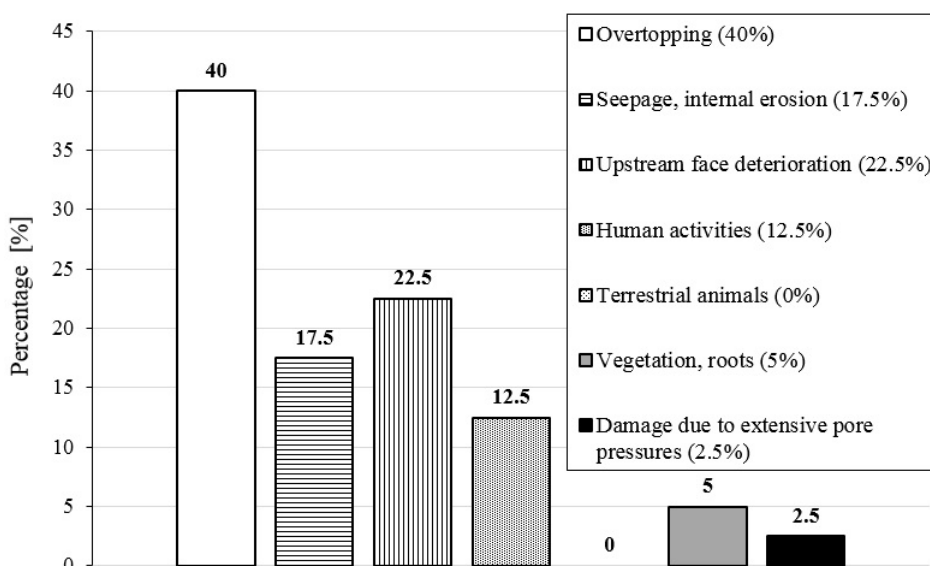


**Fig. 4.5** Occurrence of individual failure modes as a percentage of all modes, for dikes in the Odra river basin during the period from 1960 to 2009 (Glac and Říha 2012)

Based on the statistical researches mentioned above, the dike failure due to overtopping is the most frequent cause of failure in both the Morava river basin and the Odra one in the Czech Republic. Therefore, the dike reliability from the viewpoint of the dike failure due to overtopping is a significant topic.

## 5 MECHANISM OF DIKE BREACHING DUE TO OVERTOPPING

### 5.1 Dike breaching progression

The main reason for the dike breaching due to overtopping is the surface erosion of the material of the dike crest and its downstream slope. During the dike overtopping process, three hydraulic zones in terms of the flow regime may be characterized according to Fig. 5.1 (Powledge et al. 1989):

- The 1<sup>st</sup> zone is situated above the dike crest in the subcritical flow region. The flow regime in this zone is influenced by the cross section of the dike crest (regarding the width, shape of the downstream edge and the cross-sectional slope) and by the material covered the dike crest (vegetation, asphalt, etc.).
- The 2<sup>nd</sup> zone is situated above the dike crest close to the intersection line between the dike crest and the downstream slope. This zone reflects the critical regime of the flow where the flow velocity and shear stress are higher and the energy slope is steeper in this region.
- The 3<sup>rd</sup> zone is situated in the region of the rapid (supercritical) flow on the downstream slope of the dike. The flow accelerates until reaching approximately uniform flow conditions. Sheer stress and flow velocity are quite high and when they exceed critical values defining the dike resistance so the erosion initiates and then quickly accelerates.

The dike breaching due to overtopping usually occurs in the final stage taking into consideration that some characteristic stages during the breaching development can be distinguished. Form the instant of beginning of overtopping, the following stages are typical:

1. Surface of the downstream slope of the dike resists for some time the erosion load caused by the overflowing water on the dike crest and its downstream slope. Characteristics of the erosion load are essentially related to the breach discharge per unit length of the dike crest and further they are influenced by the downstream slope, the protective lining layer covering the downstream slope (e.g. the type of vegetation) and the downstream slope uniformity. The erosion load can be characterized using shear stress, flow velocity or other parameters of the overflowing water.
2. When the characteristics of the erosion load exceed critical values defining the resistance of the dike crest and its downstream slope against the surface erosion, the breach formation

initiates due to a gradual local erosion and the subsequent flow concentration. Progression of the dike breaching substantially depends on the dike shape, properties of the dike material and the existence and arrangement of the element of protective lining layer.

3. With continuation of the dike overtopping process, a relatively slow gradual scouring due to backward erosion of the dike crest and its downstream slope occurs. During this stage and while the backward erosion does not reach the upstream edge of the dike crest, a relatively small magnitude of the dike material is washed away therefore the potential significant increase of the breach discharge does not occur. If the water level in the stream drops down, the breach discharge may considerably decrease and the erosion may stop.
4. When the backward erosion of the dike material reaches the upstream edge of the dike crest, elevation of the dike crest downward decreases and the significant breach discharge is expected to occur. During this stage, the breaching process is characterised by an increase in the breach opening size (Fig. 5.2) where a significant downward erosion and a considerable lateral widening occur, i.e. a considerable amount of the dike material is washed away. Since the increase of the breach discharge results in an increase of the erosion intensity, this stage is considered the most critical one during the dike breaching progression. At the end of this stage, the elevation of the breach bottom reaches the elevation of the downstream terrain (Fig. 5.2) and the breach opening reaches its maximum size.

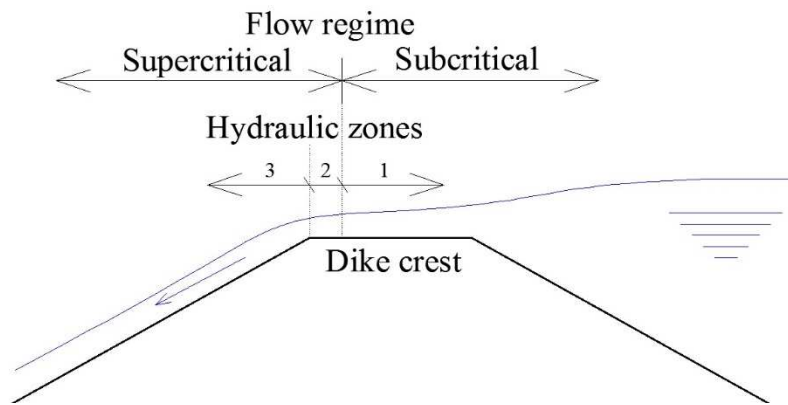


**Fig. 5.1** Flow and erosion regimes during dike overtopping (Powledge et al. 1989)

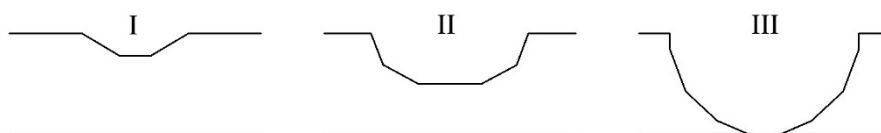


**Fig. 5.2** Diagram depicting dike breaching due to overtopping

## 5.2 Homogeneous dike breaching due to overtopping

As mentioned before, the breach formation due to local erosion starts when parameters of the erosion load exceed critical values specifying the resistance of the dike crest and its downstream slope against the surface erosion caused by the overflowing water.

In the case of homogeneous dikes, shear stress and flow velocity are the most common parameters defining the erosion load. The critical shear stress and the non-scouring velocity are the corresponding parameters defining the resistance of dike material against the erosion process.

Comparison between the flow shear stress (erosion load) and the critical shear stress (resistance against erosion) as adopted analytical method for dam breach modelling can be used (according to some authors' conclusions) only in the case of embankments without a cohesive core or in the case of dams built from homogeneous cohesive material (Jandora and Říha 2008). The same conclusion can be extended for the comparison between the flow velocity and the non-scouring velocity.

In case of homogeneous dikes and with progression of breaching due to overtopping, the breach discharge increases outwards in the perpendicular direction to the dike's axis. During the gradual backward erosion of the dike body, slope of the downstream face remains approximately identical with the initial slope (Fig. 5.3).

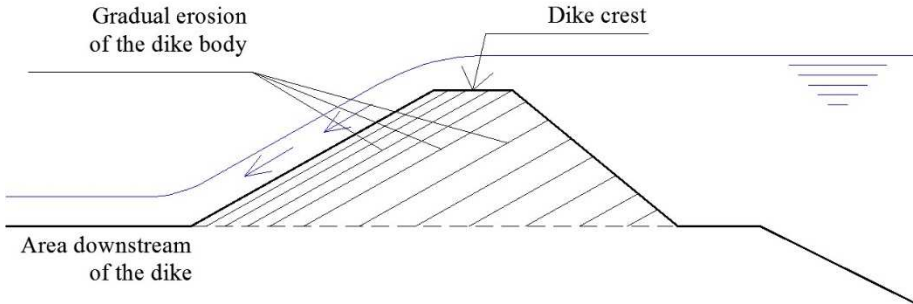


**Fig. 5.3** Diagram of progress of a homogeneous sandy dike failure (Fread 1988)

## 6 Scour resistance of the dike surface

### 6.1 Introduction

The problem of dike overtopping during flood events becomes more dangerous when the protective lining layer (probably exists) covering the dike crest and its downstream slope initiates to be scoured; and subsequently dike material of the crest and the downstream slope starts to be eroded. In case when the dike crest and its downstream slope are protected by a protective lining layer (riprap or grass layer), erosion of the dike material starts after the protective lining layer is damaged. In other words, erosion and transport of soil particles start when the erosion load induced by the overflowing water exceeds a critical value expressing the resistance of the protective lining layer and the dike material respectively.

Scour resistance of the lining layer and of the dike material against the erosion load induced by the overflowing water is one of the most significant characteristics affecting the dike safety during flood events. Therefore, parameters defining the scour resistance of the lining layer or the dike material have been the subject of several investigations since the beginning of the 20<sup>th</sup> century.

The scour resistance is usually defined by the critical value of either shear stress, flow velocity, Froude number or flow rate (usually specific discharge) (Linford and Saunders 1967, Hartung and Scheuerlein 1970, Knauss 1979, Clopper and Chen 1987, Hanson et al. 1999, Říha et al. 2009, Jandora and Špano 2011). The critical value of each variable (shear stress, flow velocity, Froude number, specific discharge) can be defined as the maximum value which does not cause particle movement yet (Jandora and Špano 2011). For determining those critical values, several authors proposed empirical formulae based on the laboratory and field measurements. For example, the resistance of various materials against water flow-induced scouring is summarized within (Floods and reservoir safety 1996). The final results of a research regarding the resistance of grass protective layers were also published within (Hanson et al. 1999). In case of rock-fill dams or riprap protection, Knauss (1979) addressed the critical specific discharge as a function of the bottom slope and the effective stones diameter, and he also took into account the construction process, particularly whether the protective layer is formed by free laid stones or by hand-placed stones. Some technical measures used for the enhancement of dam protection against overtopping were summarized within (Říha et al. 2009).

## 6.2 Assessment of the dike surface resistance

### 6.2.1 Unlined surfaces

In the traditional literature sources, the critical shear stress  $\tau_{cr}$  and the non-scouring velocity  $v_{non}$  were widely used in order to define the scour resistance of dike material in case of unlined surface. Several authors were carried out their experimental researches for deriving empirical relations predicting those critical values (Alhasan et al. 2013):

- 1. Some empirical equations predicting the critical shear stress for unlined surfaces:** A simple formula of critical shear stress related to water density and effective grain size was developed by Krey (1935). Kramer (1935) proposed the critical shear stress as a function of water density, effective grain size, density of sediment and homogeneity modulus. Schoklitsch (1952) took into account the influence of the shape factor instead of homogeneity modulus. Shields (1936) expressed the critical shear stress by means of the so-called Shields parameter  $\theta$  which is a function of the Reynolds number of sediments.
- 2. Some empirical equations determining the non-scouring velocity for unlined surfaces:** Mavis et al. (1935) developed a relation for determining the non-scouring velocity as a function of water density, density of sediments and effective grain size. Levi (1948) derived equations for cases of uniformly graded materials, gravel-sand mixtures and fine-grained soils. Gončarov (1954) derived his relations from the condition of balance between the pressure force of static moment and the dead moment force of particles for cases of effective grain size ranges from 0.1 mm to 1.5 mm and then from 1.5 mm to 20 mm. Neil (1967) derived his equation related to effective grain size and water depth within the conditions that effective grain size is  $> 3$  mm and the rate (effective grain size/water depth) ranges from 0.01 to 0.5. Šamov (1959) developed a simple relation of non-scouring velocity related to effective grain size and water depth. The frequently used equation related to water and sediments density, effective grain size and Chézy discharge coefficient was developed by Meyer-Peter (1948).

In the above-mentioned references, all relations expressing the critical shear stress or the non-scouring velocity are related to open channels. In these cases, relatively mild channels slopes were addressed and granular sediment materials with grain size rarely exceeds 100 mm were studied (Alhasan et al. 2013).



### 6.2.2 Lined surfaces

In case of dam or dike surface protected by lining layer, several researches for estimating the scour resistance of the lining materials on steeper slopes were focused on surfaces protected by grass or granular materials.

Numerous authors were carried out their experimental researches with physically modelled dam or dike in order to develop empirical relations defining the resistance of lining materials on the downstream slope using the common variables of critical shear stress  $\tau_{cr}$ , non-scouring velocity  $v_{non}$ , critical specific discharge  $q_{cr}$  or critical Froude number.

Within the framework of the research performed by Linford and Saunders (1967), the authors proposed the critical shear stress for the rock fill as a function of water and sediments density, effective rock diameter and the packing (compaction) factor which considers the case of well compacted or manually packed rock fill and the case of naturally packed rock fill. Hartung and Scheuerlein (1970) expressed the flow velocity of overflowing water as a function of water depth, slope gradient, effective grain size and flow aeration. For comparing the calculated flow velocity with a critical value, the authors defined the non-scouring velocity related to water and sediments density, effective grain size, angle of internal friction of the surface layer material, the slope angle and the degree of flow aeration.

For dams or dikes with rock fill shoulders or lining, Knauss (1979) proposed relations defining the critical specific discharges for the exposed downstream slopes. He developed his relations for effective stone sizes equal 0.50 m, 0.75 m and 1.0 m (the approximate corresponding weights of stones were 1.75 kN, 5.85 kN and 13.85 kN), and for combination of its placing methods (manual or natural packing). The final results obtained from that experimental research were summarized in Fig. 6.1.

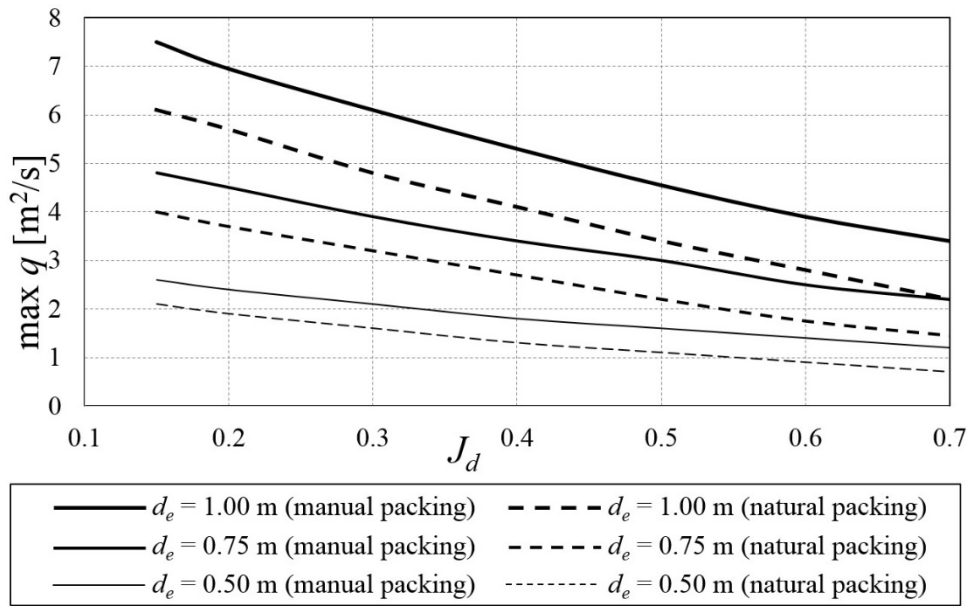


**Fig. 6.1** Critical specific discharge for downstream rock fill lining (Knauss 1979)

For assessing the resistance against erosion load for particular types of dam or dike protective lining layer using the non-scouring velocity (the limiting velocity according to Floods and reservoir safety 1996), the graphs presented in Fig. 6.2 can be used. The non-scouring velocity was defined as a function of the overflow duration, namely in the case of non-rigid materials (grass, meshes, mats, etc.).

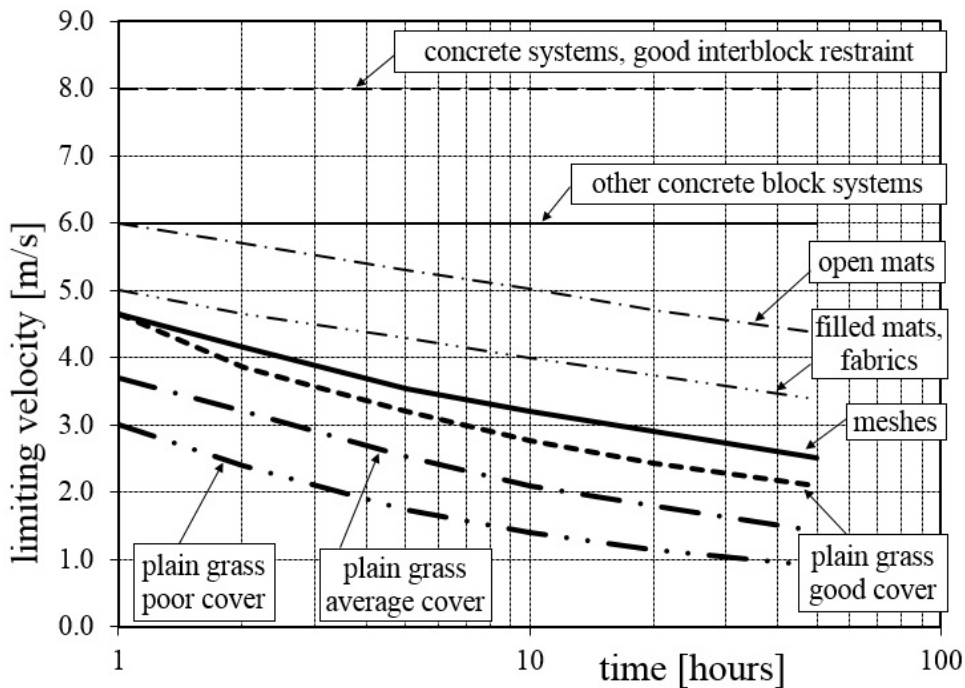


**Fig. 6.2** Non-scouring velocity for selected types of surfaces as a function of overflowing time (Floods and reservoir safety 1996)

The results of extensive research for assessing the resistance of grass cover were published within (Hanson et al. 1999). The non-scouring velocities and the critical shear stress for grass covers of different quality were summarized in Table 6.1.

**Table 6.1** Allowable critical shear stress and non-scouring velocities for grass cover (Hanson et al. 1999)

Grass cover quality	Critical shear Stress [Pa]	Non-scouring velocity [m/s]	
		Erosion-resistant soils	Easily eroded soils
dense, uniform, well developed and maintained grass carpet with well rooted turf	177	1.8	1.2
dense, uniform, well maintained grass carpet	101	1.5	0.9
grass mixture, less dense grass carpet *)	48	1.2	0.9
thin grass cover with an irregular surface **)	29	1.1	0.8
temporary grass cover, one year-old grass **)	18	1.1	0.8

\*) Unsuitable for overflowed slopes of a slope gradient larger than 10 %.

\*\*\*) Unsuitable for overflowed slopes of a slope gradient larger than 5 %.

An experimental research for estimating the resistance of some types of structural protection (such as riprap and placed stones) was carried out by Říha et al. (2009) and completed by (Jandora and Špano 2011). Those types of structural protection were tested on physical model with three downstream slopes (1:2, 1:3 and 1:4) and with combination of three riprap stone sizes. The authors carried out a cross comparison of the results via Froude number related to the critical specific discharge, water and sediments density and the effective stone diameter. Jandora and Špano (2011) indicated several limits of the lining movements like the first movement of individual stones, movement of the mass of stones and total destruction of the lining. Those limits corresponding to individual tested material (in terms of critical specific discharge for each movement limit) were determined and expressed via critical Froude number corresponding to individual downstream slope, material and movement limit. Final results of this research were compared with results presented by Knauss (1979) (Jandora and Špano 2011).

### 6.3 Conceptual approach

The problem of dike breaching due to overtopping is a complex problem. The progress of the dike breaching and its parameters can be better understood by analysing the mechanism of the dike breaching due to overtopping and distinguishing the fundamental stages and the sequential events of the breaching course.

The main cause of dike breaching due to overtopping is the problem of surface erosion of the dike material induced by overflowing water on the dike crest and its downstream slope. Therefore, the dike breaching can be divided into two processes: the overtopping process (first stage) and the erosion process (second stage). Depending on more detailed analysis, the dike breaching process due to overtopping can be analysed and divided into its sequential events, allowing the following typical phases to be distinguished (Figures 4.1 and 6.3) (Singh 1996):

1. Flood wave arrival (no overtopping) (Fig. 6.4): due to the flood event, water level in the river gradually increases but does not exceed the dike crest elevation.
2. Resistance (overtopping - no erosion) (Fig. 6.5): the dike material or the protective layer on the downstream slope resists the overflow for some time. The resistance mainly depends on the overflow velocity, the dike material and the protective layer situated on the downstream slope.
3. Breach initiation (erosion - no collapse) (Fig. 6.6): gradual breach formation at the downstream slope and dike crest is initiated due to local erosion when the non-scouring velocity of the downstream slope material is exceeded. In this phase, a small portion of the dike material from the downstream slope and the dike crest will be breached. This phase represents the duration from the beginning of the downstream erosion until the upstream slope is reached. In this phase, the breach bottom elevation approximately remains equal to the dike crest elevation.
4. Breach formation (dike collapse) (Fig. 6.7): this phase represents the breaching of the dike due to backward erosion of the upstream slope. Usually when the backward erosion reaches the upstream slope, a rapid increase in the discharge through the breach initiates, which causes more intensive erosion of the upstream slope. During this phase, it is noticeable that there is a significant lateral widening of the breach opening and that a considerable amount of the dike material is being flashed away. The elevation of the breach bottom may reach the terrain elevation of the area downstream of the dike, and the lateral widening continues until the end of the flood event.

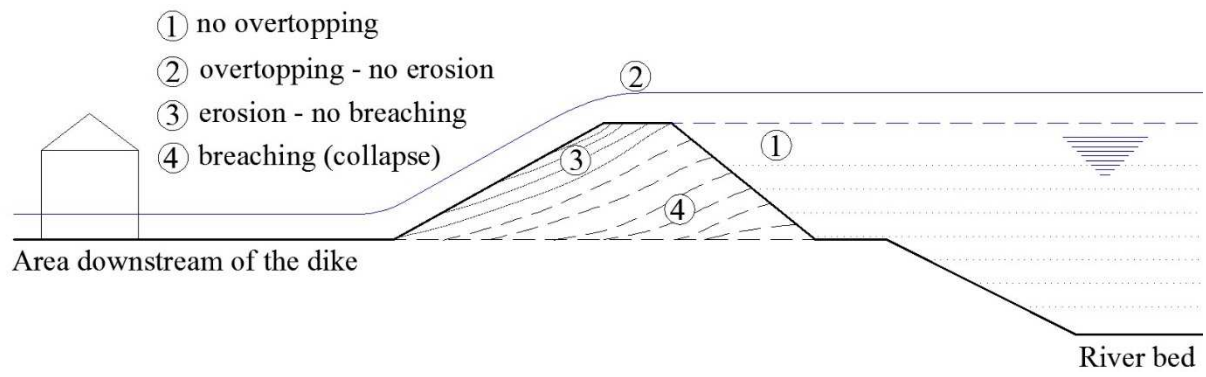


**Fig. 6.3** Diagram of the failure of a dike due to overtopping



**Fig. 6.4** First phase: no overtopping



**Fig. 6.5** Second phase: overtopping - no erosion



**Fig. 6.6** Third phase: erosion - no collapse



**Fig. 6.7** Fourth phase: dike collapse

## **7 RELIABILITY ANALYSIS**

### **7.1 General remarks**

During the design of engineering structures, the deterministic approach as a general rule is commonly used. The deterministic approach is usually derived depending on requirements of the technical standards, theory of limit states and on the results of the statistical analysis of load and physical properties of materials. In this case, destruction caused by failure or loss of stability of structures designed to fulfil the prescribed technology and maintenance does not occur with large extent to endanger lives of people. This approach can be assumed with high probability for simple designs.

In the case of complex technical systems (telecommunications, computer, energy, space, etc.), the involvement of a large number of reliable elements in complex systems does not necessarily create a reliable system. Those complex and highly sophisticated systems require new approaches for analysing their reliability and safety and for designing a safe, functionally reliable and economically satisfactory system. Therefore, methods of reliability analysis have been gradually developed. Those methods enable through the stage of project preparation to investigate variants of the proposed system in terms of its reliability and hence its safety. By applying the methods of reliability analysis, the proposed system will be with high probability reliable and will fulfil the specified function throughout its planned lifetime under specified operational and technical conditions.

Consequently, the reliability as a general feature can be defined as the ability of a system to consistently perform its required function with maintaining the values of specified operational parameters within given limits according to specified technical conditions. The reliability quantifier is the probability of accomplishing the desired function. Basic procedures for testing complex systems are described below in this Chapter, see 7.2 and 7.3.

Indeed, the reliability is often associated with the safety. From the point of view of mathematical analysis, reliability and safety are similar issues; but from the technical point of view they are considered different and often contradictory characteristics. Requirements for safety are usually addressed by the well-timed removal or renewal of an equipment if its failure due to further operation is suspected. For example, duplication of the bottom outlet valve (two valves on one bottom outlet) increases the safety of the equipment but reduces its reliability.

This is due to the fact that, the reliability of this bottom outlet is determined by the proper operation of two valves instead of one. The cost for higher safety is thus a higher probability of failure (failure probability of both valves should be summed because of their series connection).

## 7.2 Qualitative analysis

Qualitative analysis is considered the first step of the reliability analysis for any system. Since the qualitative analysis is an initial analysis to get general understanding of the reasons related to any problem, so it is very important entry for suggesting and developing ideas for the quantitative analysis.

The qualitative analysis aims to identify the weakest elements of the system and accordingly to identify the possible modes of the system failure. The first step of the qualitative analysis is defining the relationships connecting the elements of the evaluated system, their vulnerability and the possible consequences of their failure. This enables to build the various event scenarios that will be analysed by further methods such as the event tree analysis or the fault tree analysis. Those methods are verbal and largely dependent on the experience of the researcher.

In the qualitative analysis of any system we proceed as follows (Říha a kol. 2005):

- 1 Definition of the system.
- 2 Compilation of the checklists:
  - Checklist of the system elements.
  - Checklist of the event scenarios.
- 3 Compilation of diagrams of the system elements.
- 4 Compilation of the failure modes.
- 5 Analysis using one of the following methods:
  - Failure Modes and Effect Analysis (FMEA).
  - Fault Tree Analysis (FTA).
  - Event Tree Analysis (ETA).

In order to analyse the problem of dike breaching due to overtopping, the method of event tree analysis (ETA) will be further used because it can be considered the most appropriate method for analysing this problem.



### **7.2.1 Checklists of the problem**

**A.** Checklist of the problem of dike breaching due to overtopping includes the following elements:

- 1- Flood wave characteristics: involve the parameters like peak discharge, duration of the flood wave and the corresponding water level in the stream.
- 2- Overtopping characteristics: involve the initial overtopping width, flow discharge, water depth at the downstream slope and flow velocity.
- 3- Erosion characteristics: involve the non-scouring velocity which represents the resistance of the lining layer on the downstream slope, and the erodibility parameters of the dike material.

**B.** Checklist of the event scenarios of this problem consists of the following typical phases described in Chapter 6, see 6.3:

- 1- First phase: Flood wave arrival (no overtopping).
- 2- Second phase: Resistance (overtopping – no erosion).
- 3- Third phase: Breach initiation (erosion – no breaching).
- 4- Fourth phase: Breach formation (breaching - dike collapse).

### **7.2.2 Event tree analysis (ETA)**

Event tree analysis (ETA) is a logical modelling technique investigates the system responses through a single initial event in order to assess probabilities of the consequences (for both success and failure of the system) by analysing the total system (Clemens et al. 1998).

Objectives and results of the event tree analysis can be summarized as follows:

- Determining various possible event scenarios and the system conditions resulting from the initial events.
- Identifying the favourable condition of the system, which means that the elements of the system perform their functions (functional elements result in success of the system).
- Identifying the unfavourable condition of the system, which means that one of the elements is not functional and results in failure of the system.
- Classifying the different modes of system failure according to the event scenarios.

- Determining the probability of individual event scenario, which leads to the favourable (success) or unfavourable (failure) condition of the system.

Event tree of the problem of dike breaching due to overtopping is plotted in Fig. 7.2 where the possible event scenarios are presented. Conditions, phases and related parameters of the problem of dike breaching due to overtopping are plotted in Fig. 7.1.

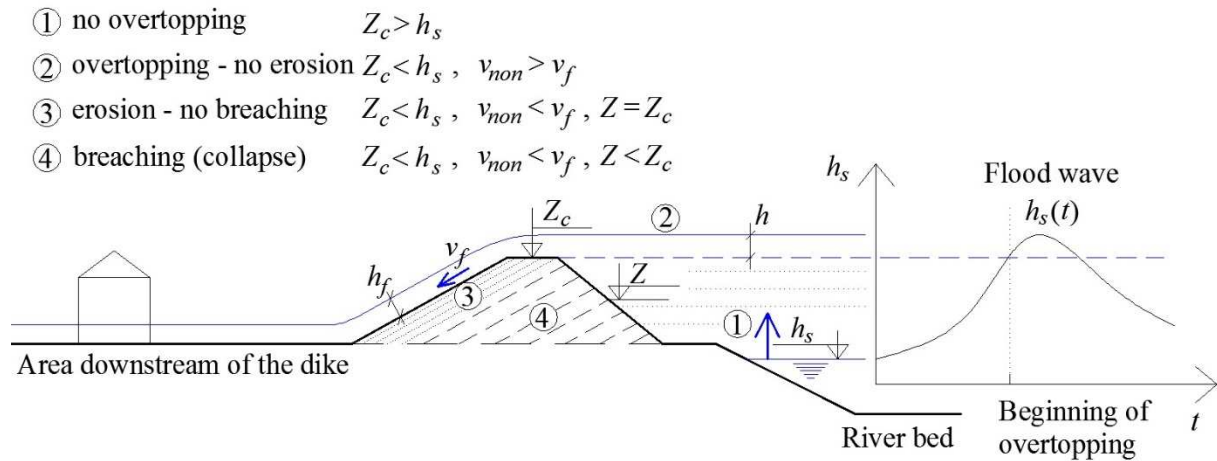


**Fig. 7.1** Schematic diagram of the events during the process of dike breaching due to overtopping

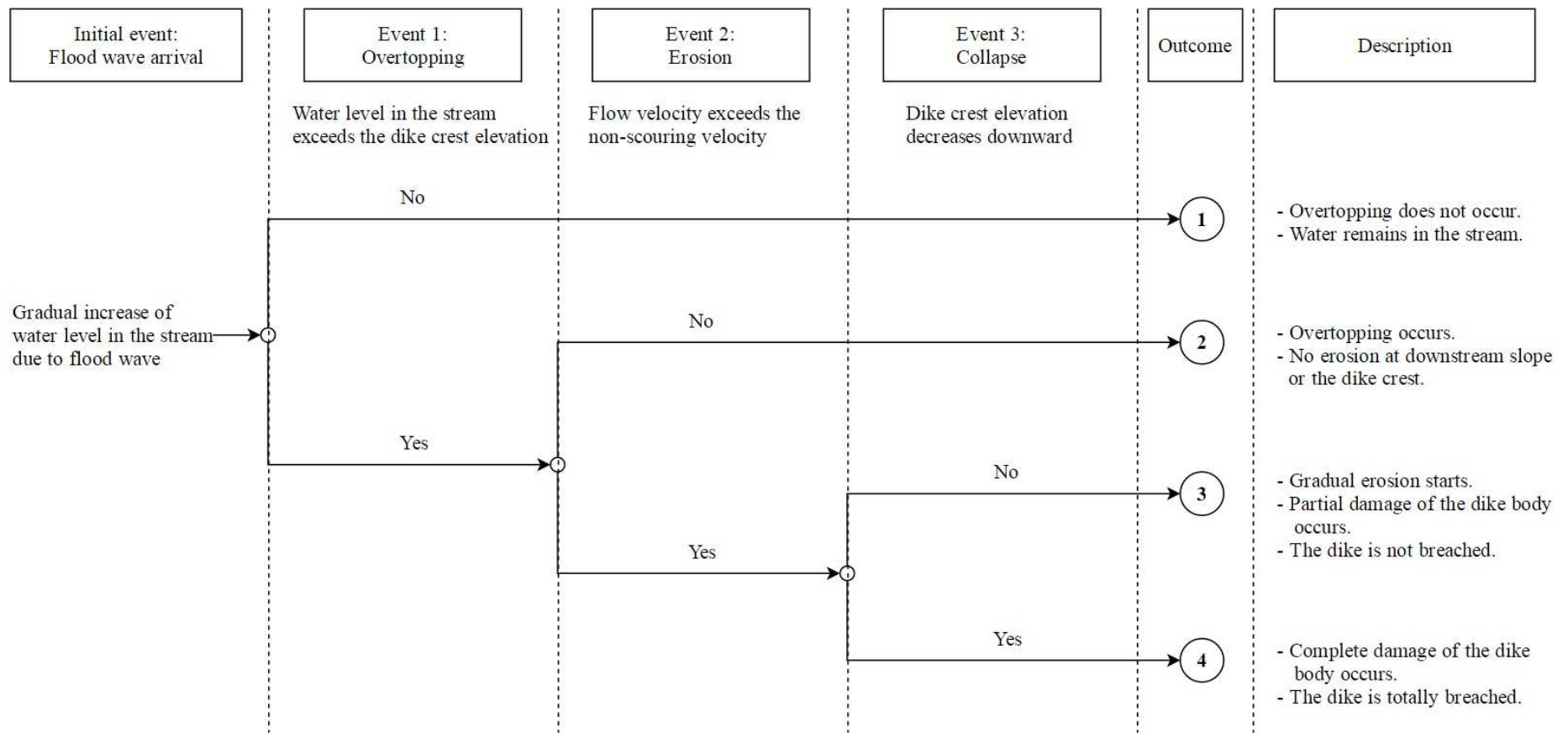


**Fig. 7.2** Event tree of the process of dike breaching due to overtopping

### 7.3 Quantitative analysis

The quantitative analysis is the next step after the qualitative analysis in the reliability assessment. The quantitative analysis aims to quantify the problem (depending on outcomes of the qualitative analysis) by generating numerical data can be used in the mathematical and statistical modelling methods. All event scenarios or some required ones identified by ETA (Fig. 7.2) obtained by the qualitative analysis can be further quantitatively analysed using an appropriate mathematical and statistical modelling method. Latin hypercube sampling (LHS) method was adopted for the purpose of this thesis.

The main objective of the quantitative analysis within this thesis is to estimate the probability of each outcome obtained from individual event scenario. For this purpose, the probability of each event investigated using the ETA method (Fig. 7.2) will be firstly estimated and then the reliability of the entire system (the dike) will be estimated based on the probability of individual event scenario. For instance, the probability  $P_B$  of dike breaching due to overtopping will be estimated based on the probability  $P_F$  of arrival of the corresponding flood wave, the probability  $P_O$  of dike overtopping and the probability  $P_E$  of dike erosion (Fig. 7.3).

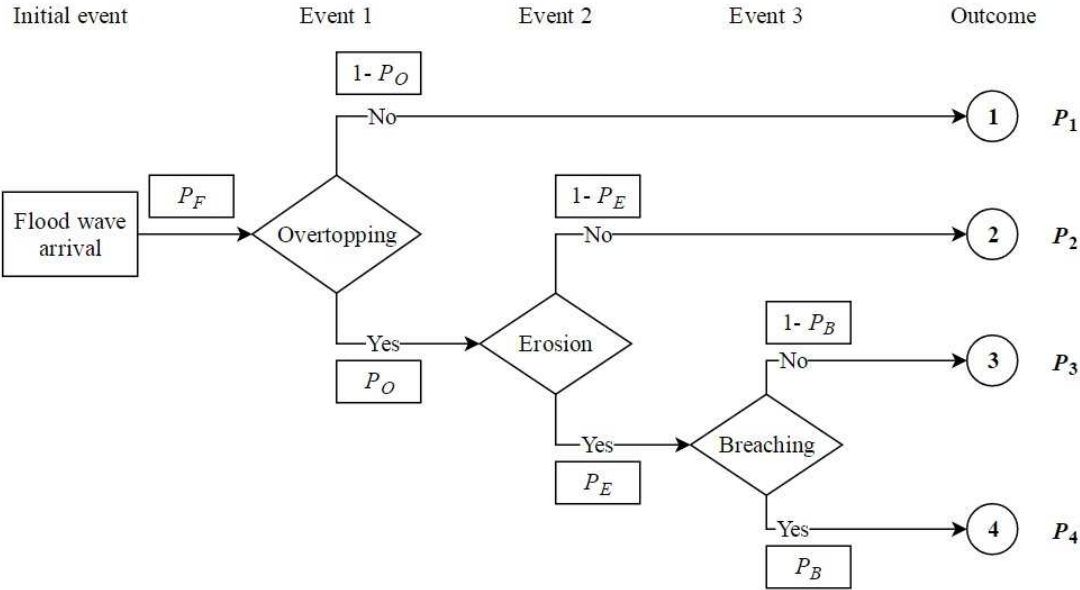


**Fig. 7.3** Event tree for estimating the probability of dike breaching due to overtopping

According to what mentioned above, parameters affecting those events in Fig. 7.3 (flood wave arrival, overtopping, erosion and breaching) should be considered random variables and their probability distributions should be specified. Therefore, the quantitative analysis requires a large number of statistical input data obtained using the LHS method.

## 7.4 Formulation of the problem

Failure (breaching) of the dike can be defined as the termination of the dike ability to perform its desired function when the value of one parameter (or several parameters) exceeds its critical value. Further, the consequent damage will be partial or complete.

Therefore, the dike reliability  $R$  can be defined as the probability that the dike strength  $S$  (or resistance) is equal to or larger than the load  $L$  applied to the dike (Fig. 7.4). This definition can be expressed as follows:

$$R = P(S \geq L) = P(S - L \geq 0) \quad (7.1)$$

Conversely, the dike failure  $F$  can be generally expressed as follows:

$$F = 1 - R = 1 - P(S \geq L) = P(S < L) \quad (7.2)$$

For the purpose of probabilistic solution, a sufficient number of simulations should be performed (Fig. 7.4). The quantities  $S$  and  $L$  will be considered random variables and their values will be randomly determined using a random sampling method (LHS) taking into consideration the probability distribution of each variable. Subsequently the probability  $P_i$  (Fig. 7.3) of each outcome obtained from individual event scenario investigated using the ETA method can be simply estimated by the frequency analysis as follows:

$$P_i = \frac{M_i}{N_{total}} \quad (7.3)$$

where  $M_i$  is the number of simulations realizing the outcome ( $i$ ) (Fig. 7.3) and  $N_{total}$  is the total number of simulations.

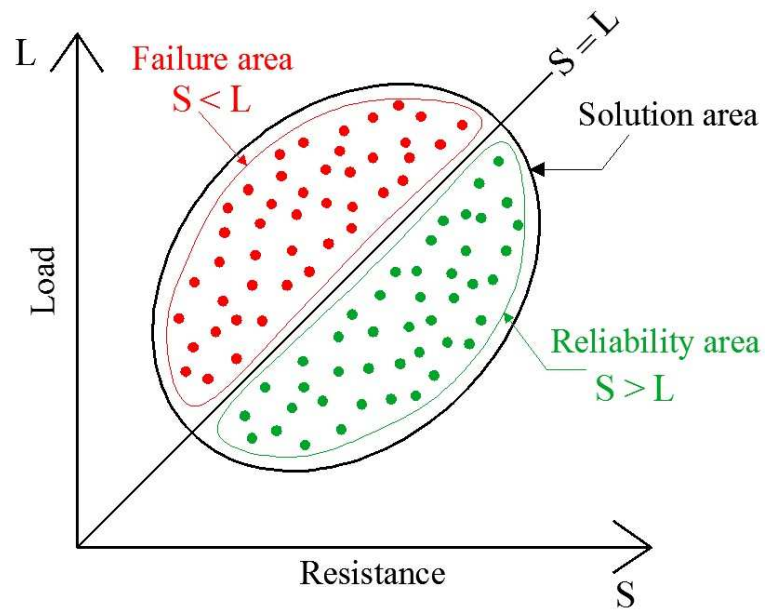


**Fig. 7.4** Definition of the reliability and the failure of a dike according to equations (7.1 and 7.2)

## 8 Model of dike breaching

The problem of dike breaching due to overtopping was addressed by several authors in order to propose mathematical models describing the breaching process and predicting its parameters. Generally, the more detailed analysis of the dike breaching mechanism produces more complex and sophisticated model involving more important parameters.

From the practical side, parameters defining the resistance of dike material or its protective layer against erosion load induced by water overflowing on the dike crest and its downstream slope; and erodibility parameters describing the subsequent erosion process are considered the most important parameters in the suggested models. For the purposes of this thesis, resistance of the dike material and its protective layer on the downstream slope is estimated by comparing the overflowing velocity at the downstream slope with the limit cross-sectional velocity known as non-scouring velocity (Fig. 6.2). Erodibility parameters expressing vertical (deepening) and horizontal (widening) progress of the erosion process are derived from real incidents of dams and dikes breached due to overtopping recorded in the past.

### 8.1 Conceptual model

The problem of dike breaching due to overtopping is a complex problem involving hydraulic and erosion transport phenomena. In this work, the dike breaching problem was divided into the process of dike overtopping followed by the process of gradual erosion of the dike material. During both overtopping and erosion, the hydraulic and erosion phenomena are complex three-dimensional processes that involve extremely turbulent three-dimensional flow comprising a mixture of water, air and soil, all with different densities. This fact creates theoretical and mathematical difficulties when solving practical problems. Therefore, the following extensive simplifications were taken into account when proposing the mathematical model:

- Water flow along the downstream slope is approximated by quasi-steady flow (Singh 1996).
- The 3D process of dike breaching is approximated by a 1D model.
- The breaching starts at the lowest point of the dike crest where the first overtopping occurs.
- The overtopping width along the dike crest is suggested as an initial value ( $b_0$ ) (Fig. 8.1). This value remains constant during the dike overtopping until the erosion starts.

- The resistance against surface erosion is evaluated with respect to the velocity of water flowing at the downstream slope. The limit cross-sectional velocity (Fig. 6.2) is used for this evaluation.
- Parallel gradual backward erosion of the downstream slope is assumed, as is shown in the diagram in Fig. 5.3 (Fread 1988).
- The shape of the breach opening is approximated by a rectangle (Fig. 8.1). Dike erosion progress is in both the downward and lateral direction. During the erosion, the bottom of the breach opening remains horizontal and the sides remain vertical.

Field and also laboratory measurements (Jandora and Říha 2008) show that in practical computations the flow along the downstream slope may be assumed to be 1D, quasi-steady and uniform. No submergence from the downstream water level behind the dike was anticipated. Uniform erosion along the breach bed and sides was also assumed.

The mathematical analysis of the problem of dike breaching due to overtopping involves the determination of time-dependent variables and the proposal of a mathematical model for the solution of those variables. Since the problem of dike breaching due to overtopping was divided into two processes (overtopping and erosion), the mathematical model consists of two parts (modules): a hydraulic module which describes the hydraulics of water flow during the dike overtopping process, and an erosion module that describes the progress of the erosion of the dike material.

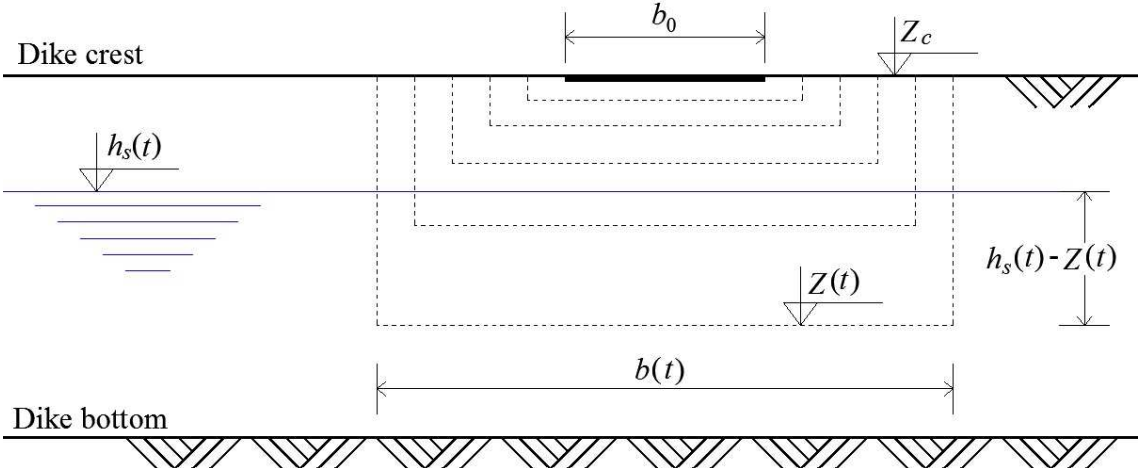


**Fig. 8.1** Proposed section of the dike breach opening



## 8.2 Mathematical model

As mentioned before, the mathematical model characterizing the dike breaching process consists of two modules: the hydraulic module and erosion module.

### A. The hydraulic module:

In order to describe water flow during dike overtopping the following state variables have been determined:

- $Q_b(t)$  flow discharge over the dike crest, or through the breach opening;
- $b(t)$  overtopping width before the erosion starts (equal to  $b_0$ ) or breach opening width during the erosion process (determined by the erosion module);
- $h(t)$  overflow head;
- $v_f(t)$  mean cross-sectional flow velocity at the downstream slope;
- $h_f(t)$  water depth along the downstream slope.

Overflow head  $h(t)$  is determined as the difference between the water level in the river  $h_s(t)$  and the elevation of dike crest  $Z_c$  (or the elevation of breach opening bottom  $Z(t)$  during the erosion process):

$$h = h_s - Z_c \quad (8.1)$$

where  $h_s$  is considered constant along the breach opening.

Water flow over the dike crest is given by the equation:

$$Q_b = m \cdot b \cdot \sqrt{2 \cdot g} \cdot h^{3/2} \quad (8.2)$$

where  $m$  is the discharge coefficient (for broad-crested weir),  $g$  is the acceleration of gravity.

The water depth  $h_f$  of the flow on the downstream slope can be derived from the Chezy formula with the assumption of uniform and quasi-steady flow:

$$h_f = \left( \frac{Q_b \cdot n}{b \cdot \sqrt{\sin \beta}} \right)^{6/10} \quad (8.3)$$

where  $\beta$  is the angle of the downstream slope,  $n$  is Manning's roughness coefficient.

Flow velocity  $v_f$  at the downstream slope is given by Chezy formula:

$$v_f = \frac{\sqrt{\sin \beta}}{n} \cdot h_f^{4/6} \quad (8.4)$$

The initial conditions for the overtopping problem - at time  $t_o$  (Fig. 4.1) - hold:

$$\begin{aligned} h(t = t_o) &= h(t_o) = 0 \\ b(t = t_o) &= b(t_o) = b_0 \end{aligned} \quad (8.5)$$

where  $b_0$  is determined as the idealized initial width of the dike crest depression at the overtopping location.

### B. Erosion module:

A simple 1D mathematical model was proposed for modelling the erosion process as it affects the dike body. Unknown variables in the erosion model are:

- $b(t)$  the breach opening width;
- $Z(t)$  the elevation of dike crest or the highest point of the breach opening bottom.

After exceeding the dike surface resistance ( $v_f > v_{non}$ ), the elevation  $Z(t)$  is determined by Equation 7.6 using the erosion module. Simple state equations can be used to calculate above mentioned variables (Singh 1996), (Jandora and Říha 2008):

$$\frac{dZ}{dt} = -\alpha_1 \cdot v_f, \text{ for } v_f > v_{non} \quad (8.6)$$

$$\frac{db}{dt} = +\alpha_2 \cdot v_f, \text{ for } v_f > v_{non} \quad (8.7)$$

where  $dZ/dt$  is the instantaneous change in the elevation of the breach opening bottom,  $db/dt$  is the instantaneous change in breach opening width,  $t$  is the time when  $t > t_b$  (Fig. 4.1),  $\alpha_1$  and  $\alpha_2$  are empirical coefficients expressing the erodibility of the dike material. The value of  $\alpha_1$  can be determined by analysing real dam failure records (Table 8.1) (Jandora and Říha 2002, 2008), and the value of  $\alpha_2$  can be estimated within the interval  $\langle \alpha_1 / 20; \alpha_1 / 5 \rangle$  (Singh 1996).

The initial conditions for the erosion problem hold:

$$\begin{aligned} b(t = t_b) &= b(t_b) = b_0 \\ Z(t = t_b) &= Z(t_b) = Z_c \end{aligned} \quad (8.8)$$

**Table 8.1** Values of coefficient  $\alpha_1$  derived from calibration of real dam breaches

Name of dam or of locality (country)	$h_d$ [m]	Downstream slope	$V$ [mil. m <sup>3</sup> ]	$B_a$ [m]	$Q_{bmax}$ [m <sup>3</sup> /s]	$\alpha_1$
Apishapa (USA)	34	1:2	22.5	86.5	6850	0.002
Baldwin Hills (USA)	49	1:1.8	110	16.5	1100	0.007
Break Neck Run (USA)	7	-	0.049	30.5	9.2	0.001
Buffalo Creek (USA)	14	1:1.3	0.61	125	1420	0.0085
Euclides de Cunha (Brazil)	53	-	13.6	131	1020	0.0014
Frankfurt (Germany)	10	-	0.35	6.9	79	0.001
Goose Creek (USA)	6	1:1.5	10.6	26.4	565	0.0013
Hatfield (USA)	6.8	-	12.3	91.5	3400	0.0020
Kelly Barnes (USA)	11.5	1:1	0.505	26.5	680	0.0050
Lake Latonka (USA)	13	-	1.59	33.5	290	0.0010
Little Deer Creek (USA)	26	-	1.73	23	1330	0.0090
Mammoth (USA)	21.3	-	13.6	9.2	2520	0.0050
Nanaksagar (India)	16	-	210	46	9700	0.0003
Salles Oliviera (Brazil)	35	-	25.9	168	7200	0.0020
Schaeffer (USA)	30.5	1:2	3.92	210	4500	0.0080
Experimental sandy dike at BUT Brno (CZ)	0.86	1:2	65.10 <sup>-6</sup>	1	0.43	0.0090
Melin dam (CZ)	5.4	1:1.39	0.35	17	150	0.003
Metelsky dam (CZ)	7.7	1:2.05	1.19	42 + 30 *	554	0.003
Luh dam (CZ)**	4.0	1:1.5	0.12	17	58	0.0001
Velky Belcicky dam (CZ)	6.7	1:2.1	1.06	42	610	0.0035

\* Two breach openings

\*\* Asphalt road on the dam crest

### 8.3 Numerical model

For the approximation of the numerical solution of equations (8.2), (8.3), (8.4) and (8.5), the Newton method was used.  $\Delta t$  refers to time step and  $t_{i+1} = t_i + \Delta t$  is discrete time.

From equation (8.1), the overflow head  $h(t_i)$  can be expressed using differences:

$$h(t_i) = h_s(t_i) - Z_c \quad (\text{during the overtopping process})$$

or

$$h(t_i) = h_s(t_i) - Z(t_i) \quad (\text{during the erosion process}) \quad (8.9)$$

For the calculation of the required hydraulic variables in the time  $t_i$ , the following equations hold:

$$Q_b(t_i) = m \cdot b(t_i) \cdot \sqrt{2 \cdot g} \cdot [h(t_i)]^{3/2} \quad (8.10)$$

$$h_f(t_i) = \left( \frac{Q_b(t_i) \cdot n}{b(t_i) \cdot \sqrt{\sin \beta}} \right)^{6/10} \quad (8.11)$$

$$v_f(t_i) = \frac{\sqrt{\sin \beta}}{n} \cdot [h_f(t_i)]^{4/6} \quad (8.12)$$

By the finite difference approximation of equations (8.6) and (8.7), the following equations are obtained:

$$\frac{dZ}{dt} \approx \frac{\Delta Z}{\Delta t} = \frac{Z(t_{i+1}) - Z(t_i)}{\Delta t} = -\alpha_1 \cdot v_f(t_i) \Rightarrow$$

$$Z(t_{i+1}) = Z(t_i) - \alpha_1 \cdot v_f(t_i) \cdot \Delta t, \text{ for } v_f(t_i) > v_{non}(t_i) \quad (8.13)$$

$$\frac{db}{dt} \approx \frac{\Delta b}{\Delta t} = \frac{b(t_{i+1}) - b(t_i)}{\Delta t} = +\alpha_2 \cdot v_f(t_i) \Rightarrow$$

$$b(t_{i+1}) = b(t_i) + \alpha_2 \cdot v_f(t_i) \cdot \Delta t, \text{ for } v_f(t_i) > v_{non}(t_i) \quad (8.14)$$

#### 8.4 Schematization of the flood wave

For starting with calculations of the hydraulic module, change in the water level in the river  $h_s(t)$  is required (equation 8.1). Therefore, the water level  $h_s(t)$  has to be derived from the flood wave passing through the studied river profile. To determine  $h_s(t)$  it is necessary to know the characteristics of the flood wave, and the geometrical characteristics and hydraulics of the stream channel (rating curve). Practically the flood wave is characterized by its peak discharge, volume and shape.

Because of the different morphology of individual catchments and the variability of climatic conditions, the shape of the flood wave (hydrograph  $Q(t)$ ) is difficult to generalize. In addition to the morphology of the catchments, the typical shape of the flood wave is affected by seasonal periods. Due to additional gradual floods induced by the melting of snow in the catchment, floods arriving in winter or spring often have a flatter shape with a longer duration and higher volume than summer floods.

In this study the flood hydrograph was approximated by a trapezoidal or triangular shape (Fig. 8.2). This approach is sufficiently variable to be able to describe the hydrographs of various flood waves. The approximated shape of the flood wave was schematically represented by the peak discharge  $Q_N$  and by three sections as follows (Fig. 8.2):

- 1- The ascending limb reflects the increase in the discharge due to the flood wave arrival. A linear increase in the discharge over time was assumed. Time interval  $t_k$  starts from the instant of the flood wave arrival and lasts until the instant when the peak discharge  $Q_N$  is

reached. It varies for each individual flood event, stream and catchment. Using data obtained from flood events (summer 2002, spring 2006 and summer 2006) in the Dyje river and depending on flood hydrographs of the Podhradí, Vranov, Znojmo and Trávní Dvůr gauging stations,  $t_k$  was assumed to range within the interval  $\langle 48; 120 \rangle$  hours.

- 2- The horizontal limb approximates the duration of the peak discharge  $Q_N$ . Time interval  $t_d$  specifies the duration from when the peak discharge is reached until the beginning of the falling limb.  $t_d$  can last less than one hour or may exceed several hours or days. Depending on the past flood events mentioned above, the minimum value of  $t_d$  was assigned as 0 hour realizing the triangular shape of the flood wave (Fig. 8.2) and the maximum value was assigned as 120 hours realizing the trapezoidal shape.
- 3- The descending limb represents the gradual decrease in the flood discharge. A linear decrease in the discharge over time was assumed and three times of  $t_k$  value was assigned for this time interval (Fig. 8.2).

The value of the peak discharge  $Q_N$  of the flood wave is provided by the Czech Hydrometeorological Institute CHMI (in Czech: Český Hydrometeorologický Ústav ČHMÚ) for an  $N$ -year flood frequency for a given river profile in the Czech Re-public.

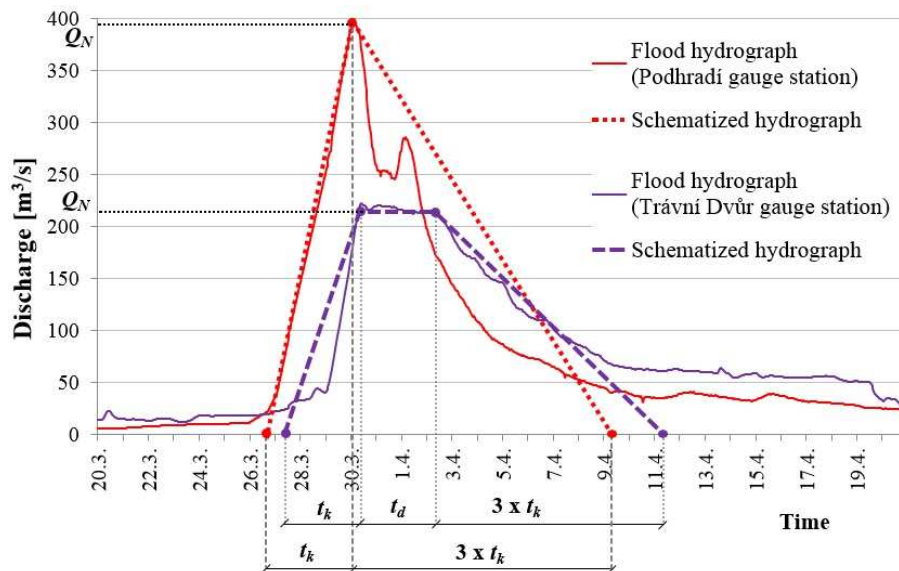


**Fig. 8.2** Schematization of the flood hydrograph at two gauge stations on the Dyje river

## 9 PROBABILITY OF DIKE BREACHING DUE TO OVERTOPPING

### 9.1 Uncertainty in input parameters

From the point of view of uncertainty, each input parameter is a variable and ranges within an interval  $\langle \min; \max \rangle$  of values which are supposed to be realistic in practical situations. Therefore, all input parameters should be individually identified and their impact on the results of the solution must be analysed.

The uncertainty in the input parameters of the dike breaching model was taken into account in order to obtain a probabilistic solution for the problem. The relevant parameters were classified into three groups:

- 1 Parameters describing the flood wave:  $Q_N, t_k, t_d$  (Fig. 8.2).
- 2 Parameters of the hydraulic module:  $b_0, m, n$  (Equations 8.5, 8.2, 8.3).
- 3 Parameters of the erosion module:  $v_{non}, \alpha_1, \alpha_2$  (Equations 8.6, 8.7).

### 9.2 Sensitivity analysis

The sensitivity analysis aims for revealing the influence of change in the value of each input parameter on the values of output parameters. The response of a mathematical model to changes in the input parameters is important in order to evaluate the model applicability and to define the input parameters that considerably affect the output parameters and thus deserve an additional attention.

In the case of dike breaching problem, the maximum breach discharge, the volume of water flowed through the breach, the breach opening size and the duration from the beginning of dike overtopping until the dike failure can be considered the most significant output parameters.

The influence of the input parameters mentioned above (in subsection 9.1) on the outputs of the dike breaching problem was taken into consideration when selecting parameters for random sampling. In this study the screening method was used to identify the non-influential input parameters. The most-used screening method in engineering is based on the so-called “One-At-a-Time” OAT design, where each input is varied while keeping the others constant (Iooss and Lemaitre 2014).

### 9.3 Estimation of the probability of dike breaching

The assessment of the probability was related to the typical phases of the dike breaching process specified in Section 6.3 (Fig. 6.3).

For the purpose of the probabilistic solution, a random sampling procedure was used where a set of simulations of dike breaching due to overtopping was generated with the consideration that the value of each uncertain input parameter changes within an interval of values with a specific probability distribution.

Using the Latin Hypercube Sampling (LHS) procedure, the sets of input parameters' values were randomly sampled and applied in the deterministic model to generate a set of output parameters.

The probability  $P_i$  of each typical  $i$ -th phase of the dike breach was estimated by frequency analysis as follows:

$$P_i = \frac{\text{number of simulations realizing the phase } (i)}{\text{total number of simulations}} \quad (9.1)$$

### 9.4 Latin hypercube sampling (LHS) method

The Latin hypercube sampling (LHS) method is an extension of quota sampling (Steinberg 1963) and can be viewed as an  $n$ -dimensional generalization of Latin square sampling (Raj 1968). Firstly, this method was used in "Uncertainty Analysis" by selecting input values  $\mathbf{x} = (x_1, x_2 \dots x_n)$  (random parameter) of a function  $y = h(\mathbf{x})$ , in order to estimate the cumulative distribution function (CDF) and the mean value of the function  $y$  (McKay et al. 2000).

According to the principle of statistical sampling, the square grid containing the sample positions can be considered a Latin square sampling (Table 9.1) if (and only if) there is only one sample in each row and each column (Raj 1968). Therefore, the Latin hypercube sampling is the generalization of this concept to a random number of dimensions (random number of parameters). From the point of view of statistical sampling, the LHS can be defined as a probabilistic procedure for generating a statistical sample of plausible sets (combinations) of parameters' values derived from a multidimensional distribution.

The LHS method is a modification of the Monte Carlo (MC) method. Contrary to the MC method the probability space for the LHS method should be divided into a specific number of intervals ( $J$ ) with the same probability. Hence the main advantage of the LHS method is the

significantly reducing the number of simulations required for the MC method in order to provide a reasonably accurate random distribution of the input parameters.

Each combination of pseudo-random values of input parameters used for the deterministic calculation is used only once according to the table of pseudo-random permutations (Table 9.1) and those pseudo-random values should be generated as one value from each interval.

**Table 9.1** One combination of pseudo-random permutations for two parameters with  $J = 6$  using the LHS method (Raj 1968)

		Intervals of the 1 <sup>st</sup> parameter					
		1	2	3	4	5	6
Intervals of the 2 <sup>nd</sup> parameter	1						*
	2			*			
	3	*					
	4					*	
	5		*				
	6				*		

The procedure of generating samples using LHS method can be summarized as follows:

- When sampling a problem with  $K$  input parameters, the range of probable values of each input parameter should be divided into a number of intervals ( $J$ ) of the same probability (Fig. 9.1). The number of intervals  $J$  depends on how many samples (values) would be generated for the input parameter.
- Then, one value from each interval is randomly selected with respect to the probability density in the interval.
- In case that all input parameters have the same  $J$ , the entire probability space consisting of  $K$  input parameters is divided into  $J^K$  cells of the same probability and thus number of the possible combinations of inputs' values according to LHS technique is equal to  $J^K$ .
- The combination or cell index indicates the intervals index of the input parameters. For example, the cell index (2, 1, 3) shows that the generated pseudo-random values of three input parameters ( $K = 3$ ) respectively lie in the 2<sup>nd</sup> interval of the 1<sup>st</sup> parameter, in the 1<sup>st</sup> interval of the 2<sup>nd</sup> parameter and in the 3<sup>rd</sup> interval of the 3<sup>rd</sup> parameter.
- For each selected (generated) combination of pseudo-random values, the deterministic calculation according Fig. 7.2 was carried out. The result of such calculation corresponds to one of the event scenarios (Fig. 7.3) and hence was applied to equation (7.3).



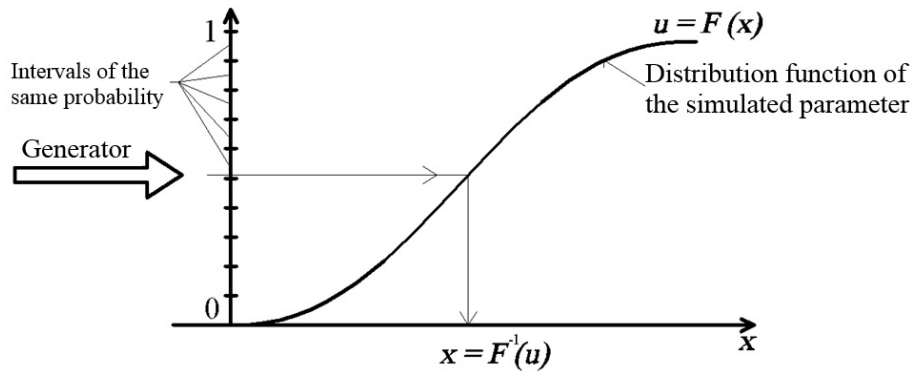


**Fig. 9.1** Generating random values of an input parameter with intervals  $J = 10$

## 9.5 Description of the outline algorithm

The algorithm describing the procedure for solving the problem of dike breaching due to overtopping consists of the following sub-problems:

- 1 Definition of the flood wave hydrograph.
- 2 Determination of overflow head using a rating curve at the river profile.
- 3 Breach discharge determined from the overflow (Equation 8.2).
- 4 Flow characteristics along the breach approximated by a 1D model of steady uniform flow.
- 5 Simulation of backward erosion (Fig. 5.3).
- 6 Determination of the breach opening size (Equations 8.6, 8.7).

# 10 Case study

## 10.1 Description of the studied dike

The studied dike is located on the left bank of the Dyje River at the stationing about 28.8 km. This location is adjacent to the village of Ladná near the town of Břeclav in the Czech Republic (Fig. 10.1). A diagram of the dike's cross section and geometrical dimensions is shown in Fig. 10.2. The location of the potential overtopping and subsequent breaching was selected during the site investigation at the lowest point on the dike crest.

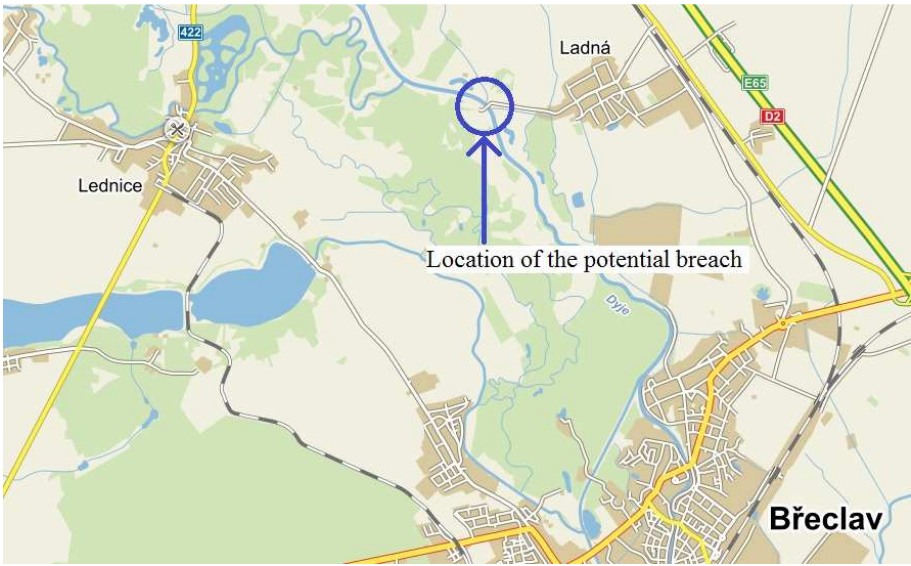


Fig. 10.1 Location of the potential breach at the Dyje river

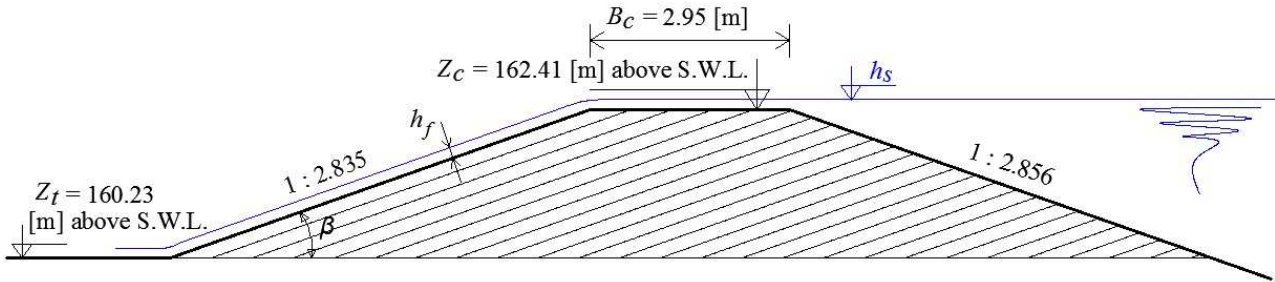


Fig. 10.2 Dike cross-section at the location of potential breach

## 10.2 Definition of the flood wave

The parameters of the flood hydrograph were set up for the chosen locality mentioned before as follows:

- 1 Values of peak discharge  $Q_N$  provided by the ČHMÚ are summarized in Table 10.1.

**Table 10.1** Values of  $N$  and  $Q_N$  (provided by the ČHMÚ)

$N$ [year]	1	2	5	10	20
$Q_N$ [m <sup>3</sup> /s]	160	230.9	341.4	436.4	540.8
$N$ [year]	50	100	500	1000	10000
$Q_N$ [m <sup>3</sup> /s]	693.3	820	1154.8	1320	1920

- 2 The duration of the ascending limb was derived from the floods in summer 2002, spring 2006 and summer 2006 along the Dyje River;  $t_k$  was considered to range within the interval  $\langle 48; 120 \rangle$  [hour].
- 3 The duration of the horizontal limb  $t_d$  was assumed to range from 0 hours (the rising limb is immediately followed by the falling limb - triangular shape) to 120 hours based on data obtained from past flood events.
- 4 The duration of the descending limb was determined based on typical observed hydrograph shapes of past flood events to be  $3.t_k$ .

## 10.3 Sensitivity analysis

In the sensitivity analysis the influence of input parameters  $Q_N$ ,  $t_k$ ,  $t_d$ ,  $b_0$ ,  $m$ ,  $n$ ,  $v_{non}$ ,  $\alpha_1$ ,  $\alpha_2$  on the output variable  $Q_{bmax}$  was assessed. In the analysis non-dimensional parameters of the inputs and the output were compared. Firstly, a reference value ( $R_i$ ) was specified for each input parameter (Table 10.2) and processed to form the following serial values  $V_i = [0.7R_i, 0.8R_i, 0.9R_i, R_i, 1.1R_i, 1.2R_i, 1.3R_i]$ . During the analysis each input parameter is substituted by its serial values while keeping the others constant equal to their  $R_i$  values. The  $Q_{bmax}$  value corresponding to each serial value for each input parameter was computed and used as a criterion in the sensitivity analysis. The procedure of sensitivity analysis for all input parameters was carried out via MATLAB software (see Appendix B).

The  $R_i$  value for the peak discharge of flood wave ( $Q_N$ ) was determined to correspond the peak discharge of flood wave with return period  $N = 100$  years ( $R_i(Q_N) = Q_{100}$ ) in order to agree with the condition that the minimum value in the  $Q_N$  serial values i.e.  $0.7R_i$  ensures the

occurrence of dike overtopping. In the case of  $t_k$  and  $t_d$ , the  $R_i$  values were determined as the average value of an interval derived from data obtained from flood events (summer 2002, spring 2006 and summer 2006) in the Dyje river (see 8.4). The  $R_i$  value for  $b_0$  was determined as idealized width of the dike crest depression at the overtopping place. The discharge coefficient  $m$  for broad-crested weir ranges within the interval  $\langle 0.3; 0.4 \rangle$  and its  $R_i$  value was determined as the average value. For Manning's roughness coefficient  $n$ , the  $R_i$  value was proposed as 0.035 corresponding to average grass cover. The  $R_i$  value for  $\alpha_1$  was chosen from Table 7.1 and the  $R_i$  value for  $\alpha_2$  was assumed to equal the average value of this interval  $\langle \alpha_1/20; \alpha_1/5 \rangle$  (Singh 1996).

**Table 10.2** Reference values ( $R_i$ ) of input parameters

Input parameter ( $i$ )	Unit	$R_i$ value
$Q_N$	[m <sup>3</sup> /s]	$Q_{100} = 820$
$t_k$	[hour]	84
$t_d$	[hour]	60
$b_0$	[m]	2
$M$	[-]	0.35
$N$	[-]	0.035
$\alpha_1$	[-]	0.001
$\alpha_2$	[-]	0.000125
$v_{non}$	[m/s]	plain grass – average cover

Since the non-scouring velocity  $v_{non}$  was expressed as a function of time (Fig. 6.2), the  $R_i$  value for  $v_{non}$  was assigned as the value of the  $v_{non}$  curve of the plain grass – average cover corresponding to the time = 1 [hour]. In order to obtain additional values of the  $v_{non}$  should be used to create the non-dimensional parameters, values corresponding to the time = 1 [hour] of the  $v_{non}$  curves of the plain grass – good cover, the plain grass – poor cover and two interpolated curves were used (Fig. 10.3).

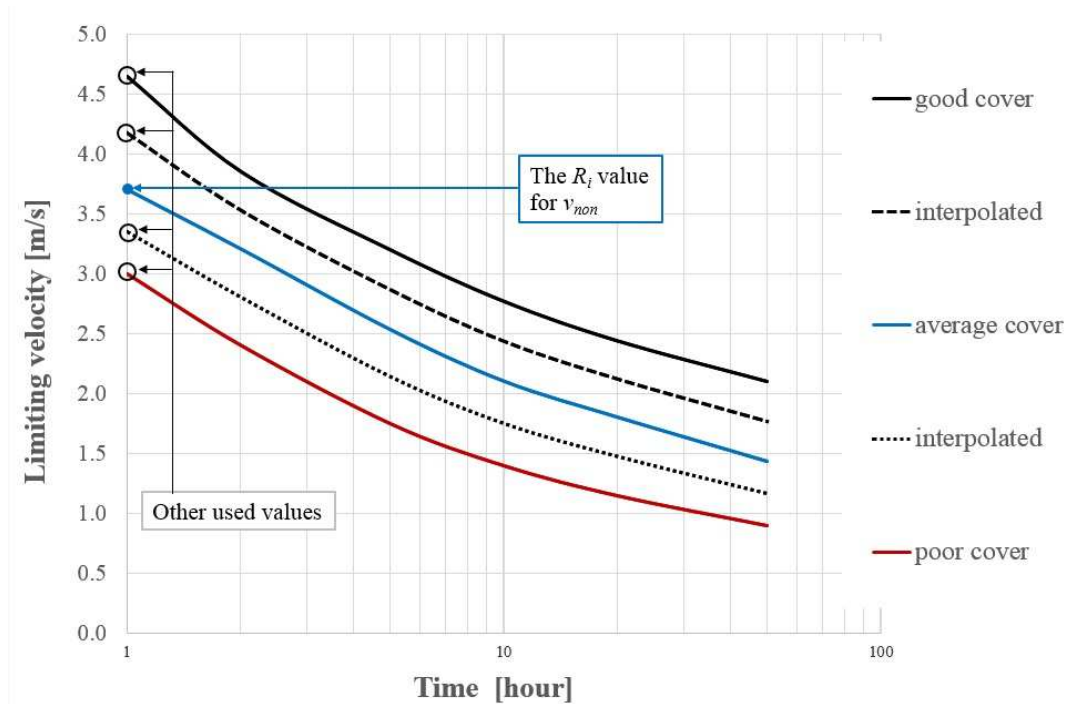


**Fig. 10.3** Original and interpolated curves of the  $v_{non}$  (Floods and reservoir safety 1996)

The resulting graph of the sensitivity analysis expressing the relation between the dimensionless input parameters ( $V_i / R_i$ ) and the dimensionless maximum breach discharge ( $Q_{bmax}(V_i) / Q_{bmax}(R_i)$ ) can be seen in Fig. 10.4 (values of input and output parameters used for creating Fig. 10.4 are summarized in Appendix A). The following conclusions can be stated:

- Parameters  $Q_N$ ,  $t_k$ ,  $t_d$ ,  $m$ ,  $n$  and  $\alpha_2$  are the most influential.  $Q_N$  has the highest influence on the output variable  $Q_{bmax}$ .  $t_k$ ,  $t_d$ ,  $m$  and  $\alpha_2$  have lower influence than  $Q_N$ , and  $n$  has reverse influence.
- Parameter  $v_{non}$  has only minor influence and parameters  $b_0$  and  $\alpha_1$  have practically no effect on the output variable  $Q_{bmax}$ .
- As a result, parameters  $b_0$ ,  $\alpha_1$  and  $v_{non}$  may be excluded from random sampling as changes to them have only a minor influence on the resulting  $Q_{bmax}$ . The input parameters  $Q_N$ ,  $t_k$ ,  $t_d$ ,  $m$ ,  $n$  and  $\alpha_2$  are the most influential parameters, so the variance ranges of those parameters and their probability distribution should be taken into account during the probabilistic solution of the dike breaching problem.

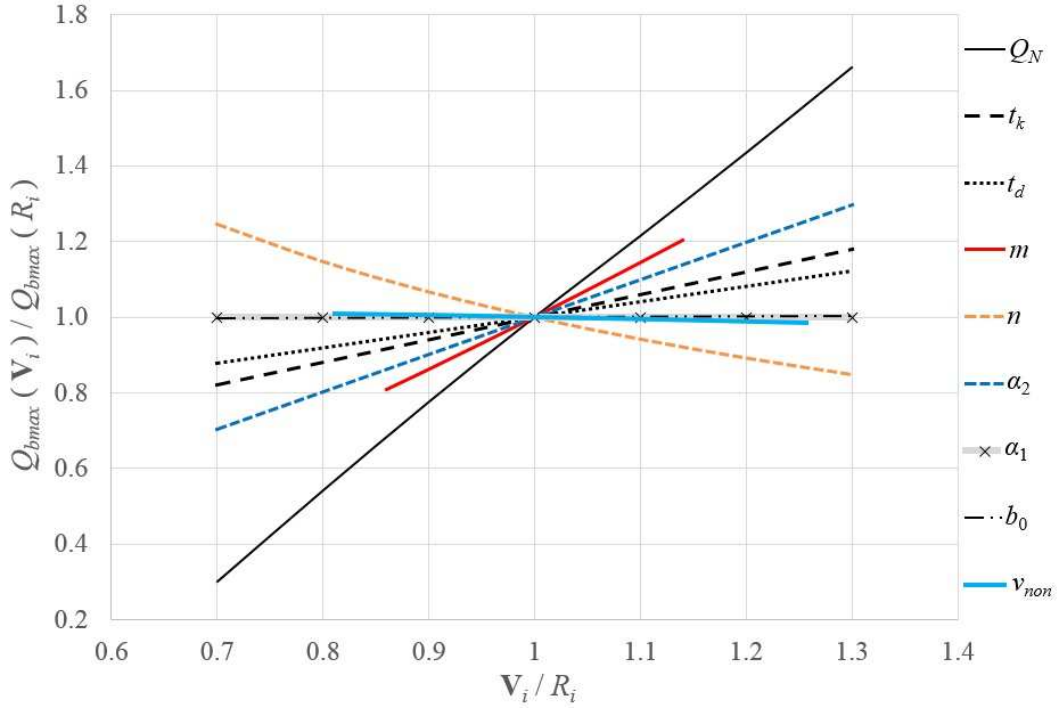


**Fig. 10.4** Sensitivity analysis results

#### 10.4 Detailed computational algorithm

The dike breaching computation is a dynamic process in which the breach discharge depends on the breach opening size (the elevation of the breach opening bottom  $Z(t)$  and the breach opening width  $b(t)$ ). The development of the breach opening depends on the capacity of flowing water to scour dike material during the breach, i.e. it depends on the flow velocity. The estimated change in the breach opening size parameters ( $\Delta Z$  and  $\Delta b$ ) due to the erosion process are used as initial inputs for the iteration in each time step.

The computational algorithm consists of the following steps (These following steps were carried out via MATLAB software (see Appendix C)):

1. Definition of the probability exceedance line ( $P$ ,  $Q_N$ ) (Fig. 10.5) to estimate the probability  $P$  of the peak discharge  $Q_N$ . This was done using the data provided by the ČHMÚ (Table 10.1) with the use of Equations 10.1 and 10.2:

$$p_N = 1 - e^{-1/N} \quad (10.1)$$

$$P = 1 - p_N = e^{-1/N} \quad (10.2)$$

where  $Q_N$  is the peak discharge in a specific profile that can be reached or exceeded once every  $N$  year,  $P$  is the probability that the  $Q_N$  will not be reached and  $p_N$  is the probability that the  $Q_N$  will be reached or exceeded and the  $p_N$  values were calculated using the probability density function of the Poisson distribution with parameter  $\lambda=1/N$ .

The fitting curve expressing the  $(P, Q_N)$  relation (Fig. 10.5) was defined via MATLAB software using  $N$  and  $Q_N$  values summarized in Table 10.1 and  $P$  values obtained from Equations 10.1 and 10.2.

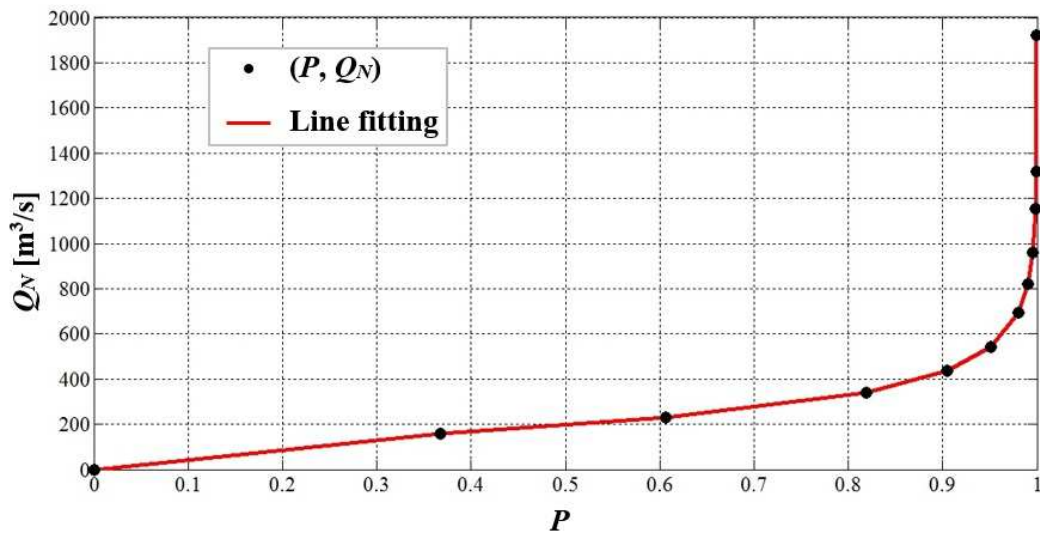


**Fig. 10.5** Fitting curve expressing the  $(P, Q_N)$  created via MATLAB software

Using the fitting curve  $(P, Q_N)$ , the random values of the variable ( $Q_N$ ) were obtained. The input parameters  $t_k, t_d, m, n$  and  $\alpha_2$  were also considered random variables. As there were no reliable data enabling the analysis of their probability density function, in this study their probability distribution was set to be uniform (see below).

2. Defining the flood wave parameters: The peak discharge and flood duration should be determined in order to obtain the hydrograph  $(Q, t)$  of the flood wave. The flood wave parameters plotted in Figures 10.6a and 10.6b are as follows:

- $Q_N$  is a value randomly chosen from the fitting curve using the LHS method (Fig. 10.5).
- $t_k$  is a value randomly chosen using the LHS method from the interval  $\langle 48; 120 \rangle$  hours with uniform distribution.

- $t_d$  is a value randomly chosen using the LHS method from the interval  $\langle 0; 120 \rangle$  hours with uniform distribution.

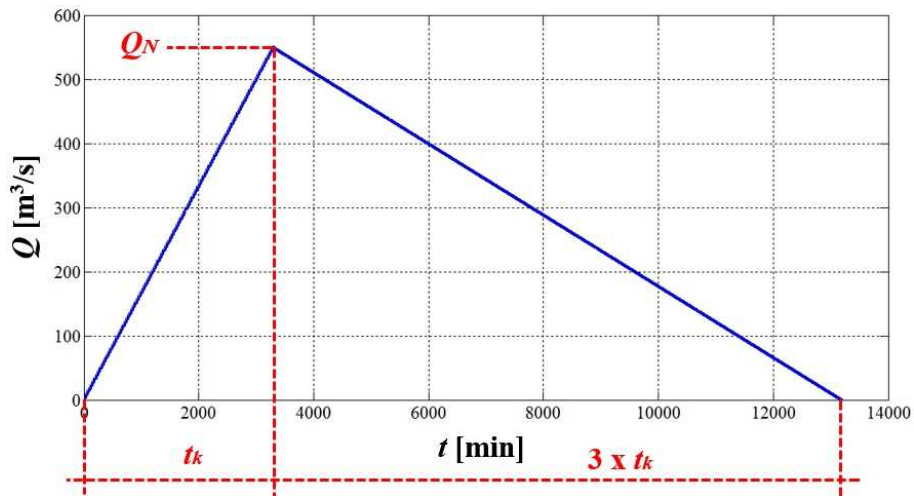


**Fig. 10.6a** Triangular flood wave hydrograph ( $Q, t$ ) created via MATLAB software

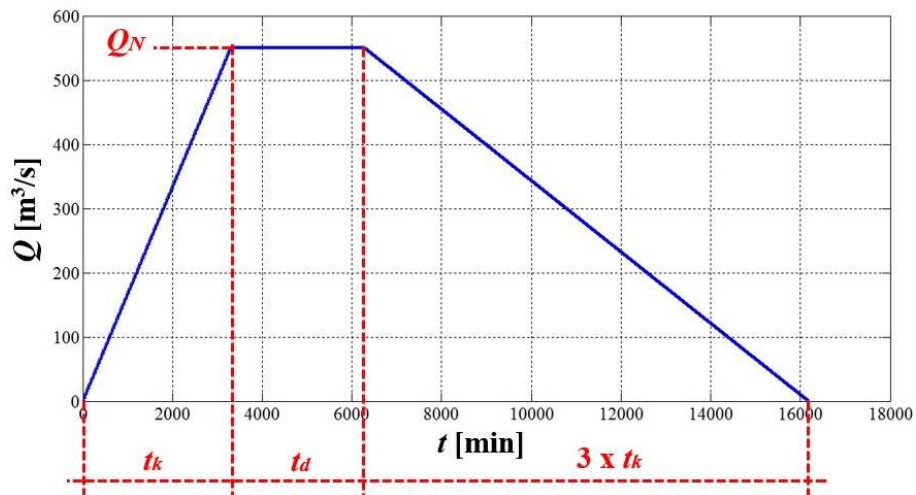


**Fig. 10.6b** Trapezoidal flood wave hydrograph ( $Q, t$ ) created via MATLAB software

3. Defining the evolution of the water level in the stream ( $h_s, t$ ) (Figures 10.8a and 10.8b). The water level in the stream (the Dyje River) is determined from the instant discharge in the river by the use of the stage-discharge curve ( $h_s, Q$ ) at the Břeclav-Ladná gauging station (Fig. 10.7).



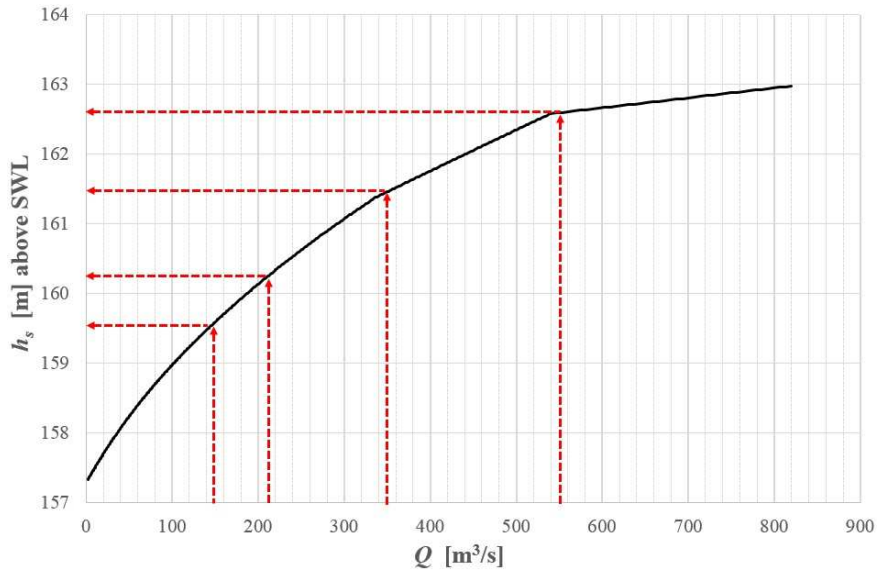


**Fig. 10.7** Stage-discharge curve at the Břeclav-Ladná gauging station

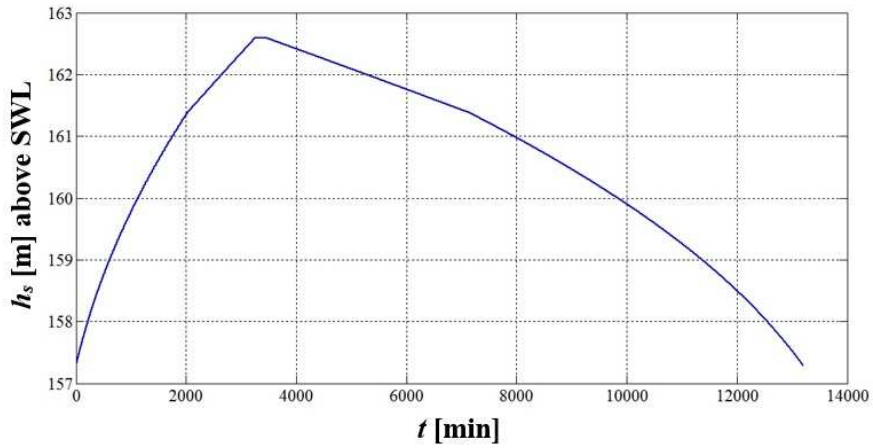


**Fig. 10.8a** Water level in the river ( $h_s, t$ ) created via MATLAB software corresponding to triangular hydrograph (Fig. 10.6a)

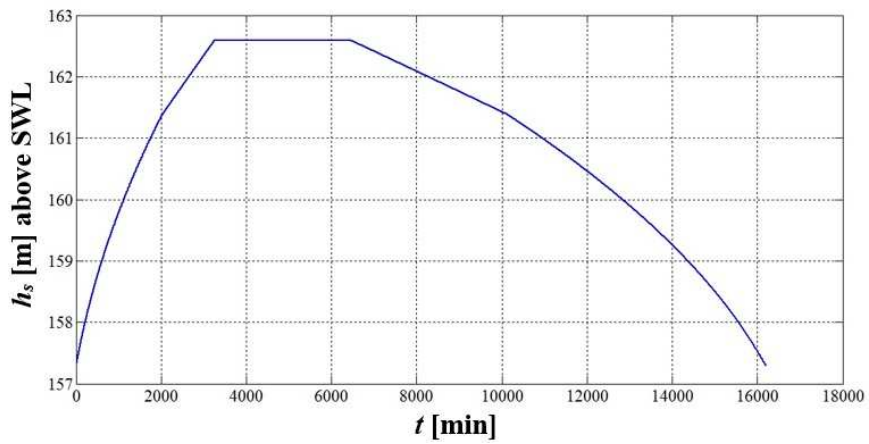


**Fig. 10.8b** Water level in the river ( $h_s, t$ ) created via MATLAB software corresponding to trapezoidal hydrograph (Fig. 10.6b)

4. Defining the dike crest elevation ( $Z_c$ ). In this thesis, two different cases of the parametric study regarding the dike crest elevation and the protective lining layer were carried out:
  - **Case 1:** The dike crest elevation  $Z_c$  was specified to be equal to the stream water level corresponding to the peak discharges with the return periods  $N = 10, 20$  and  $50$  years, i.e.  $Z_c = h_s(Q_{10}, Q_{20}$  and  $Q_{50}$ , respectively). In this case the dike crest elevation was specified for three different design discharge values in the Dyje River ( $Q_{10}, Q_{20}$  and  $Q_{50}$ ) and this enables the parametric assessment of the probabilities related to different flood protection levels.
  - **Case 2:** The dike crest elevation  $Z_c$  was specified to be equal to the stream water level corresponding to the peak discharge with the return period  $N = 10$  years (one design discharge value) i.e.  $Z_c = h_s(Q_{10})$ . The lining layer covered the downstream slope of the dike was tested for all selected types of the lining materials presented in Fig. 6.2. This enables the parametric assessment of the probabilities related to different materials of the lining layer for one flood protection level.
5. Testing whether the water level in the stream  $h_s$  exceeds the dike crest elevation  $Z_c$ . If  $h_s > Z_c$  (at time  $t > t_o$  as shown in Fig. 4.1), calculation by the hydraulic module was performed using Equations 8.9 - 8.12. During the calculation, the random variables  $m$  and  $n$  (Equations 8.10, 8.11) were determined using the LHS method, where  $m$  values were randomly chosen from the interval  $\langle 0.3; 0.4 \rangle$  and  $n$  values were randomly chosen from the interval  $\langle 0.025; 0.045 \rangle$ , both with uniform distribution. Other parameters used in the hydraulic module were determined as follows:  $b_0 = 2$  [m],  $g = 9.81$  [m/s<sup>2</sup>] and  $\beta = 19.43$  [degree].
6. Testing whether flow velocity at the downstream slope  $v_f$  exceeds the non-scouring velocity  $v_{non}$ . If  $v_f > v_{non}$ , calculation of the erosion module was performed, where the instantaneous changes in the breach opening bottom elevation and overtopping width (breach opening width) were calculated using Equations 8.13, 8.14.  $\alpha_1$  was used as a constant ( $\alpha_1 = 0.0005$ ), and the  $\alpha_2$  value was randomly chosen using the LHS method from the interval  $\langle \alpha_1/20; \alpha_1/5 \rangle = \langle 0.000025; 0.0001 \rangle$  with a uniform distribution.
7. If the elevation of the breach opening bottom reaches the elevation of the terrain behind the dike, and still  $v_f > v_{non}$ , only the breach opening width increases.

8. The procedure described in points 5 and 7 is repeated until the water level in the stream decreases together with the breaching velocity and erosion stops. The dimensions of the breach opening do not change from this time onwards.
9. Calculating the probability of each typical phase of the dike breaching due to overtopping described in Chapter 9 (see 9.3) was statistically carried out using Equation 9.1 and depending on the event scenarios described in Fig. 7.3, where:
  - $P_1$  corresponds the 1<sup>st</sup> phase (no overtopping),
  - $P_2$  corresponds the 2<sup>nd</sup> phase (overtopping – no erosion),
  - $P_3$  corresponds the 3<sup>rd</sup> phase (erosion – no collapse),
  - $P_4$  corresponds the 4<sup>th</sup> phase (dike collapse).

For the purpose of random sampling and generating the combinations of input parameters' values 50 values for  $Q_N$  (those values were randomly chosen from the  $(P, Q_N)$  curve presented in Fig. 10.5 and specified to be larger than the design discharge value ( $Q_{10}$ ) used for each case mentioned in step 4) and 10 values for each  $t_k, t_d, m, n$  and  $\alpha_2$  were randomly chosen. Therefore,  $5 \cdot 10^6$  simulations (the possible combinations according to LHS technique is equal to  $J^K = 10^{5 \cdot 50} = 5 \cdot 10^6$ ) were carried out for each case mentioned in step 4.

## 11 FINAL RESULTS

Concerning the uncertainty in input parameters of the flood wave and other parameters governing the progression of dike breaching due to overtopping, this problem should be solved as a stochastic one. To solve this problem, the numerical solution of a mathematical model describing the dike breaching due to overtopping was used, the set of input parameters' values were randomly sampled using the LHS procedure and applied in the deterministic model to generate the set of output parameters, and the probability of each typical phase of the dike breach was estimated by the frequency analysis.

The input data for the statistical modelling were as follows:

- Return periods  $N$  and the corresponding peak discharges  $Q_N$ .
- Initial breach opening width  $b_0$  and  $\alpha_1$  were proposed as deterministic parameters.
- Parameters  $t_k$ ,  $t_d$ ,  $m$ ,  $n$  and  $\alpha_2$  were specified with taking into consideration their uncertainty during the calculation. Their values were randomly chosen using the LHS technique and the uniform distribution of the values was suggested within realistic intervals proposed depending on real events (Table 11.1).

**Table 11.1** parameters of uniform distribution  $U(a, b)$

Variable	Type of distribution	$a$	$b$
$t_k$	$U(a, b)$	48	120
$t_d$	$U(a, b)$	0	120
$m$	$U(a, b)$	0.3	0.4
$n$	$U(a, b)$	0.025	0.045
$\alpha_2$	$U(a, b)$	0.000025	0.0001

The final results were performed for two cases as mentioned above (see 10.4, step 4):

- **Case 1:** The dike crest elevation was specified to be equal to three different values ( $Z_c = h_s(Q_{10}, Q_{20}$  and  $Q_{50}$ , respectively) (Table 11.2), and the downstream slope of the dike is covered with plain grass – poor cover.
- **Case 2:** The dike crest elevation is equal to  $Z_c = h_s(Q_{10})$ , and the lining layer of the downstream slope was tested for all materials presented in Fig. 6.2 (Table 11.3).

The final results were presented as probabilities related to the annual occurrence of a given phase of the breaching problem. The results were presented in Figures 11.1 and 11.2 in the form of bar graphs of the typical phases with the probability values in percentage.

**Case 1 results:**

**Table 11.2** Probabilities of the typical phases and comparison with the value obtained from equation 10.1

	$p_n$ (equation 10.1)	No overtopping	Overtopping – no erosion	Erosion – no breaching	Collapse
$Z_c = h_s (Q_{10})$	0.90484	0.90595	0.00378	0.00003	0.09024
$Z_c = h_s (Q_{20})$	0.95123	0.95688	0.00198	0.00002	0.04112
$Z_c = h_s (Q_{50})$	0.98020	0.98543	0.00189	0.00001	0.01267

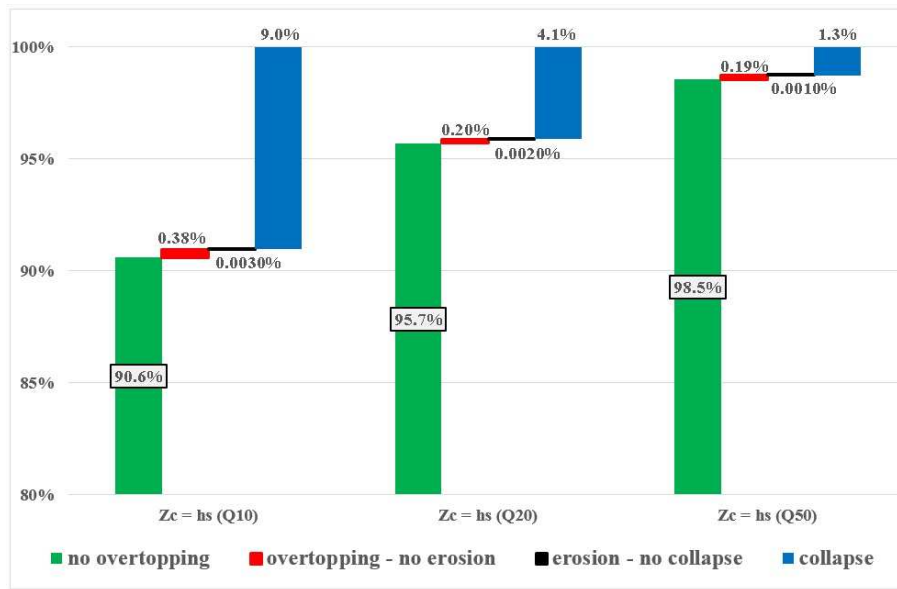


**Fig. 11.1a** Probabilities [%] of the typical phases of dike breaching due to overtopping

The next figure includes the same probabilities presented in Fig. 11.1a but in different probability scale.

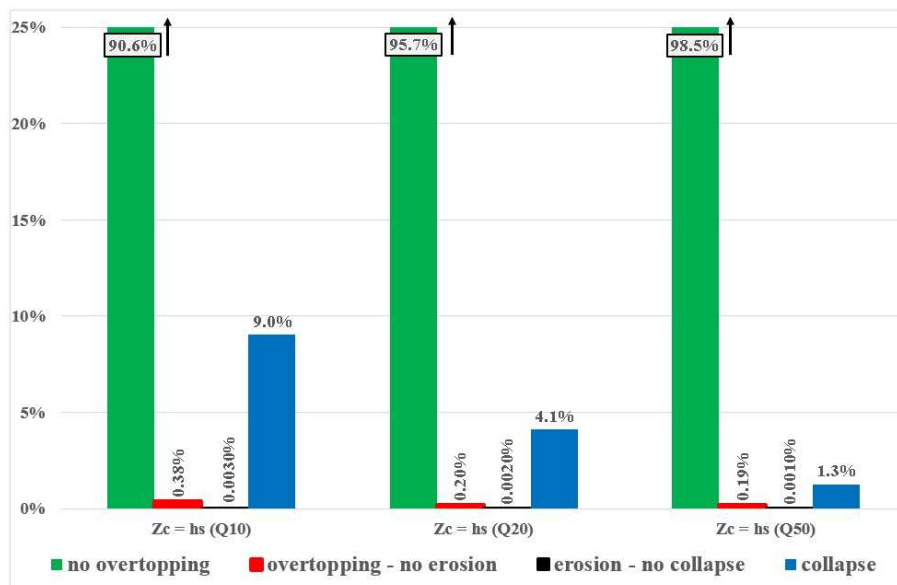


**Fig. 11.1b** Probabilities [%] of the typical phases of dike breaching due to overtopping

**Case 2 results:**

**Table 11.3** Probabilities of the typical phases for different lining materials and comparison with the value obtained from equation 10.1

	$p_n$ (equation 10.1)	No overtopping	Overtopping – no erosion	Erosion – no breaching	Collapse
A: grass poor cover	0.90484	0.90595	0.00377	0.00003	0.09024
B: grass average cover	0.90484	0.90595	0.00862	0.00003	0.08541
C: grass good cover	0.90484	0.90595	0.01505	0.00002	0.07897
D: meshes	0.90484	0.90595	0.01976	0.00002	0.07427
E: filled mats, fabrics	0.90484	0.90595	0.02993	0.00001	0.06411
F: open mats	0.90484	0.90595	0.04119	0.00001	0.05285
G: concrete block systems	0.90484	0.90595	0.07789	0.00000	0.01616
H: concrete systems	0.90484	0.90595	0.08974	0.00000	0.00431

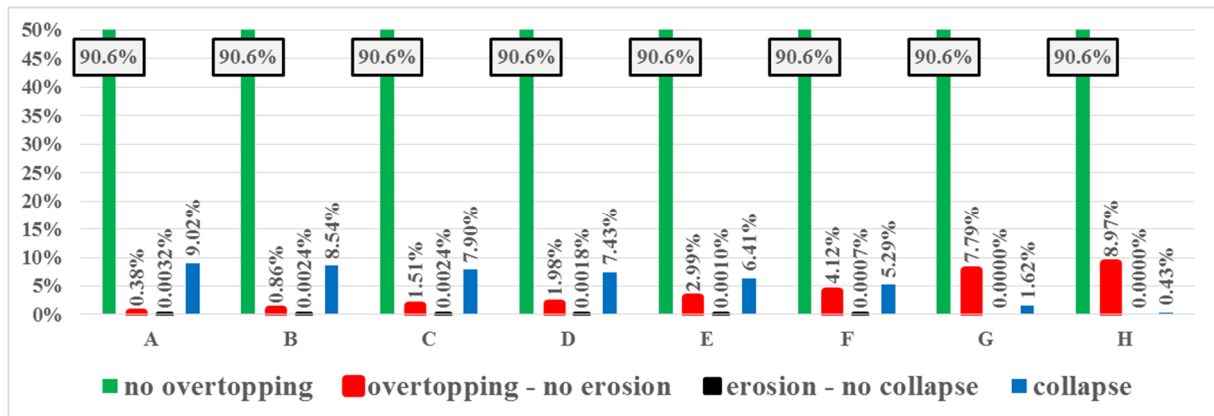


**Fig. 11.2a** Probabilities [%] of the typical phases for different lining materials

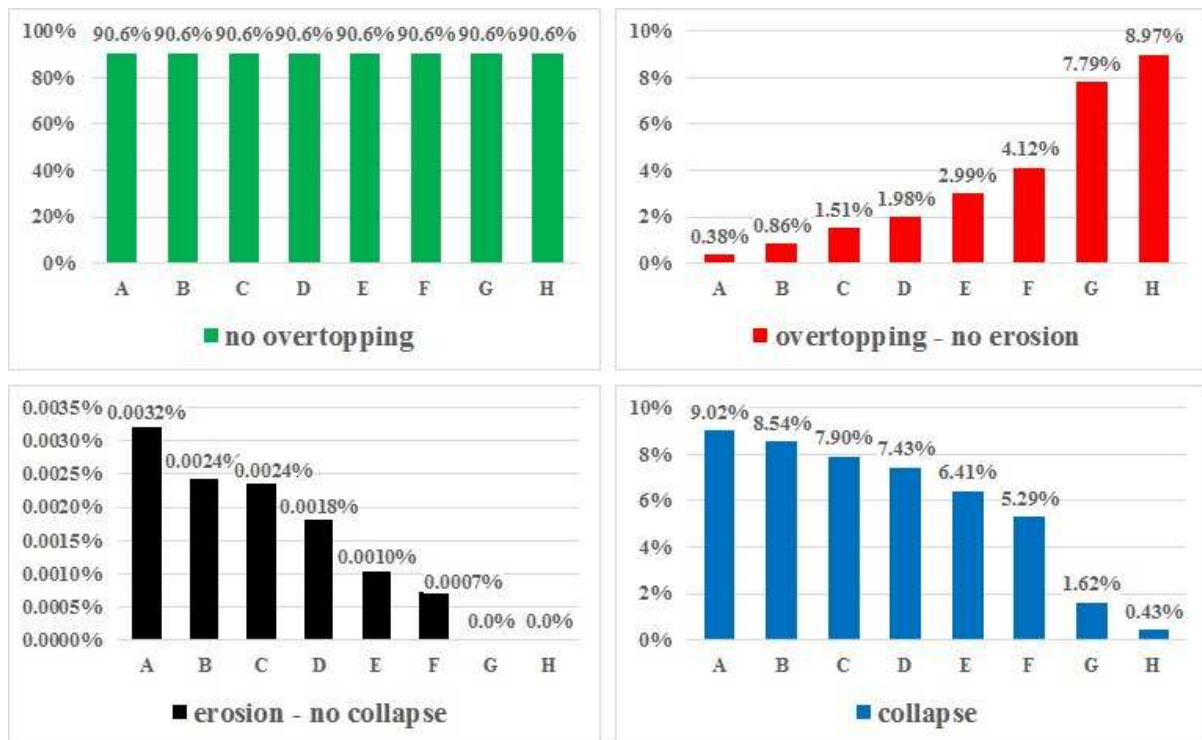


**Fig. 11.2b** Detailed Probabilities [%] of individual typical phases for different lining materials

## 12 CONCLUSIONS

### 12.1 General remarks

Dike overtopping is the most common reason of the dike failure and the statistics for dike and embankment dam failures shows that this kind of failure represents approximately as much as 40% of all embankment and dike failures. This kind of failure is induced by the erosion which begins on the downstream face and advances toward the upstream one where the erosion considerably accelerates when reaches the upstream edge of the dike crest. The erosion process is attributed to the exceedance of a critical value known as the non-scouring velocity expressing the resistance of the lined downstream slope of the dike.

Since the course of the dike breaching is significantly affected by the duration of water overflow (duration of overtopping process), so the uncertainty in the overflow duration should be taken into account through the assessment of the dike breaching probability. In more details the duration of overtopping can be considered the most important parameter to specify the beginning of erosion process (when the resistance is exceeded). Therefore, the probability of dike breaching should involve both probabilities of overtopping and erosion.

The main goal of this thesis was the reliability analyse of the flood protection dike and the probability estimation of individual phases of dike breaching due to overtopping. For this purpose, a simple mathematical model characterizing the dike breaching process was proposed depending on several assumptions mentioned in Chapter 8 (see 8.1). The mathematical model consisted of two modules: the hydraulic module and erosion module (see 8.2). The resistance of lining layer covering the downstream slope and the erosion criteria for the dike material were defined.

For the reliability assessment, the qualitative and quantitative analysis were carried out. The qualitative analysis included a checklist of the elements of the dike breaching due to overtopping and a checklist of the event scenarios of this problem discussed using the ETA method. The quantitative analysis included generating numerical data to be used in the mathematical and statistical modelling methods in order to estimate probability of individual outcome obtained from each event scenario discussed in the qualitative analysis. Before generating the numerical data, a deterministic mathematical model was developed and statistical modelling based on the LHS method was carried out in order to calculate the

probability of dike breaching.

A sensitivity analysis was performed in order to determine the sensitive parameters which further their uncertainties were taken into account before applying their values into the deterministic model. For the sensitivity analysis, the maximum breach discharge  $Q_{bmax}$  was used as the output variable to observe the influence of change in each input parameter's value ( $Q_N$ ,  $t_k$ ,  $t_d$ ,  $b_0$ ,  $m$ ,  $n$ ,  $v_{non}$ ,  $\alpha_1$  and  $\alpha_2$ ). The final sensitivity analysis results indicated that the  $Q_N$ ,  $t_k$ ,  $t_d$ ,  $m$ ,  $n$  and  $\alpha_2$  parameters are the most influential ones and should be taken into account as random variables variance when calculating the probabilities of dike breaching phases. The parameters  $b_0$ ,  $\alpha_1$  and  $v_{non}$  can be excluded from random sampling. The resulting maximum breach discharge ( $Q_{bmax}$ ) was not sensitive to parameters  $b_0$ ,  $v_{non}$  and  $\alpha_1$ . This can be attributed to the very long duration of the flood waves simulated in this work, which corresponds to a river profile lying in the lower portion of a catchment.

The final results were performed for two cases as mentioned before:

- **Case 1.** The assessment was performed for a dike which its downstream slope is covered with plain grass – poor cover, and the dike crest elevation was specified for three different design discharge values in the Dyje River ( $Q_{10}$ ,  $Q_{20}$  and  $Q_{50}$ ) as given in Table 11.2.
- **Case 2.** The assessment was performed for a dike which its downstream slope is covered with different lining materials, and the dike crest elevation was specified for one design discharge value in the Dyje River ( $Q_{10}$ ) as given in Table 11.3.

For estimating the probabilities related to the typical phases for each case, the statistical modelling was carried out for  $5 \cdot 10^6$  simulations. The final results were presented in Figures 11.1 and 11.2 in the form of bar graphs.

## 12.2 Discussion

The results for the "no overtopping" phase are in good agreement with the "accurate" results obtained from Equation 10.1 (see Tables 11.2 and 11.3). Those probabilities can be defined as the dike reliability or the probability of protection which can be obtained from a dike constructed in that studied location with specific parameters of crest elevation and other geometry, specific material of the dike body and specific layer lining its downstream slope.

The results presented in Figures 11.2a and 11.2b show that the probability of "dike collapse" decreases with the increase of resistance of the lining material. In Figures 11.1a, b and 11.2a, b



the small values gained for the probability of "dike erosion - no collapse" phase, which represents the case of partial damage in the dike body without complete failure, can be attributed to the very long duration of the flood waves in the Dyje River simulated in this work.

During this thesis, numerous specific practical and theoretical problems were solved. These can be solved in more detail during further research:

- Comprehensive sensitivity analysis including more output variables should be carried out to study the influence of erodibility parameters on the breaching process in more detail. This namely concerns locations with shorter-duration floods.
- Due to the large number of simulations, the computing time needed for this study was extensive (usually exceeding 4 days for one set of simulations). It is therefore necessary to search for more efficient sampling methods (importance sampling, etc.). This will open up the possibility of using more complex dike breach simulation techniques, including 2D models.
- An initiative to compile a database of dike failures, dike materials, resistances of individual lining materials, etc. which should provide information for the development of more reliable probability distributions of individual random variables to be used as inputs within the modelling of dike breaching.

Finally, it can be concluded that this study indicates the ability to perform the probabilistic assessment of dike failures. In practical cases, the probabilistic assessment of dike failure can be applied to identify the most vulnerable reaches and propose possible improvements for the dikes of such reaches (for instance, installing more resistant linings or designing emergency spillway, ...).

## REFERENCES

- ALCRUDO, F., MULET, J. 2007: Description of the Tous dam break case study (Spain). *Journal of Hydraulic Research*, Vol. 45, Supplement 1, 2007, pp. 45-57.
- ALHASAN, Z., JANDORA, J., ŘÍHA, J. 2013: Scour resistance of dike materials at downstream slope during overtopping. In the proceedings of the 13<sup>th</sup> International Symposium on Water Management and Hydraulic Engineering, September 9-12, 2013, Bratislava, Slovakia, ISBN978-80-227-4002-9, pp. 12.
- AURELI, F., MIGNOSA, P., TOMIROTTI, M. 2000: Numerical simulation and experimental verification of Dam-Break flows with shocks. *Journal of Hydraulic Research*, Vol. 38, No. 3, 2000, pp. 197-206.
- CALLE, E.O.F. et al. 1999: Technical Report on Sand Boils (Piping). Technical Advisory Committee on Flood Defences, The Netherlands, March 1999, (draft English version, August 2002), 142 p.
- CHINNARASRI, C., TINGSANCHALI, T., WEESAKUL, S., WONGWISES, S. 2003: Flow patterns and damage of dike overtopping. *International Journal of Sediment Research*, Vol. 18, No. 4, 2003, pp. 301-309.
- CHINNARASRI, C., JIRAKITLERD, S., WONGWISES, S. 2004: Embankment dam breach and its outflow characteristics. *Civil Engineering and Environmental Systems*, Vol. 21, No. 4, December 2004, pp. 247-264.
- CLEMENS, P.L., SIMMONS, R.J. 1998: System Safety and Risk Management. NIOSH Instructional Module, A guide for Engineering Educators, Cincinnati, Ohio: National Institute for Occupational Safety and Health, NIOSH Order No. 96-37768.
- CLOPPER, P.E., CHEN, Y.H. 1987: Predicting and minimizing embankment damage due to flood overtopping. In the proceedings of the 1987 National Conference on Hydraulic Engineering, August 3-7, 1987, Williamsburg, Virginia, United States, pp. 751-757.
- COLEMAN, S.E., ANDREWS, D.P., WEBBY, M.G. 2002: Overtopping breaching of non-cohesive homogeneous embankments. *Journal of Hydraulic Engineering*, Vol. 128, No. 9, Sep. 2002, pp. 829-838.
- DUPONT, E., DEWALS, B.J., ARCHAMBEAU, P., ERPICUM, S., PIROTTON, M. 2007: Experimental and numerical study of the breaching of an embankment dam. In the proceedings of the 32<sup>nd</sup> IAHR Biennial Congress - Harmonizing the demands from art and nature, 2007, Venice, Italy.

- FARINHA, M.L.B., CALDEIRE, L., NEVES, E.M. 2015: Limit state design approach for the safety evaluation of the foundations of concrete gravity dams. *Structure and Infrastructure Engineering: Maintenance, Management, Life-Cycle Design and Performance*. Vol. 11, No. 10, 2015, pp. 1306 - 1322.
- FLOODS AND RESERVOIR SAFETY. 1996: Institution of Civil Engineers, Thomas Telford Publications.
- FRANCA, M.J., ALMEIDA, A.B. 2004: A computational model of rock-fill dam breaching caused by overtopping (RoDaB). *Journal of Hydraulic Research*, Vol. 42, No. 2, 2004, pp. 197-206.
- FREAD, D.L. 1988: Breach: An erosion model for earthen dam failures. NWS, Maryland, 30 p.
- GONČAROV, V.N. 1954: Osnovy dinamiki ruslovyh potokov. Leningrad, Gidrometeorologičeskoje izdatelstvo. 452 p.
- GALOIE, M., ZENZ, G. 2011: One and two dimensional numerical dam-break flow modeling. In the proceedings of the international symposium on UFRIM (Urban Flood Risk Management), Graz, Austria, Sep. 2011, pp. 237-243.
- GLAC, F., ŘÍHA, J. 2012: Výsledky průzkumu poruch ochranných hrází v povodích řek Moravy a Odry. *Vodohospodársky spravodajce*, 2012, pp. 16-19.
- GORAN, G., GORAN, L. 2009: Predicting breach formation through embankment dam. In the proceedings of the International Symposium on Water Management and Hydraulic Engineering, Ohrid, Macedonia, Sep. 2009, paper A98.
- GREGORETTI, C., MALTAURO, A., LANZONI, S. 2010: Laboratory experiments on the failure of coarse homogeneous sediment natural dams on a sloping bed. *Journal of Hydraulic Engineering*, Vol. 136, No. 11, 2010, pp. 868-879.
- HANDBOOK. 2013: The international levee handbook. CIRIA, Griffin Court, 15 Long Lane, London, EC1A 9PN, UK. ISBN: 978-0-86017-734-0.
- HANSON, G.J., TEMPLE, D.M., COOK, K.R. 1999: Dam overtopping resistance and breach processes research. In the proceedings of the 1999 Annual Conference of the Association of State Dam Safety Officials, Oct. 10-13, St. Louis.
- HARTUNG, F., SCHEUERLEIN, H. 1970: Design of dam overflow rock-fill dams. In the proceedings of International Commission on Large Dams, Tenth International Congress on Large Dams, Q36, R.35, Montreal, Canada, June 1-5, 1970, pp. 587-598.

- HOLOMEK, P., ŘÍHA, J. 2000: A comparison of breach modelling methods applied to the Slusovice earth dam. *Dam Engineering*, Vol. 11, No. 3, October 2000, pp. 171-202.
- HUANG, W.C., YU, H.W., WENG, M.C. 2015: Levee reliability analysis for various flood return periods – a case study in southern Taiwan. *Journal of Natural Hazards Earth Syst. Sci.*, 15, pp. 919-930.
- IOOSS, B., LEMAITRE, P. 2014: A review on global sensitivity analysis methods. arXiv preprint arXiv:1404.2405.
- JANDORA, J., ŠPANO, M. 2011: Investigations of maximum discharge at overtopped embankment dams. *Bezpieczeństwo zapor - nowe wyzwania*, Walbrzych, Polsko 2011.
- JANDORA, J., ŘÍHA, J. 2002: Porušení sypaných hrází v důsledku přelití. Work and study of Institute of water structures, Faculty of Civil Engineering, Brno University of Technology, Book 1. ECON Publishing, 2002, 188 p.
- JANDORA, J., ŘÍHA, J. 2008: The failure of embankment dams due to overtopping. Work and study of Institute of Water Structures, Faculty of Civil Engineering, Brno University of Technology, 2008, ISBN: 978-80-214-3527-8.
- JONKMAN, B., VAN GELDER, P., VRIJLING, H. 2002: An overview of quantitative risk measures and their application for calculation of flood risk. In *ESREL 2002 European Conference*.
- JONKMAN, S.N., VAN GELDER, P.H.A.J.M., VRIJLING, J.K. 2003: An overview of quantitative risk measures for loss of life and economic damage. *Journal of Hazardous Materials A99*, 2003, pp. 1-30.
- JUN, B., OH, K. 1998: Yeonchun dam failure and downstream dam-break flood analysis. *Dam Break Modelling*, Parallel Session (parallel43), 02.09.1998.
- KADEŘÁBKOVÁ, J., GOLÍK, P., ŘÍHA, J. 2005: Historické povodně a poruchy ochranných hrází v povodí řeky Moravy. *Vodní hospodářství*, 10/2005, pp. 285-287.
- KNAUSS, J. 1979: Computation of maximum discharge at overflow rock fill dams (a comparison of different model test results). In the proceedings of the 13<sup>th</sup> ICOLD Congress, New Delhi, Q.50–R.9, pp. 143-160.
- KRAMER, H. 1935: Sand mixtures and sand movement in fluvial model. *Transactions of the American Society of Civil Engineers*, Vol. 100, No. 1, pp. 798-838.
- KRATOCHVÍL, J., STARA, V., ŘÍHA, J., JANDORA, J. 2000a: Matematické a fyzikální modelování porušení sypaných hrází v důsledku jejich přelití. *Přehradní den*, Karlovy Vary, 2000a. pp. 41-46.

- KREY, H., 1935: Elberersuche, Prussian Experiment Institute, Berlin (Unpublished report on Elbe experiments).
- LEMPERIERE, F., COURIVAUD, J.R., FRY, J.J. 2006: A new analysis of embankment dam failures by overtopping. Commission International Des Grands Barrages, Barcelona, juin 2006, pp. 1053-1065.
- LEVI, I.I. 1948: Dinamika ruslovykh potokov. Leningrad – Moskva, Gosenergoizdat, 222 p.
- LINFORD, A., SAUNDERS, D.H. 1967: A hydraulic investigation of rough and overflow rock fill dams. Report RR 888, British Hydrodynamics Research Association.
- LOVOLL, A. 2006: Breach formation in rock-fill dams results from Norwegian field tests. Commission International Des Grands Barrages, Barcelona, juin 2006, pp. 35-51.
- MAVIS, F.T., HO, C., TU, Y.C., LIU, T. Y., SOUCEK, E. 1935: The transportation of detritus by flowing water – I. University of Iowa, Studies in Engineering, 54 p.
- MEYER-PETER, E., MÜLLER, R. 1948: Formulas for bed-load transport. In the proceedings of the 2<sup>nd</sup> IAHR Congress, Appendix 2, Stockholm, Sweden, pp. 39-94.
- MCKAY, M.D., BECKMAN, R.J., CONOVER, W.J. 2000: A comparison of three methods for selecting values of input variables in the analysis of output from a computer code. Technometrics, Vol. 42, No. 1, pp. 55-61.
- MORRIS, M.W., HASSAN, M., VASKINN, K.A. 2007: Breach formation: Field test and laboratory experiments. Journal of Hydraulic Research, Vol. 45, Supplement 1, pp. 9-17.
- MORRIS, M.W., HASSAN, M., KORTENHAUS, A., VISSER, P. 2009: Breaching process – a state of the art review. FLOODsite Report T06-06-03. FLOODsite, [www.floodsite.net](http://www.floodsite.net).
- NEILL, C.R. 1967: Mean-velocity criterion for scour of coarse uniform bed-material. In the proceedings of 12<sup>th</sup> conference “International Association for Hydraulic Research”, Stockholm, pp. 46–54.
- PEYRAS, L., ROYET, P., DEROO, L., ALBERT, R., BECUE, J. P., AIGOUY, S., BOURDAROT, E., LOUDIERE, D., KOVARIK, J. B. 2008: French recommendations for limit-state analytical review of gravity dam stability. European Journal of Environmental and Civil Engineering, Vol. 12, No. 9-10.
- PICKERT, G., WEITBRECHT, V., BIEBERSTEIN, A. 2011: Breaching of overtopped river embankments controlled by apparent cohesion. Journal of Hydraulic Research, Vol. 49, No. 2, 2011, pp. 143-156.
- POWLEDGE, G.R., RALSTON, D.C., MILLER, P., CHEN, Y.H., CLOPPER, P.E., TEMPLE, D.M. 1989: Mechanics of overflow erosion of embankments. II. Hydraulic and Design

- Considerations. *Journal of Hydraulic Engineering*, Vol. 115, No. 8, August 1989, pp. 1056-1075.
- RAJ, D. 1968: *Sampling theory*. New York, McGraw-Hill, 1968.
- ROYET, P., PEYRAS, L. 2010: New French guidelines for structural safety of embankment dams in a semi-probabilistic format. IECS 2010, 8<sup>th</sup> ICOLD European Club Symposium Dam Safety - Sustainability in a Changing Environment, Innsbruck, Austria. ATCOLD Austrian National Committee on Large Dams, pp. 353-358.
- ROYET, P., PEYRAS, L. 2013: French guidelines for structural safety of gravity dams in a semi-probabilistic format. In the proceedings of the 9<sup>th</sup> ICOLD European Club Symposium, Venice, Italy, April 10-12, 2013, pp. 1-8. European Club of ICOLD. 2013.
- ŘÍHA, J. 2010: *Ochranné hráze na vodních tocích*. Grada Publishing, a.s., ISBN 978-80-247-3570-2.
- ŘÍHA, J. a kol. 2005: *Riziková analýza záplavových území*. Work and study of Institute of water structures, Faculty of Civil Engineering, Brno University of Technology, Book 7, CERM, 286 s., ISBN 80-7204-404-4.
- ŘÍHA, J. a kol. 2008: *Úvod do rizikové analýzy přehrad*. Work and study of Institute of water structures, Faculty of Civil Engineering, Brno University of Technology, Book 11, CERM, 2008, ISBN 978-80-7204-608-9.
- ŘÍHA, J., DANĚČEK, J. 2000: Matematické modelování porušení sypaných hrází v důsledku přelití. *Journal Hydrology and Hydromechanics*, Vol. 48, No. 3, 2000, pp. 165-179. ISSN 0042-790X.
- ŘÍHA, J., PARILKOVA, J., ŠPANO, M., ZACHOVAL, Z. 2009: Proposals for increasing the safety and reliability of river levees under changed climate conditions. Preparation and design of physical experiments, Brno University of Technology, Faculty of Civil Engineering, Institute of Water Structures.
- ROGER, S., DEWALS, B.J., ERPICUM, S., SCHWANENBERG, D., SCHÜTTRUMPF, H., KÖNGETER, J., PIROTON, M. 2009: Experimental and numerical investigations of dike-break induced flows. *Journal of Hydraulic Research*, Vol. 47, No. 3, 2009, pp. 349-359.
- ROZOV, A.L. 2003: Modelling of washout of dams. *Journal of Hydraulic Research*, Vol. 41, No. 6, 2003, pp. 565-577.
- ŠAMOV, G.I. 1959: *Rečnyje nanosy. Režim, rasčety I metody izmerenij*. Leningrad, Gidrometeoizdat, 375 p.

- SCHMOCKER, L., HAGER, W.H. 2009: Modelling dike breaching due to overtopping. *Journal of Hydraulic Research*, Vol. 47, No. 5, 2009, pp. 585-597.
- SCHMOCKER, L., HAGER, W.H. 2012: Plane dike-breach due to overtopping: effects of sediment, dike height and discharge. *Journal of Hydraulic Research*, Vol. 50, No. 6, 2012, pp. 576-586.
- SCHOKLITSCH, A. 1952: *Handbuch des Wasserbaues II*. Wien, Springer-Verlag, pp. 479-1072.
- SHIELDS, A. 1936: Application of similarity principles and turbulence research to bed-load movement. Translated from: "Anwendung der Aehnlichkeitsmechanik und der Turbulenzforschung auf die Geschiebebewegung", *Mitteilungen der Preußischen Versuchsanstalt für Wasserbau*, Berlin, 1936.
- SINGH, V.P. 1996: *Dam breach modeling technology*. Kluwer Academic Publishers, Dordrecht, Netherlands, 1996. ISBN: 0-7923-3925-8.
- SOARES-FRAZAO, S., IAHR working group for dam-break flows over mobile beds. 2012: Dam-break flows over mobile beds: experiments and benchmark tests for numerical models. *Journal of Hydraulic Research*, Vol. 50, No. 4, 2012, pp. 364-375.
- STEINBERG, H.A. 1963: Generalized quota sampling. *Nuclear Science and Engineering*, pp. 142-145.
- TINGSANCHALI, T., CHINNARASRI, C. 2001: Numerical modelling of dam failure due to flow overtopping. *Hydrological Sciences Journal*, Feb. 2001, pp. 113-130. ISSN: 0262-6667.
- TOLEDO, M.A., PISFIL, M.B., DIE MORAN, A. 2006: Initiation phase of rockfill dams breaching by overtopping. *Commission International Des Grands Barrages*, Barcelona, June 2006, pp. 507-517.
- United State Army Corps of Engineering. 1999: Risk-based analysis in geotechnical engineering for support of planning studies. ETL 1110-2-556, May 28, 1999.
- VISSER, P.J. 1988: A model for breach growth in a dike-burst. In the proceedings of 21<sup>st</sup> International Conference of Coastal Engineering, Malaga, Spain, pp. 1897-1910.
- VISSER, P.J. 1994: A model for breach growth in sand-dikes. In the proceedings of 24<sup>th</sup> International Conference of Coastal Engineering, Kobe, Japan, pp. 2755-2769.
- VOTRUBA, L., HEŘMAN, J., a kol. 1993: *Spolehlivost vodohospodářských děl*. Česká matice technická v ZN Brázda Praha, ISBN 80-209-0251-1.

- WAHL, T.L. 1997: Predicting embankment dam breach parameters - A needs assessment. In the proceedings of the XXV IAHR Congress, San Francisco, California, August 10-15, 1997, pp. 48-53. ISSN: 0074-1477.
- WAHL, T.L. 1998: Predicting of embankment dam breach parameters - A literature review and needs assessment. Dam safety research report, DSO-98-004 Dam Safety Office. Water Resources Research Laboratory, July 1998.
- WALFF, T.F. 2008: Reliability of levee systems. In Reliability-based design in geotechnical engineering. Taylor & Francis Group, New York. pp. 448 - 496.
- WANG, P., KAHAWITA, R., PHAT, T.M., QUACH, T.T. 2006: Modelling breach formation in embankments due to overtopping. Commission International Des Grands Barrages, Barcelona, June 2006, pp. 377-396.
- WANG, Z., BOWLES, D.S. 2006: Three-dimensional non-cohesive earthen dam breach model. Part 1: Theory and methodology. Advances in Water Resources, Vol. 29, No. 10, October 2006, pp. 1528-1545.
- WU, W. (corresponding author), ASCE/EWRI Task Committee on Dam/Levee Breaching. 2011: Earth embankment breaching. Journal of Hydraulic Engineering, Vol. 137, No. 12, pp. 1549-1564. 10.1061/(ASCE)HY.1943-7900.0000498.



## NOTATION

$a, b$	Parameters of the uniform distribution	[-]
$A_b$	Breach cross-sectional area	[m <sup>2</sup> ]
$b$	Average breach width	[m]
$b_0$	Initial value of the overtopping width along the dike crest	[m]
$b_1$	Breach width at the breach top	[m]
$b_2$	Breach width at the breach bottom	[m]
$B_c$	the cross-sectional width of the dike crest	[m]
$F$	The dike failure	[%]
$g$	Acceleration of gravity	[m/sec <sup>2</sup> ]
$h$	Water depth in the breach or the overflow head	[m]
$h_b$	Breach depth	[m]
$h_f$	Water depth along the downstream slope	[m]
$h_s$	Water level in the stream	[m] above SWL
$J$	Number of intervals with the same probability	[-]
$K$	Number of input parameters	[-]
$L$	Set of load variables applied to the dike	[corresponding variable unit]
$m$	Discharge coefficient for broad-crested weir	[-]
$M_i$	Number of simulations realizing the outcome ( $i$ )	[-]
$n$	Manning's roughness coefficient	[-]
$N$	Return period of the flood wave	[year]
$N_{total}$	Total number of simulations	[-]
$p_n$	The probability that the $Q_N$ will be reached or exceeded	[%]
$P$	The probability of the peak discharge $Q_N$	[%]
$P_B$	The probability of dike breaching due to overtopping	[%]
$P_E$	The probability of dike erosion	[%]
$P_F$	The probability of arrival of the corresponding flood wave	[%]
$P_i$	The probability of each typical $i$ -th phase of the dike breach	[%]
$P_O$	The probability of dike overtopping	[%]
$q_{cr}$	Critical specific discharge	[m <sup>2</sup> /s]
$Q$	Discharge of the flood wave	[m <sup>3</sup> /s]
$Q_b$	The breach discharge	[m <sup>3</sup> /s]

$Q_{bmax}$	The maximum breach discharge	[m <sup>3</sup> /s]
$Q_N$	Peak discharge of the flood wave with $N$ return period	[m <sup>3</sup> /s]
$R$	The dike reliability	[%]
$R_i$	Reference value for each input parameter	[corresponding parameter unit]
$S$	Set of strength (resistance) variables of the dike	[corresponding strength unit]
$s$	Average breach side slope factor	[-]
$t$	Time	[s]
$t_b$	Time of beginning of the dike breaching	[s]
$t_d$	Time interval specifies the duration of the horizontal limb of the flood wave	[s]
$t_e$	Time of beginning of the dike erosion	[s]
$t_k$	Time interval specifies the duration of the ascending limb of the flood wave	[s]
$t_{max}$	Time of reaching to the maximum breach discharge	[s]
$t_o$	Time of beginning of the dike overtopping	[s]
$v_f$	Mean cross-sectional flow velocity at the downstream slope	[m/s]
$v_{non}$	Non-scouring velocity	[m/s]
$\mathbf{V}_i$	The vector of serial values of input parameter	[corresponding parameter unit]
$Z$	Elevation of breach opening bottom during the erosion process	[m] above SWL
$Z_c$	Dike crest elevation	[m] above SWL
$\alpha_1, \alpha_2$	Empirical coefficients expressing the erodibility of the dike material	[-]
$\beta$	Angle of downstream slope	[degree]
$\tau_{cr}$	The critical shear stress	[Pa]

## LIST OF ABBREVIATIONS

1D	One Dimensional
3D	Three Dimensional
BS	Branch Standards
CDF	Cumulative Distribution Function
CHMI	Czech Hydro-Meteorological Institute
ČHMÚ	Český Hydrometeorologický Ústav
CNS	Czech National Standards
ETA	Event Tree Analysis
FDM	Finite Differences Method
FMEA	Failure Modes and Effect Analysis
FTA	Fault Tree Analysis
LHS	Latin Hypercube Sampling
MC	Monte Carlo
OAT	One-At-a-Time
TBD	Technicko-Bezpečnostní Dohled
U	Uniform distribution
USA	United States of America

## LIST OF TABLES

Table 6.1	Allowable critical shear stress and non-scouring velocities for grass cover (Hanson et al. 1999) .....	29
Table 8.1	Values of coefficient $\alpha_1$ derived from calibration of real dam breaches .....	45
Table 9.1	One combination of pseudo-random permutations for two parameters with $J = 6$ using the LHS method (Raj 1968) .....	50
Table 10.1	Values of $N$ and $Q_N$ (provided by the ČHMÚ) .....	53
Table 10.2	Reference values ( $R_i$ ) of input parameters .....	54
Table 11.1	parameters of uniform distribution $U(a, b)$ .....	62
Table 11.2	Probabilities of the typical phases and comparison with the value obtained from equation 10.1 .....	63
Table 11.3	Probabilities of the typical phases for different lining materials and comparison with the value obtained from equation 10.1 .....	64

## LIST OF FIGURES

Fig. 2.1	Event tree for dike breaching due to overtopping .....	8
Fig. 4.1	Time related parameters of the dike breaching due to overtopping .....	18
Fig. 4.2	Dike cross section and idealized trapezoidal shape of the breach opening according to Jandora and Říha (2008) .....	19
Fig. 4.3	Occurrence of individual failure modes as a percentage of all modes, for dikes in the Morava river basin during the period from 1965 to 2004 (Kadeřábková et al. 2005) .....	20
Fig. 4.4	Percentages by damage type of the extent of dike damage in the Morava river basin during the period from 1965 to 2004 (Kadeřábková et al. 2005) .....	21
Fig. 4.5	Occurrence of individual failure modes as a percentage of all modes, for dikes in the Odra river basin during the period from 1960 to 2009 (Glac and Říha 2012) .....	21
Fig. 5.1	Flow and erosion regimes during dike overtopping (Powledge et al. 1989) ....	23
Fig. 5.2	Diagram depicting dike failures due to overtopping .....	23
Fig. 5.3	Diagram of progress of a homogeneous sandy dike failure (Fread 1988) .....	24
Fig. 6.1	Critical specific discharge for downstream rock fill lining (Knauss 1979) ....	28
Fig. 6.2	Non-scouring velocity for selected types of surfaces as a function of overflowing time (Floods and reservoir safety 1996) .....	28
Fig. 6.3	Diagram of the failure of a dike due to overtopping .....	31
Fig. 6.4	First phase: no overtopping .....	31
Fig. 6.5	Second phase: overtopping - no erosion .....	31
Fig. 6.6	Third phase: erosion - no collapse .....	32
Fig. 6.7	Fourth phase: dike collapse .....	32
Fig. 7.1	Schematic diagram of the events during the process of dike breaching due to overtopping .....	36
Fig. 7.2	Event tree of the process of dike breaching due to overtopping .....	37
Fig. 7.3	Event tree for estimating the probability of dike breaching due to overtopping .....	38
Fig. 7.4	Definition of the reliability and the failure of a dike according to equations (7.1 and 7.2) .....	40
Fig. 8.1	Proposed section of the dike breach opening .....	42

Fig. 8.2	Schematization of the flood hydrograph at two gauge stations on the Dyje river .....	47
Fig. 9.1	Generating random values of an input parameter with intervals $J = 10$ .....	51
Fig. 10.1	Location of the potential breach at the Dyje river .....	52
Fig. 10.2	Dike cross-section at the location of potential breach .....	52
Fig. 10.3	Original and interpolated curves of the $v_{non}$ (Floods and reservoir safety 1996).55	
Fig. 10.4	Sensitivity analysis results .....	56
Fig. 10.5	Fitting curve expressing the $(P, Q_N)$ created via MATLAB software .....	57
Fig. 10.6a	Triangular flood wave hydrograph $(Q, t)$ created via MATLAB software .....	58
Fig. 10.6b	Trapezoidal flood wave hydrograph $(Q, t)$ created via MATLAB software ....	58
Fig. 10.7	Stage-discharge curve at the Břeclav-Ladná gauging station .....	59
Fig. 10.8a	Water level in the river $(h_s, t)$ created via MATLAB software corresponding to triangular hydrograph (Fig. 10.6a) .....	59
Fig. 10.8b	Water level in the river $(h_s, t)$ created via MATLAB software corresponding to trapezoidal hydrograph (Fig. 10.6b) .....	59
Fig. 11.1a	Probabilities [%] of the typical phases of dike breaching due to overtopping ..	63
Fig. 11.1b	Probabilities [%] of the typical phases of dike breaching due to overtopping ..	63
Fig. 11.2a	Probabilities [%] of the typical phases for different lining materials .....	64
Fig. 11.2b	Detailed Probabilities [%] of individual typical phases for different lining materials .....	64

## PUBLICATIONS OF THE AUTHOR

- ALHASAN, Z. 2013. Numerical model of the dike failure due to overtopping, the river of Morava, the city of Hodonin. In the proceedings of the 15<sup>th</sup> International Conference of PhD Students (JUNIORSTAV 2013), 7.2.2013, Brno University of Technology, Faculty of Civil Engineering, ISBN 978-80-214-4669-4, pp. 323.
- ALHASAN, Z., DRÁB, A., ŘÍHA, J. 2013. Matematické modelování porušení ochranné hráze na Dyji v Břeclavi v důsledku přelití. *Vodní Hospodářství*, 6/2013, Ročník 63, 6319 ISSN 1211-0760, pp. 202-206.
- ALHASAN, Z., DRÁB, A., ŘÍHA, J. 2013. Mathematical model of dike failure due to overtopping at the river Dyje at Breclav. In the proceedings of the XV Dam Monitoring International Conference, June 18 – 21, 2013, Jastrzębia Góra, Poland, ISBN 978-83-61102-81-6, pp. 245-255.
- ALHASAN, Z., JANDORA, J., ŘÍHA, J. 2013. Scour resistance of dike materials at downstream slope during overtopping. In the proceedings of the 13<sup>th</sup> International Symposium on Water Management and Hydraulic Engineering, September 9 – 12, 2013, Bratislava, Slovakia, ISBN978-80-227-4002-9, pp. 12.
- ALHASAN, Z., JULÍNEK, T., ŘÍHA, J., DUCHAN, D. 2014. Critical hydraulic gradient for uniform homogenous glass beads. In the proceedings of the 8<sup>th</sup> Scientific-Technical Conference, October 23 – 25, 2014, St. Petersburg, Russia, pp. 24-27.
- ALHASAN, Z., JANDORA, J., ŘÍHA, J. 2015. Study of Dam-break Due to Overtopping of Four Small Dams in the Czech Republic. *Journal of Acta Universitatis Agriculturae et Silviculturae Mendelianae Brunensis*, Vol. 63, No. 3, ISSN 1211-8516, pp. 717-729.
- ALHASAN, Z., HALA, M., JULÍNEK, T., ŘÍHA, J. 2015. Discussion on the critical hydraulic gradient for uniform homogenous glass beads. In the proceedings of the XVI Dam Monitoring International Conference, September 29 – October 2, 2015, Wierchomla, Poland, ISBN: 978-83-64979-09-5, pp. 165-172.
- ALHASAN, Z., JANDORA, J., ŘÍHA, J. 2016. Comparison of specific sediment transport rates obtained from empirical formulae and dam breaching experiments. *Environmental Fluid Mechanics*, ISSN 1567-7419, DOI: 10.1007/s10652-016-9463-2, Springer Netherlands, Published online: 14 June 2016, pp. 1-23.
- ALHASAN, Z., DUCHAN, D., ŘÍHA, J. The probabilistic solution of dike breaching due to overtopping. In the proceedings of the 4<sup>th</sup> IAHR Europe Congress, Liege, Belgium, 27–29 July 2016, Taylor & Francis Group, London, ISBN 978-1-138-02977-4, pp. 93.

## LIST OF APPENDICES

A.	Results of the sensitivity analysis .....	83
B.	An example of the source code created via MATLAB software for the sensitivity analysis procedure .....	85
C.	An example of the source code created via MATLAB software for estimating the probabilities of the typical phases of dike breaching due to overtopping .....	87



## Appendix A

### Results of the sensitivity analysis

**Table A.1** Values of the input parameters used for the sensitivity analysis

Input parameter	$0.7R_i$	$0.8R_i$	$0.9R_i$	$R_i$	$1.1R_i$	$1.2R_i$	$1.3R_i$
$Q_N$	574	656	738	820	902	984	1066
$t_k$	58.8	67.2	75.6	84	92.4	100.8	109.2
$t_d$	42	48	54	60	66	72	78
$b_0$	1.4	1.6	1.8	2	2.2	2.4	2.6
$n$	0.0245	0.028	0.0315	0.035	0.0385	0.042	0.0455
$\alpha_1$	0.0007	0.0008	0.0009	0.001	0.0011	0.0012	0.0013
$\alpha_2$	$88 \cdot 10^{-6}$	$100 \cdot 10^{-6}$	$113 \cdot 10^{-6}$	$125 \cdot 10^{-6}$	$138 \cdot 10^{-6}$	$150 \cdot 10^{-6}$	$163 \cdot 10^{-6}$
Input parameter	$0.86R_i$	$0.9R_i$	$0.96R_i$	$R_i$	$1.04R_i$	$1.1R_i$	$1.14R_i$
$m$	0.301	0.315	0.336	0.35	0.364	0.385	0.399
Input parameter	-	$0.81R_i$	$0.91R_i$	$R_i$	$1.04R_i$	$1.1R_i$	-
$v_{non}$	-	3	3.35	3.7	4.175	4.65	-

**Table A.2** Values of  $Q_N$  and resulted  $Q_{bmax}$  used for Fig. 10.4

Input parameter	$0.7R_i$	$0.8R_i$	$0.9R_i$	$R_i$	$1.1R_i$	$1.2R_i$	$1.3R_i$
$Q_N$	574	656	738	820	902	984	1066
$V_i / R_i$	0.7	0.8	0.9	1	1.1	1.2	1.3
$Q_{bmax}(V_i)$	511.15	919.43	1315.79	1695.75	2059.40	2430.98	2813.62
$Q_{bmax}(V_i) / Q_{bmax}(R_i)$	0.30	0.54	0.78	1.00	1.21	1.43	1.66

**Table A.3** Values of  $t_k$  and resulted  $Q_{bmax}$  used for Fig. 10.4

Input parameter	$0.7R_i$	$0.8R_i$	$0.9R_i$	$R_i$	$1.1R_i$	$1.2R_i$	$1.3R_i$
$t_k$	58.8	67.2	75.6	84	92.4	100.8	109.2
$V_i / R_i$	0.7	0.8	0.9	1	1.1	1.2	1.3
$Q_{bmax}(V_i)$	1393.26	1493.97	1594.76	1695.75	1796.82	1897.98	1999.23
$Q_{bmax}(V_i) / Q_{bmax}(R_i)$	0.82	0.88	0.94	1.00	1.06	1.12	1.18

**Table A.4** Values of  $t_d$  and resulted  $Q_{bmax}$  used for Fig. 10.4

Input parameter	$0.7R_i$	$0.8R_i$	$0.9R_i$	$R_i$	$1.1R_i$	$1.2R_i$	$1.3R_i$
$t_d$	42	48	54	60	66	72	78
$V_i / R_i$	0.7	0.8	0.9	1	1.1	1.2	1.3
$Q_{bmax}(V_i)$	1488.05	1557.28	1626.51	1695.75	1764.99	1834.24	1903.49
$Q_{bmax}(V_i) / Q_{bmax}(R_i)$	0.88	0.92	0.96	1.00	1.04	1.08	1.12

**Table A.5** Values of  $b_0$  and resulted  $Q_{bmax}$  used for Fig. 10.4

Input parameter	$0.7R_i$	$0.8R_i$	$0.9R_i$	$R_i$	$1.1R_i$	$1.2R_i$	$1.3R_i$
$b_0$	1.4	1.6	1.8	2	2.2	2.4	2.6
$V_i / R_i$	0.7	0.8	0.9	1	1.1	1.2	1.3
$Q_{bmax}(V_i)$	1692.38	1693.50	1694.62	1695.75	1696.87	1697.99	1699.11
$Q_{bmax}(V_i) / Q_{bmax}(R_i)$	1.00	1.00	1.00	1.00	1.00	1.00	1.00

**Table A.6** Values of  $m$  and resulted  $Q_{bmax}$  used for Fig. 10.4

Input parameter	$0.86R_i$	$0.9R_i$	$0.96R_i$	$R_i$	$1.04R_i$	$1.1R_i$	$1.14R_i$
$m$	0.301	0.315	0.336	0.35	0.364	0.385	0.399
$\mathbf{V}_i / R_i$	0.86	0.9	0.96	1	1.04	1.1	1.14
$Q_{bmax}(\mathbf{V}_i)$	1369.75	1460.78	1600.54	1695.75	1792.49	1940.40	2040.94
$Q_{bmax}(\mathbf{V}_i) / Q_{bmax}(R_i)$	0.81	0.86	0.94	1.00	1.06	1.14	1.20

**Table A.7** Values of  $n$  and resulted  $Q_{bmax}$  used for Fig. 10.4

Input parameter	$0.7R_i$	$0.8R_i$	$0.9R_i$	$R_i$	$1.1R_i$	$1.2R_i$	$1.3R_i$
$n$	0.0245	0.028	0.0315	0.035	0.0385	0.042	0.0455
$\mathbf{V}_i / R_i$	0.7	0.8	0.9	1	1.1	1.2	1.3
$Q_{bmax}(\mathbf{V}_i)$	2114.49	1946.81	1810.39	1695.75	1597.92	1513.11	1438.78
$Q_{bmax}(\mathbf{V}_i) / Q_{bmax}(R_i)$	1.25	1.15	1.07	1.00	0.94	0.89	0.85

**Table A.8** Values of  $\alpha_1$  and resulted  $Q_{bmax}$  used for Fig. 10.4

Input parameter	$0.7R_i$	$0.8R_i$	$0.9R_i$	$R_i$	$1.1R_i$	$1.2R_i$	$1.3R_i$
$\alpha_1$	0.0007	0.0008	0.0009	0.001	0.0011	0.0012	0.0013
$\mathbf{V}_i / R_i$	0.7	0.8	0.9	1	1.1	1.2	1.3
$Q_{bmax}(\mathbf{V}_i)$	1695.75	1695.75	1695.75	1695.75	1695.75	1695.75	1695.75
$Q_{bmax}(\mathbf{V}_i) / Q_{bmax}(R_i)$	1.00	1.00	1.00	1.00	1.00	1.00	1.00

**Table A.9** Values of  $\alpha_2$  and resulted  $Q_{bmax}$  used for Fig. 10.4

Input parameter	$0.7R_i$	$0.8R_i$	$0.9R_i$	$R_i$	$1.1R_i$	$1.2R_i$	$1.3R_i$
$\alpha_2$	$88 \cdot 10^{-6}$	$100 \cdot 10^{-6}$	$113 \cdot 10^{-6}$	$125 \cdot 10^{-6}$	$138 \cdot 10^{-6}$	$150 \cdot 10^{-6}$	$163 \cdot 10^{-6}$
$\mathbf{V}_i / R_i$	0.7	0.8	0.9	1	1.1	1.2	1.3
$Q_{bmax}(\mathbf{V}_i)$	1190.39	1358.84	1527.29	1695.75	1864.20	2032.65	2201.10
$Q_{bmax}(\mathbf{V}_i) / Q_{bmax}(R_i)$	0.70	0.80	0.90	1.00	1.10	1.20	1.30

**Table A.10** Values of  $v_{non}$  and resulted  $Q_{bmax}$  used for Fig. 10.4

Input parameter	$0.81R_i$	$0.91R_i$	$R_i$	$1.04R_i$	$1.1R_i$
$v_{non}$	3	3.35	3.7	4.175	4.65
$\mathbf{V}_i / R_i$	0.81	0.91	1	1.13	1.26
$Q_{bmax}(\mathbf{V}_i)$	1712.00	1705.43	1695.75	1683.39	1668.24
$Q_{bmax}(\mathbf{V}_i) / Q_{bmax}(R_i)$	1.01	1.01	1.00	0.99	0.98

## Appendix B

### An example of the source code created via MATLAB software for the sensitivity analysis procedure

This MATLAB code includes the sensitivity analysis of  $Q_N$ .

```
clear all
clc
QN = [574 656 738 820 902 984 1066];
MAX=QN;
for i=1:length(QN)
    QNi = QN(i);
    tk = 84;
    td = 60;
    tf = 4*tk+td; % tf : flood duration [hours].
    t=(0:1:tf*60);% time step [min].
    Q=t;
    for a = 1:(tf*60)+1 % matrix of flood duration.
        if a <= tk*60 % ascending limb.
            Q(a) = (a-1)*QNi/(tk*60);
        elseif a <= tk*60 + td*60 % horizontal limb.
            Q(a) = QNi;
        else % descending limb.
            Q(a) = ((tf*60)-(a-1))*QNi/(3*(tk*60));
        end
    end
    EXLdata = xlsread('hsQ.xlsx'); % Import data from EXCEL file.
    x = EXLdata(:,1); % Q values.
    y = EXLdata(:,2); % hs values.
    hs = interp1(x,y,Q,'spline'); % Interpolation function.
    Zc = 162.41; % elevation of the left-side dike crest [m] above SWL.
    b0 = 2; m = 0.35; g = 9.81;
    Qb0 = hs;
    for a=1:length(hs)
        if hs(a) <= Zc
            Qb0(a) = 0;
        else
            Qb0(a) = m*b0*sqrt(2*g)*(hs(a)-Zc)^1.5;
        end
    end
    n = 0.035; % Manning's roughness coefficient (for grass).
    beta = 19.43;% inclination angle of downstream slope [degree].
    hf0 = (Qb0*n/b0/sqrt(sind(beta))).^0.6; % water depth at down. slope.
    vf0 = sqrt(sind(beta))/n*hf0.^(4/6); % velocity at downstream slope.
    t0_hours = vf0;
    t0_hours(:)= 0;
    for a=1:length(vf0)-1
        if vf0(a+1)== 0
            t0_hours(a+1)=0;
        else
            t0_hours(a+1)=t0_hours(a)+1/60;
        end
    end
    end
    v0_non = t0_hours;
    for a=1:length(t0_hours)
        if t0_hours(a)== 0
            v0_non(a)=0;
        else
    
```

```

        v0_non(a)=3.7811*t0_hours(a)^(-0.246);
    end
end
alfa1=0.001;
delta0_z = v0_non;
delta0_z(:) = 0;
for a=1:length(v0_non)
    if vf0(a)<= v0_non(a)
        delta0_z(a) = 0;
    else
        delta0_z(a) = alfa1*vf0(a)*60; % delta(t)=1 [min]= 60 [sec].
    end
end
Zt = 160.23; % terrain elevation [m] above SWL.
Zd0 = delta0_z;
Zd0(:)= Zc;
for a=1:length(delta0_z)-1
    if Zd0(a)-delta0_z(a+1)<= Zt
        Zd0(a+1) = Zt;
    else
        Zd0(a+1) = Zd0(a)-delta0_z(a+1);
    end
end
Bc = 2.95; % width of the dike crest [m].
s = (6.18/2.18); % downstream slope.
Zu0 = Zd0;
Zu0(:) = Zc;
for a=1:length(Zd0)-1
    if Zu0(a)-delta0_z(a+1) <= Zt
        Zu0(a+1) = Zt;
    else
        if Zd0(a+1) >= (Zc - Bc/s)
            Zu0(a+1) = Zc;
        else
            Zu0(a+1) = Zu0(a)-delta0_z(a+1);
        end
    end
end
alfa2 = 0.000125;
b = Zu0;
b(:) = b0;
for a=1:length(Zu0)-1
    if and (Zd0(a+1)==Zc , vf0(a+1)<= v0_non(a+1))
        b(a+1) = b0;
    else
        b(a+1) = b(a)+alfa2*vf0(a+1)*60; % delta(t)=1[min]=60[sec].
    end
end
Qb=b;
Qb(:)=0;
for a=1:length(b)
    if hs(a) <= Zu0(a)
        Qb(a) = 0;
    else
        Qb(a)= m*b(a)*sqrt(2*g)*(hs(a)-Zu0(a))^1.5;
    end
end
Qb=real(Qb);
MAX(i)=max(Qb);
end

```

## Appendix C

### An example of the source code created via MATLAB software for estimating the probabilities of the typical phases of dike breaching due to overtopping

This MATLAB code includes estimating the probability of typical stages of dike breaching in case 1 for dike crest elevation equals to  $Z_c = h_s(Q_{10})$ .

```
clear all
clc
tic;
wb = waitbar(0, 'Please wait...');
wb1=0;

%% Generating random numbers using LHS method.
% separated LHS generator will be used for QN.
% LHS method is specified that the random values equal to the midpoint of
those intervals of each variable.
M1 = 50; % Number of intervals with equal probability, i.e. number of
random values of QN > Q10: (Zc = hs(Q10)).
x1 = lhsdesign(M1,1,'smooth','off'); % The main interval is [0 - 1]; QN
will have M1 values represent the midpoints of subintervals.
V1 = x1; % the first variable is QN.

Vi = 5; % Number of other variables: (tk, td, m, n, alfa2).
M2 = 10; % Number of intervals (equal probability) of each variable, i.e.
number of random values of each variable.
x2 = lhsdesign(M2,Vi,'smooth','off'); % The main interval is [0 - 1]; each
variable will have M2 values represent the midpoints of subintervals.
V2 = x2(:,1); % tk.
V3 = x2(:,2); % td.
V4 = x2(:,3); % m.
V5 = x2(:,4); % n.
V6 = x2(:,5); % alfa2.

% Input: Return periods N and Peak discharge corresponding to N.
N = [0 1 2 5 10 20 50 100 500 1000 10000];
pN = 1-exp(-N.^-1);
P = 1-pN;
QN = [0 160 230.9 341.4 436.4 540.8 693.3 820 1154.8 1320 1920];

% Defining the fitted curve [X=(QN) , Y=(P)].
% Fit: 'Fit(X=(QN) , Y=(P))'.
[xData1 , yData1] = prepareCurveData (QN , P);
% Set up fitttype and options.
ft1 = fitttype( 'smoothingspline' );
% Fit model to data.
[fittedmodell1, gof1] = fit( xData1, yData1, ft1 ); % fittedmodell1: is the
function identifying the graph (X=(QN) , Y=(P)).
QN_design = 436.4; % [m3/s]: The design peak discharge = Q10.
P_design = fittedmodell1(QN_design); % Probability of the peak discharge
QN_design.

case_1 = zeros(M1,M2,M2,M2,M2,M2); % no overtopping.
case_2 = zeros(M1,M2,M2,M2,M2,M2); % overtopping - no erosion.
case_3 = zeros(M1,M2,M2,M2,M2,M2); % overtopping + erosion - no breaching.
case_4 = zeros(M1,M2,M2,M2,M2,M2); % overtopping + erosion + breaching.
```

```

% V1 : QN
[xData2 , yData2] = prepareCurveData (P , QN);
ft2 = fittype( 'smoothingspline' );
[fittedmodel2, gof2] = fit( xData2, yData2, ft2 );% graph (X=(P),Y=(QN)).

P_min = P_design;
P_max = 1;
P_i = V1;
QN_i = V1; % [m3/s].

for a1 = 1:length(V1)
    P_i(a1) = P_min + (P_max - P_min) * V1(a1); % Probability of flood
    arrival. The midpoint of the interval.
    QN_i(a1) = fittedmodel2(P_i(a1)); % [m3/s] : Peak discharge
    corresponding to P_i.

    % V2 : tk
    % Determining the flood hydrograph (flood duration and flood shape).
    % Flood duration (tf) = tk + td + 3.tk.
    % Determining (tk) : depending on the 2002 and 2006 flood events.
    tk_min = 48; % [hour] = 2 days.
    tk_max = 120; % [hour] = 5 days.
    tk_i = V2;

    for a2 = 1:length(V2)
        tk_i(a2) = tk_min + (tk_max - tk_min) * V2(a2); % [hour].

        % V3: td
        % Determining (td) : depending on the 2002 and 2006 flood events.
        td_min = 0; % [hour] this represents the triangular shape of the
        flood wave.
        td_max = 120; % [hour] this represents the trapezoidal shape of the
        flood wave.
        td_i = V3; % [hour].

        for a3 = 1:length(V3)
            td_i(a3) = td_min + (td_max - td_min) * V3(a3); % [hour].

            tf = 4*tk_i(a2) + td_i(a3); % [hour]: the total flood duration.

            % Determining the Hydrograph Q(t) of the flood wave.
            t = (0:1:tf*60); % time step [min].
            [m1,n1]=size(t);
            Q = zeros(m1,n1);
            for a = 1:(tf*60)+1
                % matrix of flood duration.
                if a <= tk_i(a2)*60
                    % ascending limb.
                    Q(a) = (a-1)*QN_i(a1)/(tk_i(a2)*60);
                elseif a <= tk_i(a2)*60 + td_i(a3)*60 % horizontal limb.
                    Q(a) = QN_i(a1);
                else
                    % descending limb.
                    Q(a) = ((tf*60)-(a-1))*QN_i(a1)/(3*(tk_i(a2)*60));
                end
            end
        end
    end
end

```

```

% Determining the flood wave characteristic hs(t).
% Defining the hs(Q) curve : in the EXCEL file(Stage-Discharge
Curve, Břeclav-Ladná Gauging Station).

EXLdata = xlsread('hsQ.xlsx'); % Import data from EXCEL file
under this name 'hsQ.xlsx'.
x = EXLdata(:,1); % Q values.
y = EXLdata(:,2); % hs values.
hs = interp1(x,y,Q,'spline'); % Interpolation function.

% V4 : m
% Determining the initial overtopping characteristics (Qb0,
hf0, vf0, vnon0, Zd0, Zu0) based on b0 = 2 [m].
% Determining the elevation of the dike crest as follows:
Zc = hs(QN_design).

Zc = interp1(x,y,QN_design,'spline');
b0 = 2;
m_min = 0.3; % proposed min value of discharge coefficient.
m_max = 0.4; % proposed max value of discharge coefficient.
m_i = V4;

for a4 = 1:length(V4)
    m_i(a4) = m_min + (m_max - m_min)*V4(a4);

    g = 9.81;
    Qb0 = zeros(m1,n1);
    for a=1:length(hs)
        if hs(a) > Zc
            Qb0(a) = m_i(a4) * b0 * sqrt(2*g) * (hs(a)-Zc)^1.5;
        end
    end

% V5: n
% Determining initial characteristics (hf0[m],vf0[m/s]).
beta = 19.43; %[degree]inclination angle of downstream slope.
n_min = 0.025; % proposed min value of Manning's roughness
coefficient (for grass).
n_max = 0.045; % proposed max value of Manning's roughness
coefficient (for grass).
n_i = V5;

for a5 = 1:length(V5)
    n_i(a5) = n_min + (n_max - n_min)*V5(a5);
    hf0 = (Qb0*n_i(a5)/b0/sqrt(sind(beta))).^0.6; % water
depth at downstream slope.
    vf0 = sqrt(sind(beta))/n_i(a5)*hf0.^(4/6); % velocity
at downstream slope.
    % Determining the initial erosion process and
conditions (non-scouring velocity).
    % Determining the accumulative time steps [in hour
unit] of the overtopping process.
    t_hours_0 = zeros(m1,n1);

    for a=1:length(vf0)-1
        if vf0(a+1) > 0 % overtopping.
            t_hours_0(a+1) = t_hours_0(a) + 1/60; % [hour].
        end
    end
end

```

```

% Determining the initial non-scouring velocity values.
vnon0 = zeros(m1,n1);

for a=1:length(t_hours_0)
    if t_hours_0(a) > 0 % overtopping.
        vnon0(a) = 2.8902 * t_hours_0(a)^(-0.297); %
        [m/s2] grass with poor cover: this relation was
        derived via EXCEL.
    end
end

% Determining the initial vertical erosion rate
(deltaz0).

alfal = 0.0005;
deltaz0 = zeros(m1,n1);
for a=1:length(vnon0)
    if vf0(a) > vnon0(a)
        deltax0(a) = alfa1 * vf0(a) * 60; % [m] : time
        step = 1 [min] = 60 [sec].
    end
end

%% Determining the initial change of breach bottom
opening (Zd0 & Zu0 [m]).

% Determining the initial change of the downstream
crest point elevation (Zd0).

Zt = 160.23; % [m] above SWL: terrain elevation.
Zd0 = ones(m1,n1) * Zc; % [m] above SWL.

for a=1:length(deltaz0)-1
    if Zd0(a) - deltax0(a+1) <= Zt
        Zd0(a+1) = Zt; % [m] above SWL.
    else
        Zd0(a+1) = Zd0(a) - deltax0(a+1);%[m]above SWL.
    end
end

% Determining the initial change of the upstream crest
point elevation (Zu0).

Bc = 2.95; % [m]: width of the dike crest.
s = (6.18/2.18); % downstream slope.
Zu0 = ones(m1,n1) * Zc;

for a=1:length(Zd0)-1
    if Zu0(a) - deltax0(a+1) <= Zt
        Zu0(a+1) = Zt; % [m] above SWL.
    elseif Zd0(a+1) >= (Zc - Bc/s)
        Zu0(a+1) = Zc; % [m] above SWL.
    else
        Zu0(a+1) = Zu0(a) - deltax0(a+1);%[m]above SWL.
    end
end

```



```

% V6 : alfa2
% Determining the final variables (b, Qb, hf, vf,
v_non, Zd, Zu).

%Determining final change of overtopping width(b [m]).
alfa2_min = 0.000025; % proposed min value.
alfa2_max = 0.0001; % proposed max value.
alfa2 = V6;

for a6 = 1:length(V6)
    wb1=wb1+1;
    waitbar(wb1/(M1*M2^Vi),wb,[num2str(wb1), ' / ',
    num2str(M1*M2^Vi)])

    alfa2(a6) = alfa2_min + (alfa2_max -
        alfa2_min)*V6(a6);

    b= ones(m1,n1)*b0;
    for a=1:length(Zu0)-1
        if Zu0(a+1) < Zc
            b(a+1) = b(a) + alfa2(a6) * vf0(a+1) * 60;%
            [m] : time step = 1 [min] = 60 [sec].
        end
    end

% Determining final change of overtopping discharge
(Qb [m3/s]).

Qb = zeros(m1,n1);
for a=1:length(b)
    if hs(a) > Zu0(a)
        Qb(a)= m_i(a4) * b(a) * sqrt(2*g) * (hs(a)-
            Zu0(a))^1.5; % [m3/s].
    end
end

% The previous for-loop returns the Qb variable as
a complex number.
% But only the real part will be used.

Qb=real(Qb);

% Determining the final variables (hf & vf).
hf = zeros(m1,n1);
o = find(Qb > 0);
hf(o)=(Qb(o).*n_i(a5)./b(o)./sqrt(sind(beta))).^0.6;
clear o

vf = (sqrt(sind(beta))/n_i(a5))*hf.^(4/6); % [m/s].

% Determining the accumulative time steps in
[hours] of the overtopping process.

t_hours = zeros(m1,n1);
for a=1:length(vf)-1
    if vf(a+1) > 0
        t_hours(a+1) = t_hours(a) + 1/60; % [hour].
    end
end
end

```

```

% Determining final non-scouring velocity values.

v_non = zeros(m1,n1);
o = find(t_hours > 0);
v_non(o) = 2.8902 * t_hours(o).^(-0.297);
clear o

%Determining final vertical erosion rate (delta_z).

delta_z = zeros(m1,n1);
o = find(vf > v_non);
delta_z(o) = alfa1 * vf(o) * 60; %[m]:
time step=1 [min] = 60 [sec].
clear o

% Determining the final change of breach bottom
opening (Zd & Zu [m] above SWL).

% Determining the final change of the downstream
crest point elevation (Zd).

Zd = ones(m1,n1)*Zc; % [m] above SWL.

for a=1:length(delta_z)-1

    if Zd(a) - delta_z(a+1) <= Zt
        Zd(a+1) = Zt; % [m] above SWL.
    else
        Zd(a+1)=Zd(a)- delta_z(a+1); %[m]above SWL.
    end

end

% Determining the final change of the upstream
crest point elevation (Zu).

Zu = ones(m1,n1)*Zc; % [m] above SWL.

for a=1:length(Zd)-1

    if Zu(a) - delta_z(a+1) <= Zt
        Zu(a+1) = Zt; % [m] above SWL.
    elseif Zd(a+1) >= (Zc - Bc/s)
        Zu(a+1) = Zc; % [m] above SWL.
    else
        Zu(a+1)=Zu(a)-delta_z(a+1); %[m] above SWL.
    end

end

```

```

% Determining the probability of each case

if max(hs) <= Zc % no overtopping.
    case_1(a1,a2,a3,a4,a5,a6) = 1;

elseif max(delta_z) == 0 % overtopping - no erosion
    case_1(a1,a2,a3,a4,a5,a6) = 0;
    case_2(a1,a2,a3,a4,a5,a6) = 1;

elseif min(Zu) == Zc %overtopping + erosion - no
    breaching
    case_2(a1,a2,a3,a4,a5,a6) = 0;
    case_3(a1,a2,a3,a4,a5,a6) = 1;
    case_4(a1,a2,a3,a4,a5,a6) = 0;

else % overtopping + erosion + breaching

    case_3(a1,a2,a3,a4,a5,a6) = 0;

    case_4(a1,a2,a3,a4,a5,a6) = 1;

end
end
end
end
end
end
end

L = length(case_1(:));

P_case_1 = P_design + sum(case_1(:))/length(case_1(:))*(1-P_design);
P_case_2 = sum(case_2(:))/length(case_2(:))*(1-P_design);
P_case_3 = sum(case_3(:))/length(case_3(:))*(1-P_design);
P_case_4 = sum(case_4(:))/length(case_4(:))*(1-P_design);

P_control=P_case_1+P_case_2+P_case_3+P_case_4;
toc;

save Q10.mat

```